Chapter 2 High Pressure Behavior of Porous Geomaterials

2.1 Overview

This chapter provides a brief history of the research conducted to evaluate the behavior of porous geomaterials subjected to static and dynamic high pressure loadings. It begins with a description of test equipment used to discern high pressure material behavior. The chapter includes a chronology of high pressure testing of granular materials and a summary of the conclusions developed by the referenced investigators. After completing this chapter, the reader should have a better understanding of and appreciate the importance of the high pressure behavior of porous materials.

The term "high pressure" means many different things to different people, and therefore will be defined at this time. Terminology originally developed by Vesic and Clough (1968) is adopted to define the pressure ranges used in this report. When describing specific pressure levels, low pressure refers to pressures in the range from 0 to 1 MPa, elevated pressures range from 1 to 10 MPa, high pressures range from 10 to 100 MPa, very high pressures range from 100 to 1000 MPa, and ultra-high pressures are those greater than 1000 MPa. The term "high pressure" will still be used as a generic term to describe research at elevated pressures and above.

2.2 High Pressure Test Equipment

2.2.1 Overview

There currently exists a significant number of devices capable of conducting tests at pressure levels ranging from high to ultra-high. The number of devices is reduced significantly if one constrains the selection to test equipment that is designed to (a) conduct mechanical property tests as apposed to wave propagation tests and (b) test specimens of average size, e.g., 35 mm diameter or greater. Gas or powder gun tests are capable of achieving stress levels ranging from tens of gigapascals to tens of terapascals. However, these tests are conducted as wave propagation tests in which the response of materials to plane wave loading is of primary interest. In these tests, the stress levels are of such magnitude that material strength is often an insignificant factor. Laboratories such as Lawrence Livermore National Laboratory, Los Alamos National Laboratory, or Sandia National Laboratory have the ability to test at pressure levels of 1-4 GPa, but typically only on small specimens having diameters less than 25 mm. In contrast, the Geodynamics Research Facility of the WES has developed a number of test devices and loaders capable of testing 50-mm-diameter specimens at high to very high pressure levels. This section will focus on WES test devices; several of which are typical of devices in the general category of high pressure test equipment, while others are very unique and one of a kind.

2.2.2 100 MPa Static and Dynamic Test Devices

The dynamic high pressure triaxial shear (DHT) test device (Ehrgott and Sloan 1971), the pore pressure uniaxial strain (PPUX) test device (Akers, Reed, and Ehrgott 1986), and the static high-pressure triaxial shear (HPTX) test device (Akers, Reed, and Ehrgott 1986) are all capable of conducting back-pressure saturated, drained or undrained tests with pore pressure measurements on a wide variety of materials to peak stress levels of 100 MPa. A controlled dynamic impulse-type loading may be applied with either the DHT or the PPUX when used in combination with the WES 100-kip SECO ram loader (Ehrgott and Sloan 1971). The SECO ram loader is capable of applying a variable peak force of up to 445 kN under controlled rise, dwell, and decay times;

rise times of 3 to 120 milliseconds (ms), dwell times of 0 to 1000 ms, and decay times of 20 ms to 10 seconds (s) are possible. These devices are described in more detail below.

The DHT test device applies a controlled dynamic confining pressure pulse to any cylindrical test specimen having a maximum height of 114 mm and a maximum diameter of 51 mm. As shown in Figure 2.1, the DHT test device consists of a pressure vessel or chamber, pressure supply system, pressure decay system, base assembly, and stroke limiter. Confining pressure is generated by applying compressed nitrogen to an amplifying piston in the base assembly. As the amplifying piston moves up into the chamber, it compresses the confining fluid and generates confining pressure. The device components allow a maximum 100 MPa confining stress to be generated with programmed rise, hold, and decay times; minimum rise, hold, and decay times are 3, 0, and 20 ms, respectively; maximum rise, hold, and decay times are 1, 1, and 10 s, respectively. When interfaced with the SECO ram loader (Figure 2.2), dynamic shear tests may be conducted, i.e., both confining pressure and axial force are applied under controlled conditions. During a typical dynamic shear test, a programmed dynamic pressure pulse is applied to the test specimen with the DHT. At a programmed point in time, the ram loader is activated. The loader applies a dynamic vertical force to the loading piston within the DHT test device, generating an increasing deviatoric stress in the test specimen. Should a test specimen fail catastrophically, a stroke limiter controls the maximum travel of the loading piston and prevents damage to the internal instrumentation. The device's internal instrumentation includes two vertically oriented LVDT's to measure the specimen's vertical deformations, a lateral deformeter to measure radial deformations, an internal pressure cell to measure confining pressure, and piston and/or base load cells to measure axial force. Pore fluid pressure is measured with a pressure cell mounted within the specimen's base pedestal.

The PPUX device was designed to conduct static drained or undrained uniaxial strain tests or dynamic undrained uniaxial strain tests on back-pressure saturated test specimens. As shown in Figure 2.3, the PPUX device was machined into an upper and lower assembly. Major components in the upper assembly include the dynamic sliding piston, the dynamic insert plug,

the fluid chamber pressure cell, and a chamber pressure port. The lower assembly consists of the test specimen, vertical deformeter (an LVDT), LVDT footing, membrane and retaining ring, and a system that provides back-pressure saturation, drainage, and pore pressure measurement capabilities. The test device will accommodate either remolded or undisturbed 23-mm-high and 97-mm-diameter test specimens. Two design factors minimize the effects of sidewall friction between the specimen and test device; first, a nominal 1-to-4 specimen aspect ratio was designed into the device and second, the LVDT footing measures the central vertical displacement of the specimen.

During static or quasi-static tests, a hydraulic pump supplies pressure to the PPUX. To generate dynamic pressures, the PPUX device is placed under the SECO ram loader. The loader drives the PPUX's sliding piston into the fluid filled chamber, thereby applying a vertical stress to the surface of the test specimen. The chamber pressure cell measures the fluid pressure and therefore the vertical stress applied to the specimen. Applying the vertical stress with a fluid eliminates the deleterious shear stresses that develop when a piston is used to load the test specimen. An internal drainage valve and a pore pressure cell are located beneath the test specimen in order to minimize the volume of pore fluid subject to compression. Accurate pore pressure measurements have been made during tests with times to peak stress as fast as 25 to 35 ms.

The HPTX test device was designed to conduct quasi-static drained or undrained shear tests on back-pressure saturated test specimens. It has three major components: the chamber top cap, base, and cylinder walls (Figure 2.4). Two top caps are available for the device, one for compression tests and one for extension tests. The internal instrumentation includes two vertically oriented LVDT's to measure the specimen's vertical deformations, a lateral deformeter to measure radial deformations, and a piston load cell to measure axial force. The device accepts a maximum specimen diameter of 76 mm, which enables testing of soils with maximum grain diameters of 13 mm. Confining pressure is generated with a hydraulic pump and a constant rate

of deformation loader provides axial driving force during shear. Pore fluid pressure is measured with a pressure cell mounted external to the base of the device.

2.2.3 600 MPa Static Shear Test Device

The WES 6-kbar static shear test device is very similar to the HPTX device; it has seven major components: the chamber top and bottom plugs, top and bottom seal plugs, instrumentation cage, loading piston, and cylinder walls (Figure 2.5). Like the HPTX, two top plugs are available for the device, one for compression tests and one for extension tests. Internal instrumentation includes two vertically oriented LVDT's to measure vertical deformations, a lateral deformeter to measure radial deformations, and an internal base load cell to measure axial force. The device accepts a maximum specimen diameter of 54 mm. Confining pressure is generated with a high pressure pump and amplifying accumulator, and a 2.2 MN stress-controlled loader provides axial driving force during shear.

2.2.4 One-GPa Static and Dynamic Test Device and Loader

Two test devices currently under development at WES will be capable of applying a 1 GPa confining stress under quasi-static or dynamic loading rates and then failing a cylindrical test specimen in shear under quasi-static or dynamic loading rates. These devices are similar in concept to the DHT and SECO loader. The two major components are the 1 GPa pressure vessel and actuator and the 11.1 MN static/8.9 MN dynamic loader. The pressure vessel (Figure 2.6) contains the test specimen, pressure vessel liners, and seal plates. The test chamber accepts a cylindrical test specimen having a maximum diameter of 51 mm. The amplifying piston, which amplifies the applied driving pressure by a factor of 45 to 1, generates the confining pressure for both static and dynamic tests. A key component in the pressure vessel is the bottom dynamic seal plate. A fluid port in this plate must allow confining fluid to flow into the specimen chamber without restriction as it is being compressed by the amplifying piston. The plate must also be able to absorb a 11.1 MN force applied to the specimen pedestal. The confining fluid is a mixture of kerosene and hydraulic oil; the two fluids must be proportioned so as to minimize both fluid compressibility and viscosity. A separate axial loader (Figure 2.7) applies either a

maximum 11.1 MN static or a maximum 8.9 MN dynamic vertical driving force to the loading piston. The minimum risetime of the loader is approximately 5 ms, maximum hold and decay times of several seconds are possible, and the minimum decay time is approximately 5 ms.

2.3 Material Property Research Prior to 1959

Bishop and Eldin (1953) studied the effects of stress history, isotropic versus anisotropic consolidation, and mode of failure on the angle of internal friction. Drained and undrained triaxial compression and extension tests, at maximum effective confining pressures of less than 0.7 MPa, were conducted on fully saturated and dry specimens of Folkestone Bed sand. This sand was the medium to fine fraction of a well-graded sand from the Folkestone Beds near the river Darent in Kent; the maximum and minimum porosities were 46.2 and 33.2 percent, respectively. Over the range of stresses investigated, the authors found: (1) the angle of internal friction was independent of the magnitude of the confining pressure[1], (2) a consistent decline in friction angle was observed with increasing initial porosity, and (3) it was necessary to correct for the work performed in changing the specimen volume in drained tests in order to match the friction angle from undrained tests. At a confining pressure of 37 kPa, the authors found that the friction angles from dry and fully saturated specimens were different; the friction angles for the dry specimens were 2 degrees higher for loose sand and 6 degrees for dense sand. The authors emphasized that the above differences could be the result of dissimilar soil structure produced by the techniques used to prepare fully saturated and dry specimens.

Nash (1953) conducted triaxial compression tests on fully saturated and air-dry specimens of a closely graded river sand having maximum and minimum porosities of 47 and 38 percent, respectively. The maximum confining pressure used in the test program was approximately 1 MPa. The author found that: (1) the hydrostatic compression responses of fully saturated and

[1] The use of the medium to fine fraction of the sand may be one reason Bishop and Eldin did not observe a decrease in angle of internal friction with increasing pressure.

dry specimens were the same and (2) if tested under the same conditions, the friction angles from fully saturated and dry specimens were the same. Like Bishop and Eldin (1953), Nash found a consistent decrease in friction angle with increasing initial porosity.

Golder and Akroyd (1954) described a triaxial compression cell they constructed to test geologic materials at confining stress levels of up to 6.9 MPa (1000 psi). The higher than normal stress levels were required to determine the friction angle of soils and soft rocks, e.g., soft sandstone and shale, located under dams or dock walls. They successfully tested a clayey sand at confining stress levels up to approximately 5.7 MPa, a sandstone to 3.8 MPa, and a crushed rock stabilized with cement to 4.3 MPa. The authors did not describe the moisture conditions of the specimens tested; the stress levels above are assumed to be effective stresses.

One-dimensional compression tests conducted on dry and saturated soils to vertical stress levels of 69 MPa were reported by Roberts and de Souza (1958). Their tests were conducted as consolidation tests, that is, specimens were incrementally loaded using a gas/fluid accumulator, hydraulic ram, load cell, piston, and consolidometer. Specimen dimensions were either 28.7 or 69.8 mm in diameter and 8.9 to 19.1 mm in height. Soils tested included Boston Blue clay, Venezuelan clays, 20-40 Ottawa sand, a well rounded graded quartz sand, and an angular uniform quartz sand. The authors used the term "critical pressure" to define the vertical stress level at which the sand grains commenced to shatter and the compressibility of the sand dramatically increased. For stress levels greater than the critical pressure, the authors found that: (1) the maximum compression index C_c of the sands was equal to or greater than that of the clays and (2) deformations were significantly time dependent during each load increment. The time dependent compression was attributed to a process of grain fracture and crushing followed by redistribution of stresses leading to additional grain crushing. Results from gradations tests on posttest specimens indicated that the uniform quartz sand became more graded with each additional increment of vertical stress. The authors concluded that, for a sand with a given initial angularity, the magnitude of the critical pressure was "dependent almost exclusively on the initial void ratio" and the critical pressure increased with decreasing initial void ratio.

2.4 Material Property Research from 1960 to 1969

Schultze and Moussa (1961) conducted one-dimensional compression tests to maximum vertical stress levels of 1.1 MPa on 25 different clean dry sands having a variety of grain shapes, gradings, and initial densities. The test specimens were initially 112.8 mm in diameter and 45 mm in height. No additional information was provided on the test equipment. The grain diameters ranged from 0.06 to 5 mm. Four to sixteen different initial densities of each sand were tested representing relative densities between 0 and 100 percent. Schultze and Moussa concluded that the stress-strain response of all sands could be mathematically represented by the equation

$$\varepsilon = a\, p^{k} \qquad 2.1$$

where ε is the vertical strain and p is the vertical stress. From this equation, the authors developed additional functional forms to account for initial density, grading and grain shape, the influence of water, and the influence of cohesive admixtures. For the sands investigated, the authors did discern similar stress-strain behavior for dry and fully saturated specimens.

Hall and Gordon (1963) documented drained and undrained triaxial compression tests conducted on several soils used in the construction of the shell, transition, and impervious zones of Oroville Dam. The materials tested fell into the following five classification categories, a clayey gravelly sand (SC), a sandy clayey gravel (GC), a silty sandy gravel (GP-GM), a clayey gravel (GP-GC), and a gravel (GP). Maximum confining pressures in the test program were 4.5 MPa. At confining pressures below 0.9 MPa, 305-mm diameter by 701-mm high specimens were tested; the maximum particle size tested was 76.2 mm. At confining pressures greater than 0.9 MPa, 152-mm diameter by 351-mm high specimens were tested; the maximum particle size was 38.1 mm. Volumetric strains measured during the shear portion of the drained tests on gravel exhibited dilation at low confining stresses (<1.4 MPa) and compaction at the high confining stresses (1.4< σ_c <3.4 MPa). Despite the maximum confining stress of 4.5 MPa, all of

the drained tests on the silty sandy gravel dilated. The pervious materials, i.e., the silty sandy gravel, the clayey gravel, and the gravel, exhibited a reduction in measured effective friction angle with increasing confining pressure. The authors made the following conclusions; (1) the decrease in friction angle was attributed to grain crushing and fracture, and a majority of the grain deterioration occurred during shear; (2) particle degradation was a function of the initial grading, the better graded soils exhibited less grain crushing and fracture; and (3) clayey and silty materials did not exhibit a reduction in friction angle.

Hirschfeld and Poulos (1963) conducted drained triaxial compression tests to maximum confining stress levels of 3.9 MPa on a glacial sand and on undisturbed Cannonsville silt specimens. The authors described Cannonsville silt as an angular to sub-angular, non-plastic silt with a natural water content ranging from 20 to 22 percent. The sand was derived from a glacial outwash deposit and had been scalped of all particles sizes greater than a No. 10 sieve. The minimum and maximum void ratios of the sand were 0.41 and 0.85, respectively; the test specimens had an average relative density of 20 percent. Constant rate of strain triaxial compression tests were conducted on both materials, and volume strains were measured during the consolidation and shear phase of each test. The authors found that, during the initial shear loading, all of the specimens compacted irrespective of confining pressure. At the highest confining stress levels, both materials exhibited compaction to axial strains of 16 to 20 percent, whereas at the lower confining stress levels dilational volumetric strains occurred. The friction angles of both materials decreased over the 0.1 to 3.9 MPa confining stress range investigated. The authors explained that if the strengths at the higher stress levels were extrapolated from the lower stress levels, the strength of the silt would have been overestimated by 35 percent and the sand by 10 percent. Unfortunately, the authors made no effort to investigate the effect of grain crushing on the response of the materials. Using Rowe's stress-dilatancy theory, they developed a modified failure envelope for the sand that was linear over the entire range of stresses investigated, and concluded that "the volume changes that occur during shear are the principal cause of the curvature of the (failure) envelope for the sand." The same theory could not fully explain the curvature of the silt failure envelope.

Kjaernsli and Sande (1963) conducted one-dimensional compression tests to maximum stress levels of 2.65 MPa on several crushed rock and gravel specimens. The materials tested were crushed angular particles of syenite, gneiss, and limestone, rounded particles of gravel, and subrounded particles of morainic materials. The maximum particle size of all the materials was less than 128 mm and the minimum particle size was not specified. The tests were performed

Table 2.1.
Summary of materials tested by Kjaernsli and Sande (1963)

Material	No. Tests	Uniformity Coefficient	Crushing %	Initial Porosity %	Relative Density %
Syenite	7	1.4 - 26	0 - 44	28 - 51	7 - 100
Gneiss	3	1.4 - 56	0 - 42	34 - 47	1 - 41
Limestone	2	1.4 - 30	0 - 40	33 - 45	na
Gravel	7	1.4 - 57	0 - 10	19 - 43	4 - 100
Morainic	1	100	0	26.7	87

with a stress-controlled consolidometer having an inside diameter of 500 mm, a height of 250 mm, and a wall thickness of 20 mm; the vertical stress was applied with a 498-mm diameter plate loaded by a piston. A total of twenty tests were conducted on the five different materials. Table 2.1 lists the materials tested and the range of values of uniformity coefficient, initial porosity, and relative density for the specimens tested. The column labeled "Crushing" is a measure of the grain crushing that occurred in the tests. Crushing was defined as the change in percent passing between pre- and posttest specimens at the pretest 0 percent passing grain diameter. One test was conducted over a period of one year, and this specimen was flooded with water twice. From this test the authors concluded that: (1) the deformations under each load increment were time dependent, (2) the introduction of water into the specimen increased the deformations, and (3) grain crushing was a principal cause of volume compression. The authors made the following summary conclusions: (1) volume compression decreases as the hardness of

the parent material increases, (2) rounded smooth-surfaced aggregates compress less than angular rough-surfaced aggregates, (3) volume compression is inversely related to relative density, and (4) well-graded aggregates compress less than poorly graded aggregates.

Kolbuszewski and Frederick (1963) investigated the effect of particle shape and size on compressibility and shear strength. Hydrostatic compression and direct shear tests were conducted on glass beads and two sands, a rounded Leighton Buzzard sand and an angular Biddulph Medium sand. Maximum stress levels were only 0.5 MPa. For different sized particles having the same shape, the authors found: (1) compressibility and the dilatancy component increased with increasing size and (2) the angle of internal friction was insensitive to particle size. As the angularity of equal sized particles increased, the authors found: (1) the compressibility of loose specimens increased dramatically and dense specimens exhibited a slight decrease in compressibility and (2) the angle of internal friction and the dilatancy component increased.

Leslie (1963) documented consolidated drained triaxial compression tests conducted by the South Pacific Division of the U.S. Army Corps of Engineers on fully saturated specimens of a variety of gravelly materials with both natural and artificial gradings. The materials tested included a rounded Ottawa sand, a quarried granite, and alluvial soils with subrounded and subangular particles. The specimens tested were 152 and 304 mm in diameter and had maximum particles sizes of 38 and 76 mm. A series of tests was conducted on five materials with parallel gradings and uniformity coefficients of 3.3; the confining pressure for all the tests was 0.42 MPa. From this series, the author reported that: (1) the maximum obtainable density increased with increasing maximum particle size; (2) the angle of internal friction increased with increasing density; and (3) at maximum density, the maximum friction angle was generated from a material with an intermediate grading. The author compared the friction angles of two soils having duplicate gradings[2]. From these tests, the author concluded the denser and less friable material had the greater friction angle. In order to quantify particle breakdown, the author compared

[2] Unfortunately the two soils had significantly different mineralogy and ranges of void ratio.

posttest gradings for several of the materials tested. The author reported that: (1) particle breakdown increased with increasing confining pressure; (2) more particle breakdown occurred during shear than during hydrostatic loading; and (3) at a confining stress level of 0.41 MPa, materials of equal uniformity coefficient and mineralogy exhibited increased particle breakdown with increased maximum particle size. Over the effective confining pressure range of 0 to 4.48 MPa, the author also found the angle of internal friction decreased with increasing confining pressure for all materials tested, and concluded that "the shear strength of alluvial gravelly soils under high lateral pressures may not exceed a range between 35 and 40 degrees."

Vesic and Barksdale (1963) appear to be the first researchers to publish in the open literature results of triaxial shear tests at confining pressures of up to 69 MPa. They conducted drained triaxial compression and constant mean normal stress tests on dry and saturated specimens of Chattahoochee River sand; all specimens were prepared dry. This sand had a uniformity coefficient of 2.5, a mean particle size of 0.37 mm, and maximum and minimum void ratios of 1.10 and 0.61, respectively; specimens were tested at a relative density of 78 percent. The authors found considerable curvature in the failure envelope over the range of confining pressures investigated; secant friction angles were 44° at pressures below 0.07 MPa, 39° at 0.49 MPa, and 30° at pressures below 69 MPa. The authors reported the dilatancy component of the shear strength contributed to the curvature of the failure envelope; the dilatancy component was greatest at a stress level of 2.45 MPa and was negligible above 4.90 MPa. During constant mean stress tests at 4.71 MPa, the authors detected no volume change during shear, and at higher stress levels specimens exhibited compressive volume changes. Significant grain crushing was observed in the tests (Figure 2.8) and more grain crushing occurred during shear than during hydrostatic compression (Figure 2.9). The authors concluded that: (1) dense cohesionless soils only exhibit dilatancy at "low" confining stress levels; (2) above a "critical pressure", which was 4.9 MPa for Chattahoochee River sand, grain crushing was a dominant component during shear; (3) the frictional component of the shear strength was proportional to the normal stress over the entire range of stresses investigated; and (4) the dilatancy component of the shear strength is

negligible above the critical pressure and achieved a maximum at approximately one half the critical pressure.

Hendron (1963) published the results of uniaxial strain tests conducted on four oven-dried sands to maximum vertical stress levels of 22.7 MPa. The tests were conducted to investigate the effects of initial relative density on the constrained modulus, the coefficient of earth pressure at rest (K_o), and the energy absorption capacity of each sand. The uniaxial strain device used by Hendron permitted the measurement of radial stresses, i.e., the entire stress tensor was defined. The four sands tested included: Minnesota sand, a uniform rounded silica sand, Pennsylvania sand, a coarse angular silica sand, Sangamon River sand, a medium to fine sub-angular sand, and Wabash River sand, a well-graded sub-angular to sub-rounded sand. The author found that the initial stiffness of all four sands increased with increasing relative density. The vertical stress level at which softening occurred in the stress-strain curves and the constrained modulus peaked, due to the onset of grain crushing, increased with increasing relative density. The author explained this behavior with the following logic. Since a loose sand has fewer contact points per unit volume than a dense sand at the same applied vertical stress, the loose sand will have higher grain to grain contact stresses. Due to the higher contact stresses, grain crushing will commence at a lower vertical stress level in a loose sand. In comparing test results from the four sands, Hendron also showed that the characteristics of the sand grains significantly influenced the magnitudes of the constrained moduli. For example, the constrained moduli of the rounded Minnesota sand were 9-10 times greater than the moduli of the angular Pennsylvania sand at the same relative density (Figure 2.10).

In evaluating the vertical and radial stress data from the four sands, Hendron found the following: (1) the magnitude of K_o was constant at low and intermediate pressures; (2) at higher pressures, there was a slight increase in the K_o values; (3) during unloading, the vertical stresses decreased at a faster rate than the radial stresses; and (4) during the later stages of unloading, the radial stresses exceeded the vertical stresses. At low and intermediate pressures, the K_o values increased with decreasing initial relative density. Since the angle of internal friction decreases

with increasing confining pressure for many materials, Hendron presumed that K_o values should increase with pressure. His data clearly showed that K_o was inversely related to angle of internal friction.

Hendron found that the energy absorbed as a percentage of the total energy input for the first cycle of loading decreased with increasing relative density for three of the four sands; the angular Pennsylvania sand exhibited a constant value with respect to relative density (Figure 2.11). The energy absorbed as a percentage of the total energy input during subsequent cycles to stress levels approximately one-third of the peak stress in the first cycle, exhibited a relatively flat response with increasing relative density. Hendron attributed the dissipation of energy in dry sand to three different mechanisms: (1) work input by the stresses to produce irrecoverable volume changes due to rearrangement of grains, (2) "energy is absorbed in the form of surface energy as crushing creates new surfaces," and (3) absorption of energy during subsequent load-unload cycles due to the differences in loading paths.

Hendron also revealed that above a certain stress level "all the measurable physical properties are the same and are independent of the initial void ratio before loading." For example, when the Pennsylvania sand stress-strain data were plotted as void ratio versus vertical stress, data from tests at different initial relative densities merged into one loading curve (Figure 2.12).

Clough (1964) extended the research work reported by Vesic and Barksdale (1963) by conducting additional drained triaxial compression and constant mean normal stress tests on dry and saturated specimens of Chattahoochee River sand. As in the earlier testing, the maximum applied confining stress level was 69 MPa. Clough's test program investigated: (1) the shape of the failure surface; (2) the effect of initial density on compressibility and shear behavior; (3) grain crushing during shear and hydrostatic compression; and (4) volume change behavior during hydrostatic compression, triaxial compression, and constant mean normal stress tests. The author provided the following properties for the sand; the maximum and minimum void ratios were 1.09 and 0.593, respectively; the maximum and minimum densities were

1.674 Mg/m^3 and 1.278 Mg/m^3, respectively; and the sand classified as a uniform slightly micaceous medium grained quartz sand. The shear tests were conducted at relative densities of 18.1 and 78.5 percent.

In analyzing the shear strength data, Clough concluded that: (1) the loose specimens were well represented by a linear failure envelope over the entire stress range (0 to 69 MPa), (2) the failure envelope for the dense specimens exhibited significant curvature at the lower stress levels (stresses less than 3 MPa), and (3) the failure envelope for both the loose and dense specimens

Table 2.2.
Range of friction angles for dense sand (Clough 1964)

Range of Confining Pressures (MPa)	Degrees
0. to 0.07	44.0
0.07 to 1.20	39.1
1.20 to 2.94	27.9
2.94 to 62.1	32.4

was linear at stress levels above 4.9 MPa with a friction angle of 32.4°. Table 2.2 lists the measured secant friction angles for the dense specimens at four pressure ranges. The curvature in the failure envelope was attributed to the dilatant characteristics of the dense sand at low pressure; a characteristic the loose specimens did not exhibit. By conducting constant mean normal stress tests in the low stress regime, and thereby measuring only shear induced volume changes, Clough found a strong correlation between the curvature of the failure envelope and the magnitude of the dilatant volumetric strains at failure (Figure 2.13).

Data from the hydrostatic loading phase of the shear tests revealed identical volume change behavior in both the dry and fully saturated test specimens. The author reported the major portion of the volume change occurred at stress levels below 20 MPa, and above this stress level, the compressibility of the loose and dense specimens were analogous. Volume strains during

hydrostatic loading were also time dependent at stress levels above 2.1 MPa; this behavior was attributed to grain crushing and to readjustment of the grain structure.

Clough explained that specimens with initial void ratios of 0.7 and 1.0 had void ratios of 0.45 and 0.47 after hydrostatic loading to 20 MPa. At stress levels above 20 MPa, loose and dense specimens in both the triaxial compression and the constant mean normal stress tests exhibited analogous compressive volumetric strains at failure. The similar behavior was attributed to the comparable void ratios at the higher stresses. In general, the loose specimens always exhibited compressive volumetric strains at failure; the dense specimens (as noted above) exhibited dilatant strains at failure at stress levels below 3 MPa.

Clough compared posttest gradings to evaluate the magnitude of grain crushing. At pressures above 3 MPa (30 kg/cm^2), the posttest gradings of loose and dense specimens had similar distributions; the same was found for dry and fully saturated specimens (Figure 2.14). Clough concluded that initial void ratio and moisture conditions had no influence on grain crushing. As reported by earlier researchers, grain crushing was more extensive during shear than during hydrostatic loading.

Bishop, Webb, and Skinner (1965) described eight tests (3 consolidated-drained and 3 consolidated-undrained triaxial compression tests and 2 special tests) conducted on saturated loose specimens of Ham River sand. Maximum and minimum porosities of this sand were 48 and 38 percent, respectively. The maximum applied confining pressure was 6.9 MPa. The three drained tests exhibited only a small drop in friction angle, from 33.5° to 30.2°, with increasing pressure. Axial strains of between 25 and 30 percent were required to fail these specimens. All of the undrained tests generated positive pore pressures during shear. One undrained test, with an initial effective confining pressure of 6.83 MPa, had a friction angle of only 21.3° at peak deviator stress and a friction angle of 34.2° at ultimate failure. It produced a pore-pressure parameter A at peak deviator stress of 1.0 and a value of 1.83 at ultimate failure. The authors

noted that this behavior conflicted with critical state theory, and attributed the differences to grain crushing or "structural breakdown".

In his 1965 Rankine Lecture, Bishop (1965a) provided a synopsis of the behavior of soils under high stress levels. Most of the results presented were from drained and undrained triaxial compression tests conducted at Imperial College on saturated specimens of Ham River sand to maximum confining pressures of 27 MPa. The author produced Figure 2.15, which presents drained failure envelopes reported in the literature for several materials. The author stated that for granular materials (sands, gravels, and rockfills) the curvature of the failure envelope was associated with grain crushing and was more distinct for materials that (a) "are initially dense or heavily compacted" and (b) "are initially of relatively uniform grain size." Grain crushing diminishes the volume increase at failure and thereby yields a reduced friction angle at failure. In comparing the friction angles from drained tests on loose and dense specimens of Ham River sand, Bishop found a 5-degree difference at a pressure of 0.7 MPa, but only a 0.2 degree difference at 6.9 MPa, i.e., the magnitude of the friction angles converges with increasing confining pressure. Dense specimens, which dilated at stress levels below 3.4 MPa, compacted during shear at stress levels above 3.4 MPa. Bishop found a strong correlation between friction angle and dilatancy rate ($d\varepsilon_v / d\varepsilon_a$) and concluded that "the curvature of the failure envelope is thus largely accounted for by the decrease in the rate of dilatancy with increasing stress." The author reported grain crushing occurred at the higher stress levels, and the grain crushing was more severe during shear than during hydrostatic compression. Bishop commented that the posttest gradings were approaching that of a glacial till, which has a constant friction angle over a broad range of pressure levels (Insley and Hillis 1965). Bishop reported that undrained shear tests on loose specimens of Ham River sand exhibited an unstable behavior similar to quick clays. For a specimen with an initial effective stress of 6.2 MPa, the mobilized friction angle at peak deviator stress was 62 percent of the value at ultimate failure.

As a panelist at the Sixth International Soil Mechanics Conference, Bishop (1965b) again addressed aspects of soil behavior under "high" confining stress levels, where Bishop defined

high confining stress as 7 to 70 MPa. Bishop discussed the often difficult task of determining peak stress in drained triaxial compression tests on cohesionless materials where significant grain crushing occurs at large strains. He described a simple stress analysis of particle packing and contact in which particle size drops out of the final equations for contact pressure. From this analysis, he concluded that the magnitude of grain crushing and fracture was controlled by the strength and compressibility of the individual particles and not their size, and therefore grain crushing and fracture can occur at relatively low stress levels. The author also showed that soils with a narrow initial grading, and thus a high initial porosity, generate larger volumetric strains during shear than well-graded materials. Thus, a well-graded material would be a better source of fill for high dams, both grain crushing and changes in friction angle would be reduced.

Insley and Hillis (1965) conducted drained and undrained triaxial compression tests on 152-mm (6-inch) diameter specimens of a well-graded, slightly plastic glacial till at three compaction moisture contents. Effective confining stress levels in the test program ranged from 0.35 to 3.10 MPa. The authors found little variation in friction angle over the range of stress levels investigated for all three compaction moisture contents. This behavior was attributed to the presence of fines, the grading of the material, and the similar nature of the volume change behavior during shear. The fines were thought to inhibit any substantial fluctuation in the volumetric strain response of the material during shear.

Lee and Seed (1966, 1967) documented a series of triaxial compression tests conducted to investigate "the relationship between strength, volume changes and confining pressure in drained tests at high confining pressures." Tests were conducted on two sands, Sacramento River and a dense Ottawa sand. A more extensive series of tests was conducted on Sacramento River sand, a fine uniform sand having maximum and minimum void ratios of 1.03 and 0.61, respectively, subangular to subrounded grain shapes, and grains consisting primarily of feldspar and quartz minerals. The Ottawa sand had well-rounded grains, which "exhibited a high resistant to crushing". The fully saturated test specimens were initially 35.6 mm (1.4 in.) in diameter and 86.4 mm (3.4 in.) high, and were tested to maximum confining pressures of 13.73 MPa. The

authors noted that the grading of the sand made corrections for membrane penetration unnecessary, standard end platens were deemed sufficient for all tests, and a 49-kPa seating load was required to form the test specimens.

Lee and Seed described a series of tests in which specimens were prepared at relative densities of 100 percent and tested at confining pressures ranging from 0.098 to 11.77 MPa. The following observations were associated with increasing confining pressure: (1) the stress-strain curves transitioned from brittle to ductile like behavior, (2) the axial strain to failure increased, and (3) the sand exhibited less dilatancy. All of the drained tests at confining pressures above 2.9 MPa exhibited compressive volumetric strains during shear. The authors made several notable comments concerning the stress-strain behavior: (1) "The stress-strain volume change characteristics of dense sand at high confining pressures are not unlike those of loose sand at low pressures." and (2) "For each confining pressure, the volume changes which accompany the shearing deformations tend to produce samples with the same void ratio at failure, even though the initial void ratios may be vastly different."

Lee and Seed indicated the slopes of the Mohr envelopes decreased with increasing confining pressure up to 3.92 MPa; the slopes of the dense sand decreased from 41 to 24 degrees and the loose sand decreased from 34 to 24 degrees. At confining pressures above 3.92 MPa, the Mohr envelopes exhibited a slight increase in slope and at higher pressures the envelopes were approximately linear. At the highest confining pressures, the loose and dense specimens had equivalent strengths, i.e., the measured strengths were independent of the initial specimen densities. In contrast to the Sacramento River sand, results from tests on dense Ottawa sand indicated the failure envelope had a gradually decreasing slope over the entire range of stress levels investigated (0.10 to 13.73 MPa). The authors attributed the differences in the character of the failure envelopes to the high crushing resistance of the Ottawa sand.

For Sacramento River sand, Lee and Seed also determined the critical void ratio, the critical confining pressure, and the Mohr envelope under constant volume conditions. At confining

pressures below 3.92 MPa, the authors found that the critical void ratio and the critical confining pressure were uniquely related to each other, and were "completely independent of the initial void ratio of the test specimen."

Grain crushing was evident in the posttest specimens of both the Ottawa and Sacramento River sand. For the later sand, the percent passing the #200 sieve increased from 2 percent (the original grading) to 50 percent when loaded to a confining pressure of 13.73 MPa (Figure 2.16). Lee and Seed found it necessary to add grain crushing and re-arranging effects as a strength component in a relationship for the overall strength of a cohesionless material. Grain crushing had considerable influence on the strength mobilized at constant volume. The authors stated that "crushing of grains in tests at high confining pressures will absorb energy causing the angle of friction corrected for dilatancy effects to be greater than φ_u, the angle of sliding friction." In their relationship, the measured shear strength was the sum of the strength due to sliding friction, dilatancy effects (a positive value for dilational volume strains and a negative value for compressive volume strains), and grain crushing and re-arranging effects (Figure 2.17).

Lee and Farhoomand (1967) conducted a series of drained constant stress ratio tests to investigate the effects of grain size, grain shape, grading, stress level, and stress ratio on the compressibility and grain crushing of saturated specimens of a crushed granitic gravel. Five angular soils of uniform grading, one graded angular soil, and two subrounded soils of uniform grading were manufactured from the granitic source material and tested. The maximum grain size was 19.0 mm (¾ inch), and all of the materials were tested at a relative density of 100 percent. The maximum applied confining pressure was 13.73 MPa and three stress ratios of 1.0, 2.0, and 2.8 were used during the test program. From their investigation, the authors found both the grain crushing and compression behavior of the granitic materials to be time dependent; minor volume changes were still occurring two hours after the application of a load increment. For the three stress ratios and eight different materials investigated, Lee and Farhoomand found that the volumetric strains exhibited by these materials were a unique function of the applied

major principal stress and independent of the applied minor principal stress[3]. The authors claimed that these observations supported the experiments and conclusions drawn by Rutledge (1947). In comparing the volume compression and grain crushing of soils with different gradings and grain shape, Lee and Farhoomand reported: (1) an angular soil exhibited more volume compression and grain crushing than a subrounded soil of equivalent grading, (2) volume compression increased with increasing grain size for angular soils, (3) a uniform soil exhibited more volume compression and more crushing than a graded soil with the same maximum grain size, (4) grain crushing at a given confining pressure increased with increasing stress ratio, and (5) coarse soils exhibit more volume compression and grain crushing than fine soils.

Lee, Seed, and Dunlop (1967) documented an investigation of the effect of moisture conditions on the drained strength of clean sands. Static triaxial compression tests were conducted on oven dried, air dried, and saturated specimens of Antioch sand at confining pressures ranging from 0.1 to 13.73 MPa and at 100 percent relative density. The Antioch sand was dredged from the Sacramento River near Antioch, California. The maximum and minimum void ratios were 1.14 and 0.75, respectively. A petrographic analysis indicated the sand was composed of 50% quartz grains, 20% aggregate grains (grains made up of an aggregate of minerals), 10% heavy minerals, 10% other, and less than 1% mica. At all levels of confining stress, the authors found that the oven dried specimens exhibited the greatest strengths and degree of dilation, the saturated specimens had the lowest strengths and least dilation, and the air dried specimens were always intermediate between the two. The same trends were observed in the initial moduli during shear. The saturated specimens also exhibited the greatest amount of grain crushing during shear, and the oven dried specimens the least. Similar tests conducted on both Monterey and Ottawa sands disclosed no weakening due to the introduction of pore water. The authors attributed the water sensitivity of Antioch sand to the weathered and cracked aggregate grains that composed 20% of the solid volume.

---

[3] A possible explanation for this behavior is shear induced volume changes, which, at the higher stress ratios, compensate for the smaller pressure induced volume changes.

Vesic and Clough (1968) presented a summary of results reported by Clough (1964) and some additional data and analyses. All of the data was collected from tests on Chattahoochee River sand. In reviewing Clough's data, the authors found that "there exists a mean normal stress beyond which the curvatures of the strength envelopes for all initial void ratios vanish and beyond which the shear strength of the sand is not affected by its initial void ratio." The authors identified this mean normal stress as the "breakdown stress (σ_B)", and further defined it as the stress level "at which all dilatancy effects disappear and beyond which particle breakage becomes the only mechanism, in addition to simple slip, by which shearing displacement in the slip planes becomes possible." The breakdown stress for this material was approximately 9.8 MPa. The authors processed the test data to derive values of Poisson's ratio and tangent Young's modulus to mean normal stress levels of 69 MPa. Above the breakdown stress, these elastic parameters were identical for initially loose and dense specimens. Values of Poisson's ratio increased from 0.25 at the breakdown stress to 0.30 at 59 MPa, while values of tangent Young's modulus increased from 200 to 1000 MPa over the same stress range.

The authors developed the following relation between secant friction angle and mean normal stress at stress levels less than the breakdown stress

$$\varphi_s = \varphi_f + (\varphi_n - \varphi_f) \frac{\log \frac{\sigma_B}{\sigma_0}}{\log \frac{\sigma_B}{\sigma_n}} \qquad 2.2$$

where φ_s is the secant friction angle corresponding to the normal stress σ_0, φ_n and σ_n are the reference secant friction angle and mean normal stress, φ_f was defined by the authors as "the angle of interparticle friction" and is the limiting secant friction angle above the breakdown stress. With low pressure failure data and a knowledge of the breakdown stress, a nonlinear failure surface can be approximated with the above relationship.

Lee, Seed, and Dunlop (1969) presented test data from dynamic triaxial compression tests conducted on dry specimens of Antioch sand at confining pressures ranging from 0.1 to 1.47 MPa, at relative densities of 38 and 100 percent, and under a maximum strain rate of 2.5 per second. The strength increase measured during the dynamic tests was attributed to "the effect of strain rate on the energy required for particle crushing." A special series of undrained triaxial compression tests was also conducted on Sacramento River sand to investigate time-dependent grain crushing. The undrained tests conducted by the authors were a form of instability test. Specimens were anisotropically consolidated to some percentage of the drained strength. Under conditions of free drainage, these specimens were always stable. When the drainage line was closed and a small transient increment of axial load was applied, the pore fluid pressure increased with time until failure occurred. The time to failure decreased as the magnitude of the axial load increased. Similar behavior was observed without the application of axial load; however, the time to failure was more prolonged. Again, the authors attributed this behavior to time-dependent grain crushing. Grain crushing caused the specimen to compact, which in turn, increased the pore fluid pressures.

Hendron, Davisson, and Parola (1969) documented undrained uniaxial strain tests conducted to peak vertical stress levels of 138 MPa on remolded and undisturbed specimens of silty clay and sandy silt. The tests were conducted to investigate the influence of degree of saturation on high pressure stress-strain behavior and to disprove the concept that large strains would develop in fine-grained materials at high pressure due to grain crushing. Some of their data is suspect, since the specimens within the test device were not sealed and pore fluid could drain out of the specimen and flow through the loading mechanism. The authors made the following conclusions: (1) degree of saturation and initial void ratio were the primary variables controlling the high-pressure stress-strain behavior and (2) provided their initial physical properties were the same, remolded and undisturbed specimens exhibited identical stress-strain behavior above 21 MPa.

Banks and MacIver (1969) assembled a survey of published high pressure triaxial shear test data on granular materials. The authors condensed into tabular and graphic (see Figure 2.18) forms the test data of many researchers referenced in this chapter. From the accumulated data, they developed an empirical relation to account for the variation in the secant angle of internal friction with increasing confining pressure. Their relation was written as

$$\varphi_s = \varphi_n - P \log \frac{\sigma_0}{\sigma_n} \qquad 2.3$$

where φ_s is the secant friction angle corresponding to the normal stress σ_0, φ_n and σ_n are the reference secant friction angle and normal stress, and P is the change in friction angle over one log cycle. Unlike the equation developed by Vesic and Clough (1968), the above equation has no limiting stress level, i.e., no breakdown stress, above which the secant friction angle remains constant. A friction angle of zero will be calculated at some pressure level.

Marachi, et al. (1969) presented an extensive report on the strength and deformation characteristics of rockfill materials. The authors investigated two topics that are of interest in this chapter, grain crushing and the effects of particle size on the strength and compressibility of granular materials. The authors investigated the effects of particle size by conducting drained triaxial compression tests on saturated specimens of three different modeled rockfill materials. The materials were "modeled" by maintaining parallel grading curves with different maximum grain sizes. Therefore, to first order, the only variable in this modeling process was maximum grain size. The three materials tested were a rockfill (an angular argillite) from the shell zone of Pyramid Dam, a rockfill (a well-rounded to rounded amphibolite) from the shell zone of Oroville Dam and a crushed basalt (angular, fine grained olivine basalt). Three different maximum grain sizes were tested for each material, requiring specimen diameters of 914, 305, and 71 mm (36, 12, and 2.8 inches). Tests were conducted at four effective confining stress levels; the maximum stress level was 4.5 MPa. The authors found that the volumetric strains due to hydrostatic loading of the crushed basalt and the Oroville Dam materials were the same for the three grain sizes; the Pyramid Dam material showed a slight increase in volume compression with increasing

maximum grain size. When corrected for the small differences in initial void ratio, all three materials exhibited a decrease in the angle of internal friction with increasing maximum grain size (Figure 2.19), and all three materials exhibited a decrease in the angle of internal friction with increasing confining stress (Figure 2.20).

The authors found that the volumetric strains at failure were the same for the intermediate and large size specimens and the small size specimens exhibited the smallest values. In general, the axial strains at failure increased with increasing maximum grain size. Both the volumetric strains and the axial strains at failure were more compressive with increasing confining pressure. The authors obtained posttest gradings from all of the tests and analyzed the results to ascertain the effect of modeling on the grain crushing characteristics of the rockfills. Grain crushing was evident in all of the tests; the Pyramid Dam materials exhibited the greatest measure of degradation and the Oroville Dam materials the least. As reported by earlier investigators, more grain crushing was induced during the shear phase of the test compared with the hydrostatic loading phase, and the degradation increased with increasing confining pressure. Using the breakage factor B, a numerical measure of grain crushing, the authors revealed that grain crushing increased with maximum particle size at each confining stress level for all three materials (Figure 2.21). By plotting the breakage factor B versus the angle of internal friction (Figure 2.22), the authors found: (1) a unique relationship between the two parameters for each of the three materials and (2) "the relationship between the angle of internal friction and the particle breakage factor B is independent of the particle size...for materials that have parallel gradations and the same initial void ratio."

Leussink and Brauns (1969) conducted an analytical investigation of particle breakdown and its effect on the shear strength of granular materials. They modeled granular materials as regular packings of elastic-brittle spheres and simulated the response of these materials under hydrostatic and deviatoric stress states. Their analysis revealed that the critical principal stress ratio (or shear strength) decreased rapidly after exceeding a "critical lateral pressure" (Figure 2.23). They found that "the failure of the array is due to sliding effects up to the critical pressure, and is due to

particle breakage beyond this lateral pressure." As illustrated in their figure, the critical lateral pressures increased with decreasing coefficients of friction, and particle breakage initiated at higher confining pressures as the applied stresses became more hydrostatic. The later result has been confirmed by several investigators who observed greater grain crushing during the shear phase of their tests.

2.5 Material Property Research from 1970 to Present

Tai (1970) extended the work reported by Clough (1964) and Vesic and Clough (1968) by conducting drained and undrained triaxial compression tests on saturated specimens of Chattahoochee River sand. He also conducted drained and undrained triaxial compression tests on saturated specimens of Ottawa sand. Tai's test program deviated from Clough's in several areas. Tai tested larger diameter specimens (71-mm) than Clough, his maximum applied confining stress level was only 35 MPa, and his tests were conducted at relative densities of 0.2, 0.5, and 1.0. In analyzing the drained test results, Tai found significant differences between the volume change behavior of Ottawa and Chattahoochee River sands and attributed the differences to the larger grain size, greater grain strength, the uniform grading, and the more spherical grain shapes of the Ottawa sand. Initial grain degradation was observed at confining stresses of 13.8 and 1.72 MPa for the Ottawa and Chattahoochee River sands, respectively.

Tai reported that the drained behavior of the two sands during shear was notably different. Values of axial strain at failure for loose and dense Ottawa sand specimens (Figure 2.24) gradually increased over a range of mean normal stresses from 0 to 24 MPa (0 to 3500 psi) and exhibited little to no increase above 24 MPa. The critical mean normal stress for dense specimens of Ottawa sand was 13.8 MPa (2000 psi), and 1.7 MPa (250 psi) for loose and intermediate density specimens. Above these pressures, the values of volumetric strain at failure followed the same trends as the axial strains at failure. The axial and volumetric strains at failure of loose and intermediate density Chattahoochee River sand specimens (Figure 2.25) increased rapidly, peaked between 6.9 and 13.8 MPa, and then decreased with increasing values of mean

normal stress. Dense specimens exhibited a gradual increase with increasing mean normal stress after an initial sharp rise between 0 and 13 MPa. Tai found that the breakdown stress (Vesic and Clough 1968) for Chattahoochee River sand was 5.5 MPa (800 psi) for both the intermediate and dense specimens (Figure 2.26); breakdown stress values of 58.6 and 8.3 MPa (8500 and 1200 psi) were obtained for dense and intermediate Ottawa sand (Figure 2.27). Tai also found the equation developed by Vesic and Clough for the secant friction angle (Equation 2.2) was applicable to both sands over the range of stresses investigated.

Tai's undrained test results revealed that the maximum shear stress occurred at a smaller axial strain than the maximum stress ratio in all of the Chattahoochee River sand tests and in the Ottawa sand tests at the higher confining stress levels (σ_c > 13 MPa). For the Chattahoochee River sand and Ottawa sand tests, the mobilized friction angles at peak deviator stress were 35 and 40 percent, respectively, lower than the values at ultimate failure. Most of the low and intermediate density Chattahoochee River sand specimens exhibited A-Factors at ultimate failure greater than 1 and in several specimens values greater than 2.0 were measured. Bishop (1965a) obtained similar results on Ham River sand and commented on the unstable nature of this type of response.

Murphy (1970, 1971) extended the work of Clough (1964), Vesic and Clough (1968), and Tai (1970) by conducting hydrostatic compression and drained triaxial compression tests on dry and saturated specimens of sand- and silt-sized grains at confining pressures of 35 and 310 MPa[4]. Murphy investigated the effects of initial density, saturation, grading, and stress level on the four "monomineral" soils listed in Table 2.3. Physical and material properties of the four materials are also presented in Table 2.3. The materials tested were selected to represent the common rock forming minerals and provide a wide range of hardness values.

[4] Tai also conducted tests at the 35 MPa stress level; this allowed Murphy to use Tai's results in his own analyses.

Table 2.3.
Materials tested by Murphy (1970)

Materials		Quartz	Feldspar	Calcite	Chlorite
Mohs Hardness		7	6	3	1-2.5
Specific Gravity		2.65	2.61	2.72	3.10
Sand	d_{10}, mm	0.25	0.25	0.25	0.25
	C_u	1.25	1.25	1.25	1.25
	d_{50}, mm	0.30	0.30	0.30	0.30
	C_R	1.0	1.0	1.0	1.0
	e_{max}	0.78	1.28	1.10	1.33
	e_{min}	0.52	0.79	0.67	0.83
	γ_{max}, Mg/m^3	1.749	1.456	1.629	1.691
	γ_{min}, Mg/m^3	1.483	1.144	1.294	1.325
Silt	d_{10},mm	0.022	0.002	0.018	0.018
	C_u	2.65	20.0	3.60	3.33
	d_{50}, mm	0.052	0.030	0.058	0.050
	C_R	2.0	3.4	2.0	1.0

Murphy maintained that the breakdown stress (Vesic and Clough 1968) was exceeded at a confining pressure of 35 MPa for all four materials. However, the secant friction angles for three of the four sands were lower at the 310 MPa confining pressure; the values were lower by 3.3, 5.0, and 6.5 degrees for the feldspar, calcite and chlorite specimens. The quartz sand specimens exhibited a negligible increase in secant friction angle (0.3 degrees). The nonlinear behavior in the failure surface well above the breakdown stress required modification of the original hypothesis introduced by Vesic and Clough. Murphy suggested there were three regions of specimen behavior. The first region was below the breakdown stress where the material behavior was strongly influenced by void ratio. A second region was above the breakdown stress where the material behavior was unaffected by initial void ratio and was dominated by grain crushing, and where the failure surface was linear. A third region was above the limit of "post breakdown

linearity". In this region, grain crushing during the consolidation phase dominated the material's shear behavior. The material's shear strength, which had a grain degradation strength component, diminished in proportion to the amount of grain crushing during consolidation. Murphy indicated the magnitude of the breakdown stress was dependent on the crushing strength of the grains. He implied that grain strength or grain mineral hardness controlled the ultimate volumetric strain capacity of a material, and the grain degradation component of the shear strength decreased as the volumetric strain during consolidation, as a percentage of the total capacity, increased.

Murphy's concept for the strength components of both hard and soft minerals are depicted in Figures 2.28 and 2.29. To prove his concept indirectly, Murphy plotted failure data in two different formats for the four materials tested. Figure 2.30 presents the failure data at the 310 MPa confining stress plotted versus the log of mineral hardness. Figure 2.31 presents all of the available failure data for the four materials plotted versus the log of mean normal stress. The relationship between strength and mineral hardness is evident in both figures.

Murphy investigated several other factors affecting the mechanical response of these four materials, e.g., saturation, end restraint, initial density, and grain size. His observations and conclusions are summarized in this and the following sections. Saturation effects (dry versus fully saturated) on shear strength and total volumetric strain were only examined at the 35 MPa confining stress level. For the materials tested, Murphy found that saturation did not affect the drained shear response. Under hydrostatic loading, total volumetric strains decreased when quartz specimens were saturated, whereas the saturated feldspar, calcite, and chlorite specimens exhibited increased strains. The author concluded that "saturation influences the mechanical behavior of cohesionless materials by means of a complex interdependence of crushing strength, grain microstructure, grain size, grain shape, grain size distribution, angle of mineral friction and state of stress."

Murphy investigated the effects of end restraint by comparing the response of specimens tested at a confining stress of 35 MPa with and without lubricated ends. If the axial stresses measured on specimens with nonlubricated ends were accurately corrected for the changing diameter of the specimen, Murphy found no variation in the measured strengths. At large strains, specimens with lubricated ends maintained a general cylindrical shape whereas the specimens with rough ends were inclined to bulge.

Murphy determined that total volumetric strain increased with decreasing initial relative density for all four materials. This observation does not conflict with earlier conclusions regarding material response below the breakdown stress. Above the breakdown stress, specimens with different initial relative densities approach a common void ratio. In comparing the shear response of sand- and silt-sized materials, Murphy found that the silt-sized soils had the greater strengths. He attributed this observation to differences in the grain degradation component of the shear strength, which was controlled by the crushing characteristics of the grains. In his final summary, Murphy concluded "that mineralogical composition, particularly as it dictates crushing strength and hardness, is the most significant factor influencing the high and very high pressure behavior of granular assemblies."

Holland (1971) and Mazanti and Holland (1970) documented unconsolidated-undrained hydrostatic compression, triaxial compression, constant stress ratio, and uniaxial compression tests conducted to maximum confining stress levels of 69 MPa on two partially-saturated recompacted soils, McCormick Ranch sand and Watching Hill clay. The McCormick Ranch sand was obtained from the McCormick Ranch test site near Albuquerque, New Mexico. It classified as a clayey sand (SC), had liquid and plastic limits of 27 and 15 percent, respectively, and was recompacted to a density of 1.874 Mg/m^3 (117 pcf) and a water content of 11.4 percent. The Watching Hill clay was obtained from the Watching Hill test site at the Defence Research Establishment, Suffield, Canada. It classified as a silty clay with fine sand (CL), had liquid and plastic limits of 36 and 17 percent, respectively, and was recompacted to a density of 1.490 Mg/m^3 (93 pcf) and a water content of 12.5 percent. The authors' test program was unique in that

they used an internal lateral deformeter to measure the specimens' radial deformations. Measurement of radial deformations allowed the authors to calculate radial strains, volume strains, bulk modulus, and shear modulus and conduct uniaxial strain tests on partially-saturated specimens. At confining pressures of approximately 20 MPa, the air porosity in both materials was crushed out and the specimens responded as fully-saturated materials, i.e., the failure surfaces were essentially flat and the specimens exhibited stiffer bulk moduli. The authors did not conduct posttest analyses of the materials for grain crushing.

Emerson and Hendron (1971) described a uniaxial strain device capable of testing gravel sized materials to vertical stress levels of 11 MPa statically and 5.5 MPa dynamically (with a minimum rise time of 3 milliseconds). The test specimens were 1200 millimeters in diameter and 355 millimeters in height. In their test program, static and dynamic tests were conducted on four materials, a 20-30 Ottawa sand, a well-graded crushed dolomitic limestone, a well-graded Wabash River gravel composed of subrounded to rounded igneous and sedimentary rocks, and a well-graded North Dakota river gravel composed primarily of igneous rocks. Their test program was designed to investigate the effects of grain shape, specimen grading, saturation, and loading rate on one-dimensional compression. The authors found the stress-strain response of the Wabash River gravel was much stiffer than the crushed angular limestone. They concluded from these tests that deformations will increase as the angularity of the specimen's grains increase. From the tests on the two river gravels, the authors concluded that the constrained modulus was a function of the grain crushing strength, the higher the strength the stiffer the response.

Emerson and Hendron reprocessed the Wabash River gravel to obtain four uniformly graded materials with different maximum particle sizes. Below 2.1 MPa, the constrained moduli increased with increasing particle size. The authors attributed this behavior to the greater crushing strength of the larger particles. The stress-strain behavior of these four materials was identical above 2.1 MPa. The authors were unable to discern changes to the uniaxial stress-strain behavior due to changes in grading. However, only a very limited number of tests were conducted to investigate that effect. The addition of water prior to or during a test reduced the

grain crushing strength of the Wabash River gravel and increased the magnitude of the axial strains. Dynamic tests were only conducted on crushed limestone specimens. The authors calculated a 40% increase in constrained modulus due to the faster loading rates of the dynamic tests.

Lo and Roy (1973) documented drained triaxial compression tests conducted on three artificial sands of the same initial grading to maximum confining pressures of 11 MPa. The three artificial sands, in order of decreasing grain crushing strength, were aluminum oxide, quartz sand, and limestone sand. All of the tests were conducted with enlarged lubricated end platens. The authors found that the stress-strain and volume change behavior of these materials were significantly influenced by grain mineralogy. All three materials exhibited an increasing axial strain to failure with increasing confining pressure, and the rate of increase in strain to failure was greatest in the weak-grained materials. The rate of volume change increased (where the sign convention is compression positive) with increasing confining pressure for all three materials. The authors stated that "the increase of strain to failure and the suppression of dilatancy may be explained by the increase in the amount of grain degradation, since the total energy input is progressively apportioned to energy dissipated in particle breakage." The confining pressure at the zero dilatancy rate increased with increasing grain hardness. For the limestone sand, the authors found that the dilatancy rate returned to zero at confining pressures above 6.9 MPa, and presented data from other investigators illustrating the same behavior (Figure 2.32). The authors identified this behavior with the "breakdown stress" of the material. They claimed that above this stress level the dilatancy rate would remain zero and the friction angle would remain constant. Like other investigators, the authors found that the secant friction angle decreased with increasing confining pressure. They showed that the rate of decrease in friction angle increased with increasing grain hardness or strength.

In 1985, the author conducted a laboratory test program to investigate the effects of loading rate on the drained and undrained uniaxial strain (UX) response of a calcareous beach sand (Akers 1986). The beach sand had the following physical and composition properties. The

minimum and maximum dry densities of four samples ranged from 1.532-1.540 Mg/m^3 and 1.740-1.744 Mg/m^3, respectively and the grain densities ranged from 2.78-2.80 Mg/m^3. Mineralogy tests indicated the beach sand was composed of 74-percent calcite and 26-percent aragonite by volume. The beach sand classified as a poorly graded clean sand (SP) by the USCS; the grading curve is plotted in Figure 2.33 (curve labeled Pretest Gradation Curve). The drained UX tests were conducted on partially-saturated samples having nominal water contents of 5 percent and relative densities (D_r) of either 0 or 45 percent. All of the tests were conducted in the WES pore pressure uniaxial-strain test device (Akers, Reed, and Ehrgott 1986).

Figure 2.34 presents the stress-strain curves from four tests (D_r=45%) conducted at four different loading rates (time to peak vertical stress of 0.006, 0.146, 15, and 30 s). These test results reveal a distinct increase in constrained modulus with faster loading rates. A controlling factor in the loading rate sensitivity of the beach sand was grain crushing. Less grain crushing occurred when the specimens were loaded dynamically as evidenced in Figure 2.33. This figure compares the posttest gradation curves for static and dynamically loaded specimens with a pretest gradation curve. It is obvious from these results that less grain crushing took place during the dynamic test.

Another set of drained UX tests were conducted by applying a dynamic loading to the specimens and then holding the peak stress for a given period of time. These tests were conducted to investigate the grain crushing response of the beach sand after dynamic loading. Figure 2.35 compares the stress-strain curves from two tests, one loaded to peak stress in 30 seconds and the other loaded to peak stress in 50 ms and then the applied stress was maintained for 900 ms. During the 900-ms period the stress was held constant, the specimen continued to deform, i.e., the axial strains increased from 18 to 21.5 percent, an increase of 3.5 percent. These results suggest that under the quasi-static loading rates, the beach sand grains crushed and rearranged themselves into more stable configurations. The millisecond loading times imposed during the dynamic tests did not allow the sand grains to reach a state of equilibrium in terms of

grain crushing. Thus, grain crushing contributed significantly to the rate sensitive nature of this material.

Colliat-Dangus, Desrues, and Foray (1988) documented drained triaxial compression tests conducted on a siliceous sand and a marine calcareous sand to maximum confining stress levels of 15 MPa. The authors' test program was conducted in two phases. In the first phase of the test program, the authors compared the mechanical response of loose and dense specimens tested with and without lubricated ends at confining stresses below 3 MPa. They used x-ray tomography to evaluate density variations in posttest specimens. From these tests, the authors concluded that specimens tested with lubricated ends and a height-to-diameter ratio of 1 exhibited improved stress and strain homogeneity. The authors used these specimen conditions in the second phase of their test program. The second phase consisted of drained triaxial compression tests to confining stress levels of 15 MPa. The authors observed basic material behavior reported by other investigators, e.g., decrease in secant friction angle with increasing confining pressure, time dependent volume change at elevated confining pressures, and significant grain crushing, which increased with increasing confining pressure. Test results on the calcareous sand revealed that the calculated secant friction angle dropped below the interparticle friction angle, which was always considered a lower limit. This response was attributed to the high porosity and brittleness of the grains.

As part of the material characterization phase of various high-explosive test programs, four sand backfill materials (identified as Sands A-D) were tested by the WES over a period of four years (1989-1992) to very high pressures under several different laboratory boundary conditions. All of the materials classified as poorly graded clean sands (SP) by the Unified Soil Classification System (USCS); the gradation curves for the four materials are presented in Figure 2.36. Sand A was identified as a concrete sand, Sands B and C were fine to medium plaster sands as specified by ASTM C-35-76, and Sand D was identified as a fine to medium flume sand. Table 2.3 lists the as-placed and as-tested composition and physical properties of the four materials. All of the very high pressure tests were conducted in the WES 6-kbar (600 MPa)

Table 2.4.
Physical properties of Sands A-D

SP Sands: Composition and Physical Properties						
	Water Content %	**Dry Density Mg/m^3**	**Grain Density Mg/m^3**	**Porosity %**	**Saturation %**	**Volume Air %**
Sand A	5.0	1.78	2.70	34.1	26.1	25.2
Sand B	4.7	1.75	2.69	35.1	23.4	26.9
Sand C	3.5	1.69	2.67	36.7	16.1	30.0
Sand D	5.6	1.61	2.64	39.0	23.1	30.0

test device as unconsolidated-undrained tests, i.e., no pore air or water was allowed to drain from the membrane-enclosed specimens. The 600 MPa peak confining pressures in these tests were approximately twice those used by Murphy (1970). Specimens were tested primarily under hydrostatic compression, K_o (or uniaxial strain), and triaxial compression boundary conditions. All of the cylindrical specimens had a minimum 2-to-1 aspect ratio and no end treatment was employed. Since undrained tests were conducted, volume strains were calculated from the vertical and lateral strains assuming a right-circular-cylinder deformed specimen shape.

Before describing the mechanical responses of these sands, a few comments must be made about the behavior of partially-saturated materials at high pressures. Air porosity or degree of saturation are key variables that control the response of partially-saturated undrained materials at high pressure. At some pressure, all partially-saturated materials tested under undrained conditions will reach a point of void closure. At void closure, all of the highly-compressible air porosity within an undrained test specimen is collapsed, crushed, or "closed out", and the specimen enters a state of full saturation. At stress levels above void closure, effective stress theory dictates that most of the additional applied stress is carried by the pore fluid, resulting in little increase in specimen strength with additional applied confining pressure. Consequently, void closure controls the peak strength of the material and softens the uniaxial-strain stress path. In addition, the bulk and constrained moduli of test specimens become much stiffer at stress

levels above void closure, since specimen compressibility is controlled by the less compressible pore fluid and grain solids.

To enable constitutive modelers to develop fits for a specific material, the multitude of test results are typically distilled into a set of recommended mechanical response curves. Typically the modeler receives a set of recommended failure envelopes, uniaxial strain stress paths, and stress-strain curves such as those presented in Figures 2.37-2.39 for the four SP sands. These figures indicate that two of the four sands (Sands A and B) were loaded to stress levels above void closure; Sand A reached void closure at an axial stress of approximately 565 MPa and Sand B at an axial stress of 460 MPa (Figure 2.39). The failure envelopes of both Sands A and B attained limiting strength values of 220 and 325 MPa, respectively (Figure 2.37). The K_o stress paths of Sands A and B softened at mean normal stress levels of between 300 and 400 MPa (Figure 2.38). In contrast, Sands C and D, which had air-void volumes of 30 percent, were not loaded to stress levels above void closure. The failure envelopes and the K_o stress paths for these two sands exhibited a consistent increase in principal stress difference with increasing mean normal stress. To first order, all of the sands exhibited very similar behavior up to the point of void closure for Sands A and B. Prior to void closure, the failure envelopes were linear and had Coulomb friction angles of between 29 and 30 degrees. During unloading, the vertical stresses in the K_o tests decreased at a faster rate than the radial stresses as indicated by the stiffer K_o response. When the entire deviatoric load was removed, i.e., at zero principal stress difference, an appreciable mean normal stress still remained on the K_o test specimens.

During the period April 1987 to January 1989, Applied Research Associates conducted a laboratory test program to characterize both the drained and saturated-undrained mechanical response of intact Salem limestone (Chitty and Blouin 1993). The types of tests performed included hydrostatic compression, triaxial compression, K_o (uniaxial strain), and strain path; tests were conducted at confining stresses ranging between 0 and 400 MPa. All of the drained tests were conducted on air-dried specimens. The authors described the intact rock as light grey in color and having a mineral composition of 97% calcite, 1.2% magnesium carbonate, 0.69%

silica, 0.44% alumina, 0.18% iron oxide, and 0.49% other trace minerals. The limestone had the following mean physical and composition properties: the grain density was 2.7 Mg/m^3, the dry density was 2.359 Mg/m^3, the porosity was 12.8 percent and the P-wave sonic velocity was 4.528 km/s. The mechanical property tests were conducted in a device similar to that of the WES 6-kbar chamber. During each test, measurements of axial and radial deformation, pore-fluid and confining pressure, and axial load were made. No endcap treatment was used for these tests.

Based on all of the available load and unload drained hydrostatic compression data, a composite or recommended drained hydrostatic compression response curve was developed by the authors (Figure 2.40). The initial loading was essentially elastic and had a bulk modulus of 23.5 GPa (235 kb). At a pressure of approximately 150 MPa, the cementation within the limestone began to degrade, producing a much softer bulk modulus (3.5 GPa) and a more rapid crushing of the material. At a pressure of 350 to 400 MPa (3.5 to 4.0 kb), at which point half of the material's available air porosity had been crushed out, the bulk modulus began to increase again. The unloading behavior was initially elastic but significant curvature was exhibited at low stress levels.

The authors constructed a composite or recommended drained K_o stress-strain response curve (Figure 2.41) from all of the available K_o stress-strain data. The K_o stress-strain response was qualitatively similar to the hydrostatic compression behavior. The initial loading was essentially elastic and had a constrained modulus of 42.0 GPa (420 kb). The material began to crush at an axial stress of approximately 170 MPa, and the tangent modulus in the early crush regime was 4.9 GPa; at larger strains (>4%), the material became stiffer. A typical drained K_o stress path (plotted as axial stress versus confining pressure) is presented in Figure 2.42. The different slopes of the stress path during initial loading, unloading, and in the crush regime, indicate that the incremental values of K_o and Poisson's ratio varied significantly.

A multitude of data from drained triaxial compression tests was accumulated and reported by the authors. Typical axial and radial strain response curves at different confining stress levels are

presented in Figure 2.43. This figure indicates that over the range of stress levels investigated, the response of the limestone changed from brittle at low stress levels to ductile at high stress levels. For the same set of tests presented in Figure 2.43, Figure 2.44 presents the volume strains during shear and Figure 2.45 the pressure-volume results. During the initial shear loading, all of the specimens compacted and then, as the failure stress was approached, dilated. The magnitude of the shear induced compaction was a strong function of the position of the stress state on the material's pressure-volume curve prior to shear loading.

The failure points from the drained triaxial compression tests and the failure envelope derived by the authors are presented in Figure 2.46. Below a mean normal stress of approximately 100 MPa, the drained failure envelope is linear with an intercept of 16 MPa and friction angle of 29 degrees (in a Mohr-Coulomb stress space). Above a mean normal stress of 100 MPa, the failure envelope is nonlinear.

The authors conducted one saturated undrained K_o test; the total and effective stress paths from this test are plotted in Figure 2.47. Since the pore fluid carries a significant portion of the applied stress, the total stress path is much softer than the effective stress path. The authors indicated that the calculated effective stress path from this test closely matched the stress paths from the drained tests.

Stress difference versus axial and radial strain curves from five saturated undrained triaxial compression tests are plotted in Figure 2.48 and the effective stress paths from the five tests are plotted in Figure 2.49. There was good agreement between the failure points from the undrained tests and the drained failure envelope. Unlike the drained triaxial compression tests, the undrained tests exhibited little increase in strength with increasing axial strains at the higher confining stress levels (100 MPa and above), and the axial strains at failure were less than 1 percent.

2.6 Summary

The previous sections provide a short synopsis of earlier research in high pressure testing of porous geomaterials. As an aid to the reader, the major conclusions developed by the cited researchers are summarized in Tables 2.5 and 2.6. The influence of several grain characteristics on mechanical properties such as friction angle and volumetric strain are summarized in Table 2.5. In a similar format, the influence of other factors such as time and stress level on mechanical properties are summarized in Table 2.6. A key at the end of each table defines abbreviations used. To avoid developing erroneous conclusions from these tables, the reader should read the appropriate sections of the text and be aware of the materials tested and the maximum stress levels used in each investigation. For example, at low stress levels the measured friction angles of sands were a strong function of the initial void ratio or relative density, whereas at high stress levels the measured friction angles were independent of initial void ratio. If one were to ignore the peak stress levels used by the investigators, then an inaccurate conclusion would be inferred.

The following text gives two examples of how the reader should interpret these tables (see the first two lines in Table 2.6). Bishop and Eldin concluded that measured friction angles were not a function of stress level but were a function of the initial density or void ratio, and the friction angles were not the same for dry and fully saturated test specimens. Nash concluded that measured friction angles were a function of the initial density or void ratio, and the pressure-volume responses and the measured friction angles were the same for dry and fully saturated test specimens.

The following statements concerning material behavior of granular materials were developed based on the observations and conclusions made by a majority of the investigators. First, friction angles were not constant over a wide range of pressures for sands and gravels due to the effects of grain crushing, grain reorientation, and dilation. Second, at stress levels below the "breakdown stress", dilation was the most significant factor in the change in friction angle. Finally, more grain crushing took place during shear loading than during hydrostatic loading.

The following observations and conclusions were made by many of the investigators.

1. Grain crushing was strongly time dependent. Several investigators described the sounds of grains cracking minutes to tens of minutes after the application of an increment of loading. Others mentioned deformations that continued for extended periods of time. Mineral hardness, grain strength, and grain compressibility were important factors in grain crushing.

2. A material dependent critical pressure or breakdown stress was observed by several researchers who tested at stress levels greater than 50 MPa. The dilatancy component of strength was negligible above the breakdown stress.

3. At low stress levels the measured friction angles of sands were a strong function of the initial void ratio or relative density, whereas at high stress levels the measured friction angles were independent of initial void ratio.

The information presented in this chapter should give the reader a better understanding of and an appreciation for the importance of research in high pressure material behavior. Since a significant quantity of research data is not available to the general public, this should not be considered an all inclusive study.

Table 2.5.
Mechanical properties influenced by grain characteristics

Authors	Nominal Peak Stress MPa	Test Type	Material	Grain Characteristics					
				Grading	Angularity	Max. Size	Miner-ology	Strength	Crushing
Bishop & Eldin (1953)	0.7	TX	Sand						
Nash (1953)	1.0	TX	Sand						
Golder & Akroyd (1954)	7.0	TX	Sand,Rock						
Roberts & de Souza (1958)	70	UX	Sand,Clay					ε_v	ε_v
Schultze & Moussa (1961)	1.1	UX	Sand		σ-ε				
Hall & Gordon (1963)	4.5	TX	Sand,Gravel	$\Delta\varphi$,ΔV_s,GC		$\Delta\varphi$		$\Delta\varphi$	$\Delta\varphi$
Hirschfeld & Poulos (1963)	3.9	TX	Sand,Silt						
Kjaernsli & Sande (1963)	2.6	UX	Rock,Gravel	ε_v	ε_v		ε_v	ε_v	ε_v
Kolbuszewski & Frederick (1963)	0.5	HC,DS	Sand,Glass	φ	φ,ε_v,ΔV_s	$\varphi\neq$,ε_v,ΔV_s			
Leslie (1963)	4.5	TX	Sand,Rock	φ,$\Delta\varphi$,GC	n	GC,n		φ	
Vesic & Barksdale (1963)	70	TX,CP	Sand						
Hendron (1963)	22.7	UX	Sand		M		M_i		BS
Clough (1964)	70	TX,CP	Sand						
Bishop, Webb, & Skinner (1965)	7.0	TX	Sand						
Bishop (1965a)	--	--	--	$\Delta\varphi$					$\Delta\varphi$,ΔV_s
Bishop (1965b)	70	TX	Sand	GC$\neq$,ε_v,n		GC$\neq$		GC	
Insley & Hillis (1965)	3.1	TX	Glac. Till	$\Delta\varphi$					

Authors	Nominal Peak Stress MPa	Test Type	Material	Grain Characteristics					
				Grading	Angularity	Max. Size	Miner-ology	Strength	Crushing
Lee & Seed (1966)	13.7	TX	Sand					GC,φ	$\Delta\varphi$,φ
Lee & Farhoomand (1967)	13.7	CSR	Soils	GC,ε_v	GC,ε_v	ε_v			
Lee, Seed, & Dunlop (1967)	13.7	TX	Sand						
Vesic & Clough (1968)	69	TX,CP	Sand						
Lee, Seed, & Dunlop (1969)	1.5	TX	Sand						φ
Hendron, Davisson, & Parola (1969)	138	UX	Silt,clay						
Banks & MacIver (1969)	--	--	--						
Marachi, et al. (1969)	4.5	HC,TX	Rockfill			$\Delta\varphi$,ΔV_s, GC	GC		
Leussink & Brauns (1969)	--	--	--						
Tai (1970)	35	TX	Sand	ε_v	ε_v	ε_v	ε_v,ΔV_s,GC	ε_v,ΔV_s,GC	
Murphy (1970, 1971)	310	TX	Granular	φ,GC		φ,GC	φ,ε_v	φ,ε_v	φ,ε_v,BS
Holland (1971), Mazanti & Holland (1970)	70	HC,TX UX,CSR	Soils						
Emerson & Hendron (1971)	11	UX	Sand, gravel	$M\neq$	ε_v	M		M	M
Lo & Roy (1973)	11	TX	Sand				$\Delta\varphi$,ΔV_s,BS ,ε_v,σ-ε	$\Delta\varphi$	ΔV_s
Colliat-Dangus, Desrues, & Foray (1988)	15	TX	Sand						
Akers (1986)	70	UX	Sand					GC	ε_v

Authors	Nominal Peak Stress MPa	Test Type	Material	Grain Characteristics					
				Grading	**Angularity**	**Max. Size**	**Miner-ology**	**Strength**	**Crushing**

KEY: ε_v = volumetric strain σ-ε = stress-strain $\Delta\varphi$ = friction angle change ΔV_s = shear induced dilation GC = grain crushing
φ = friction angle n = initial porosity M = constrained modulus M_i = initial constrained modulus BS = breakdown stress
TX = triaxial compression HC = hydrostatic compression UX = uniaxial strain CP = constant mean normal stress DS = direct shear
CSR = constant stress ratio

Table 2.6.
Mechanical properties influenced by other factors

Authors	Nominal Peak Pressure MPa	Test Type	Material	Time	Stress		Initial D_r/n/e	Dilation	Dry = Saturated
					Stress Level	Breakdown Stress			
Bishop & Eldin (1953)	0.7	TX	Sand		$\varphi \neq$		φ		$\varphi \neq$
Nash (1953)	1.0	TX	Sand				φ		P-V,φ
Golder & Akroyd (1954)	7.0	TX	Sand,Rock						
Roberts & de Souza (1958)	70	UX	Sand,Clay	ε_v	GC	GC,M	BS		
Schultze & Moussa (1961)	1.1	UX	Sand						σ-ε
Hall & Gordon (1963)	4.5	TX	Sand,Gravel		$\Delta\varphi$,ΔV_s				
Hirschfeld & Poulos (1963)	3.9	TX	Sand,Silt		$\Delta\varphi$,ΔV_s			$\Delta\varphi$	
Kjaernsli & Sande (1963)	2.6	UX	Rock,Gravel	ε_v			ε_v		$\varepsilon_v \neq$
Kolbuszewski & Frederick (1963)	0.5	HC,DS	Sand,Glass						
Leslie (1963)	4.5	TX	Sand,Rock		GC		φ		
Vesic & Barksdale (1963)	70	TX,CP	Sand		$\Delta\varphi$,ΔV_s,GC	ΔV_s,GC		$\Delta\varphi$	
Hendron (1963)	22.7	UX	Sand		K_o	M	M_i,BS,K_o E,GC		
Clough (1964)	70	TX,CP	Sand	ε_v	$\Delta\varphi$,ΔV_s,GC		$\Delta\varphi$	$\Delta\varphi$	P-V,GC
Bishop, Webb, & Skinner (1965)	7.0	TX	Sand		$\Delta\varphi$				
Bishop (1965a)	--	--	--				$\Delta\varphi$	φ,$\Delta\varphi$	

Authors	Nominal Peak Pressure MPa	Test Type	Material	Time	Stress		Initial D_r/n/e	Dilation	Dry = Saturated
					Stress Level	Breakdown Stress			
Bishop (1965b)	70	TX	Sand						
Insley & Hillis (1965)	3.1	TX	Glac. Till		$\Delta\varphi^{\neq}$				
Lee & Seed (1966)	13.7	TX	Sand		$\Delta\varphi,\Delta V_s$,GC		$\Delta\varphi,\sigma$-ε		
Lee & Farhoomand (1967)	13.7	CSR	Soils	GC,ε_v	ε_v				
Lee, Seed, & Dunlop (1967)	13.7	TX	Sand						$\varphi^{\neq},\Delta V_s^{\neq}$, GC$^{\neq}$,$M_i^{\neq}$
Vesic & Clough (1968)	69	TX,CP	Sand			$\varphi,\Delta\varphi,\Delta V_s$, GC			
Lee, Seed, & Dunlop (1969)	1.5	TX	Sand	GC					
Hendron, Davisson, & Parola (1969)	138	UX	Silt,clay				σ-ε		
Banks & MacIver (1969)	--	--	--		$\Delta\varphi,\varphi$				
Marachi, et al. (1969)	4.5	HC,TX	Rockfill		$\varphi,\Delta V_s$,GC				
Leussink & Brauns (1969)	--	--	--						
Tai (1970)	35	TX	Sand		ΔV_s	φ	BS		
Murphy (1970, 1971)	310	TX	Granular		$\Delta\varphi,\varphi$				$\varepsilon_v^{\neq},\varphi$
Holland (1971), Mazanti & Holland (1970)	70	HC,TX UX,CS R	Soils						
Emerson & Hendron (1971)	11	UX	Sand, gravel	M	M				$\varepsilon_v^{\neq}$,M$^{\neq}$
Lo & Roy (1973)	11	TX	Sand		ΔV_s				

Authors	Nominal Peak Pressure MPa	Test Type	Material	Time	Stress		Initial D_r/n/e	Dilation	Dry = Saturated
					Stress Level	Breakdown Stress			
Colliat-Dangus, Desrues, & Foray (1988)	15	TX	Sand	ε_v	$\Delta\varphi$,GC				
Akers (1986)	70	UX	Sand	ε_v,GC	ε_v,GC				ε_v

KEY: ε_v = volumetric strain σ-ε = stress-strain $\Delta\varphi$ = friction angle change ΔV_s = shear induced dilation GC = grain crushing
φ = friction angle n = initial porosity M = constrained modulus M_i = initial constrained modulus BS = breakdown stress
P-V = pressure - volume TX = triaxial compression HC = hydrostatic compression UX = uniaxial strain
CP = constant mean normal stress DS = direct shear CSR = constant stress ratio

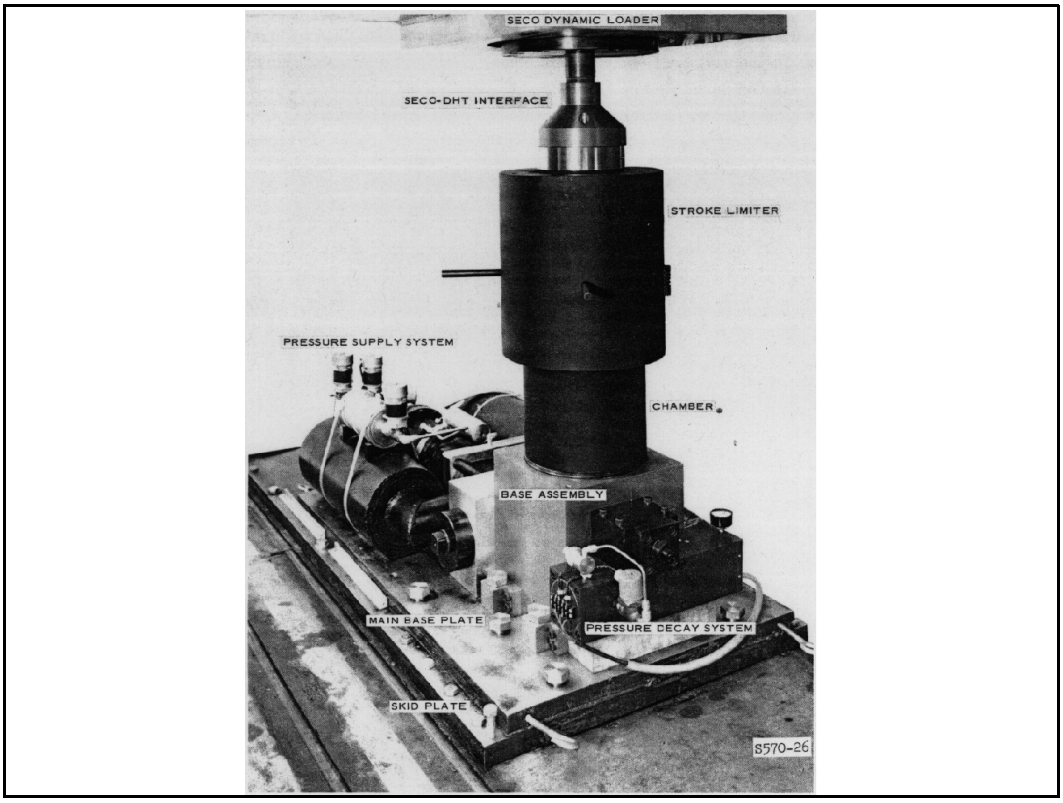

Figure 2.1. DHT test device

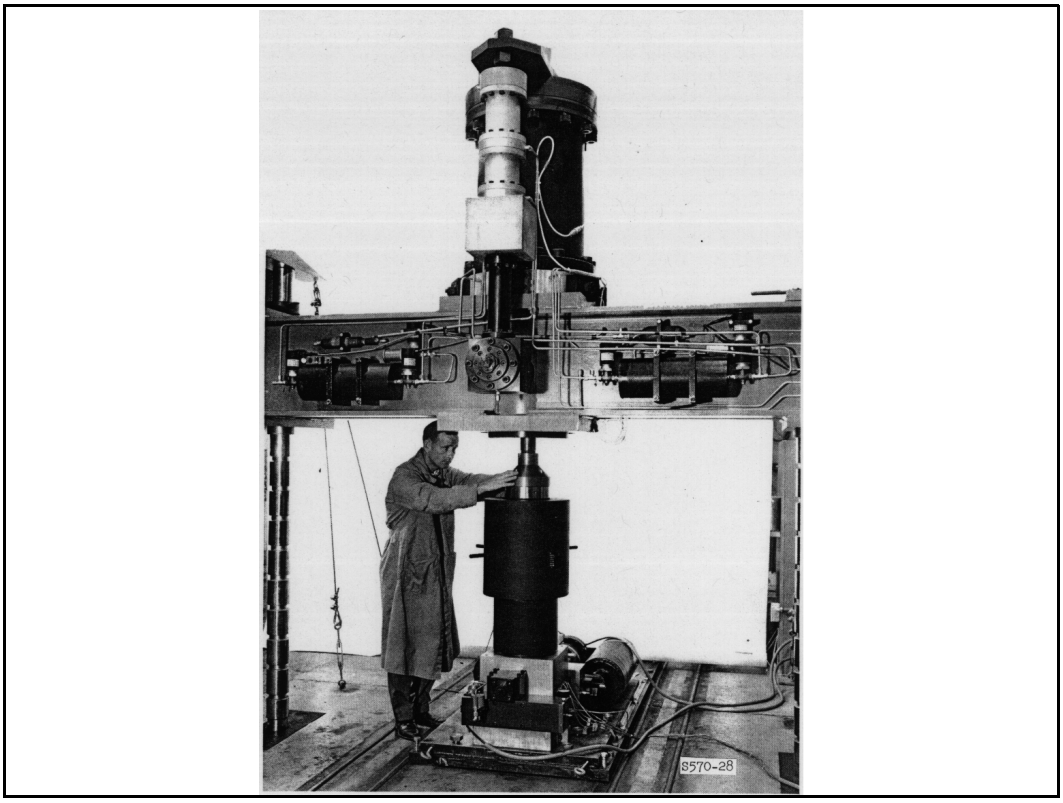

Figure 2.2. DHT and SECO ram loader

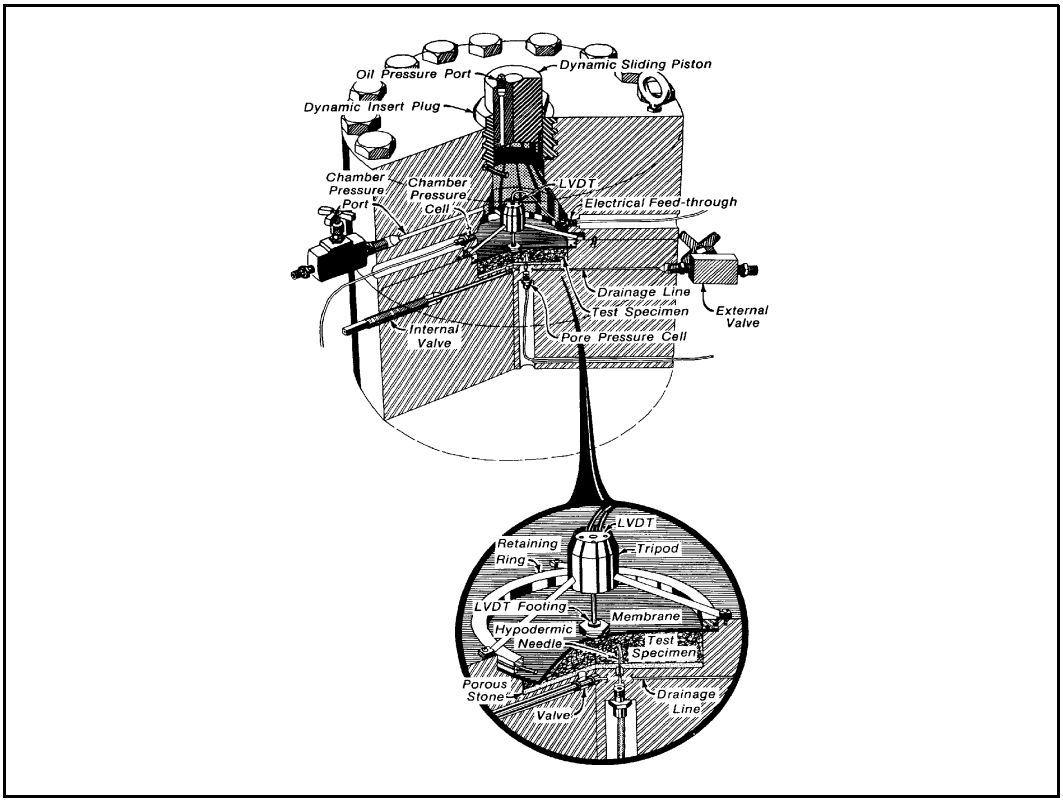

Figure 2.3. PPUX test device

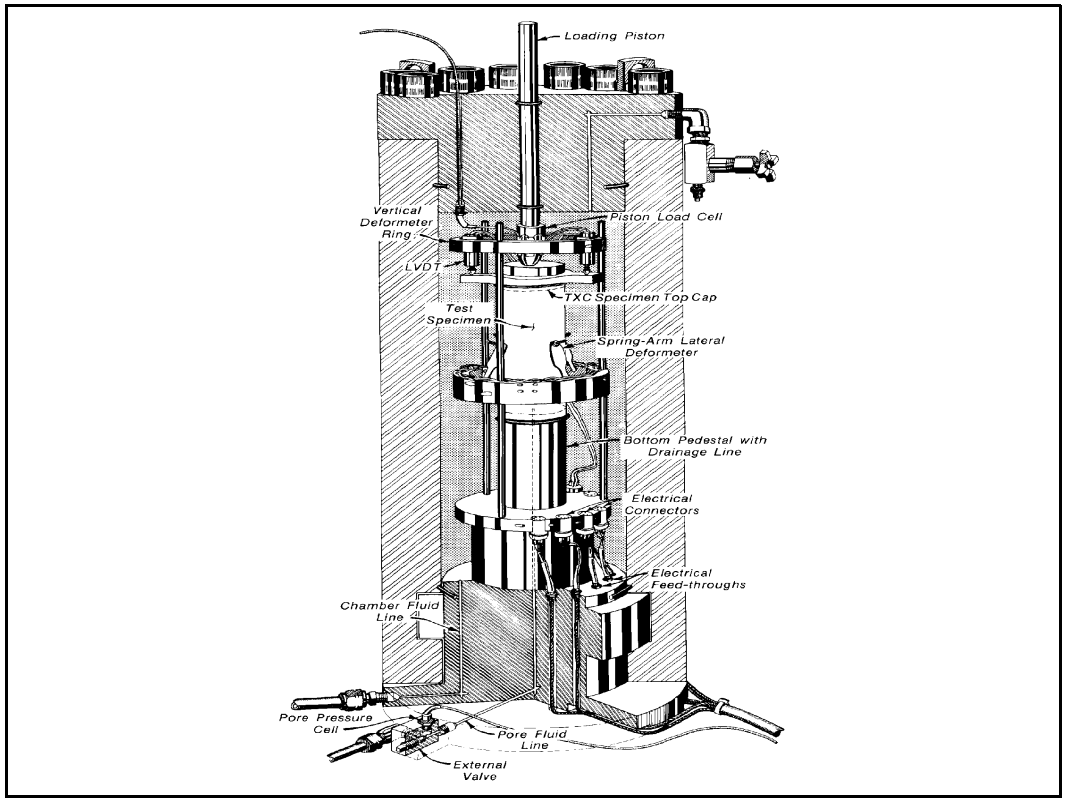

Figure 2.4. HPTX test device

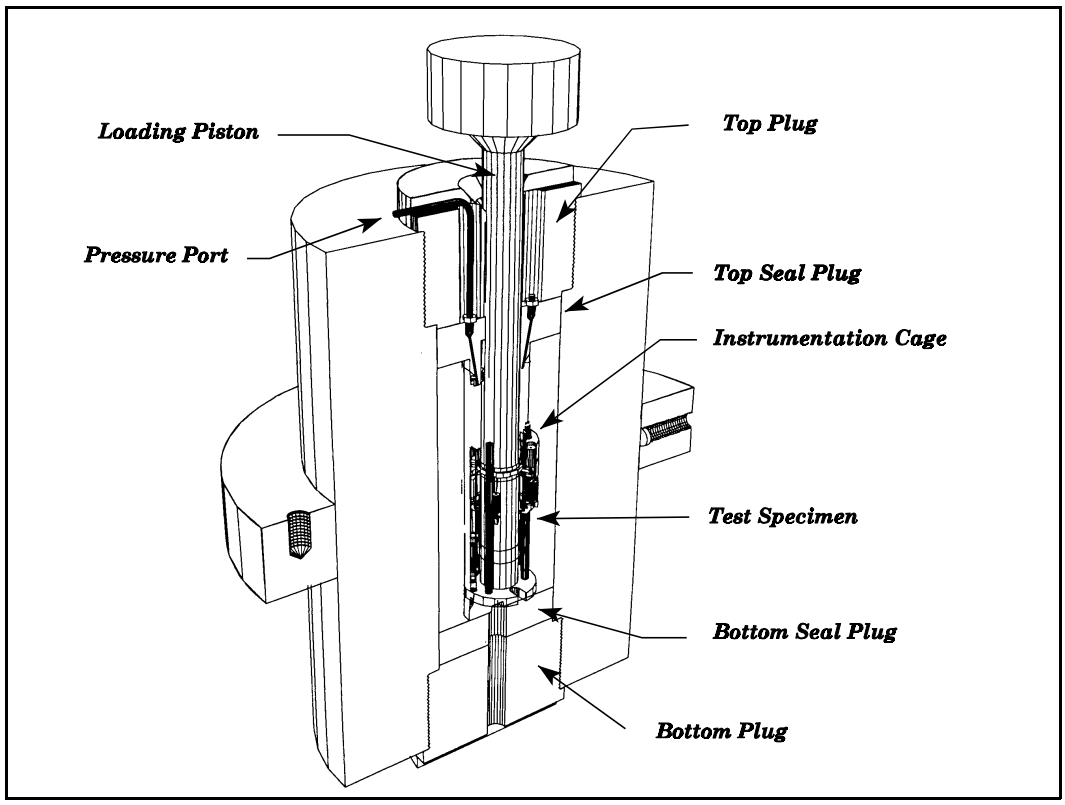

Figure 2.5. WES 6-kbar test device

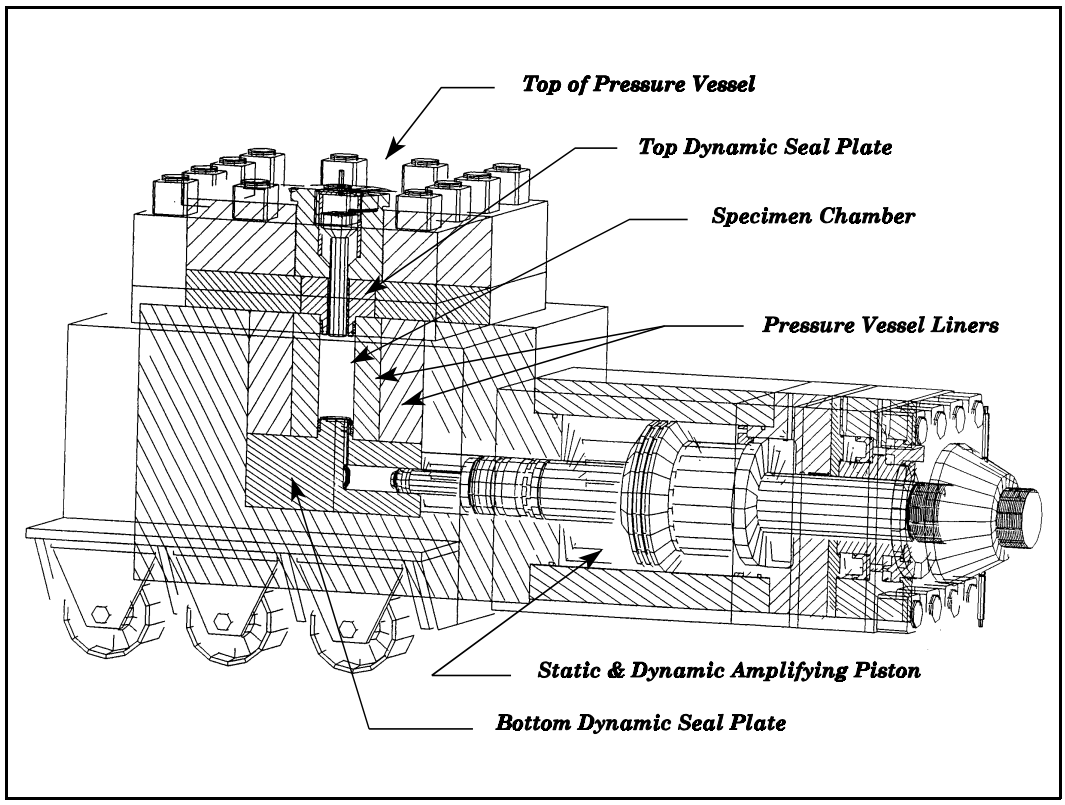

Figure 2.6. WES 10-kbar test device

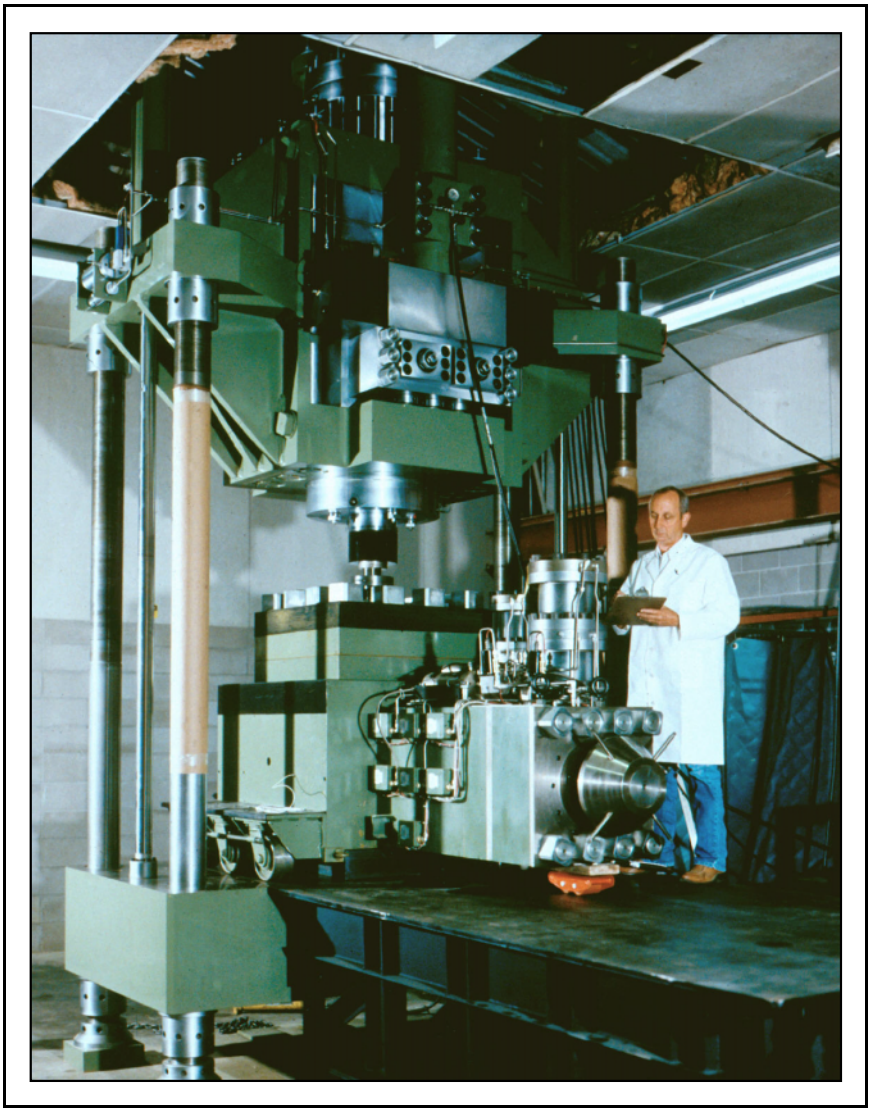

Figure 2.7. 9 MN dynamic loader and 1 GPa pressure vessel

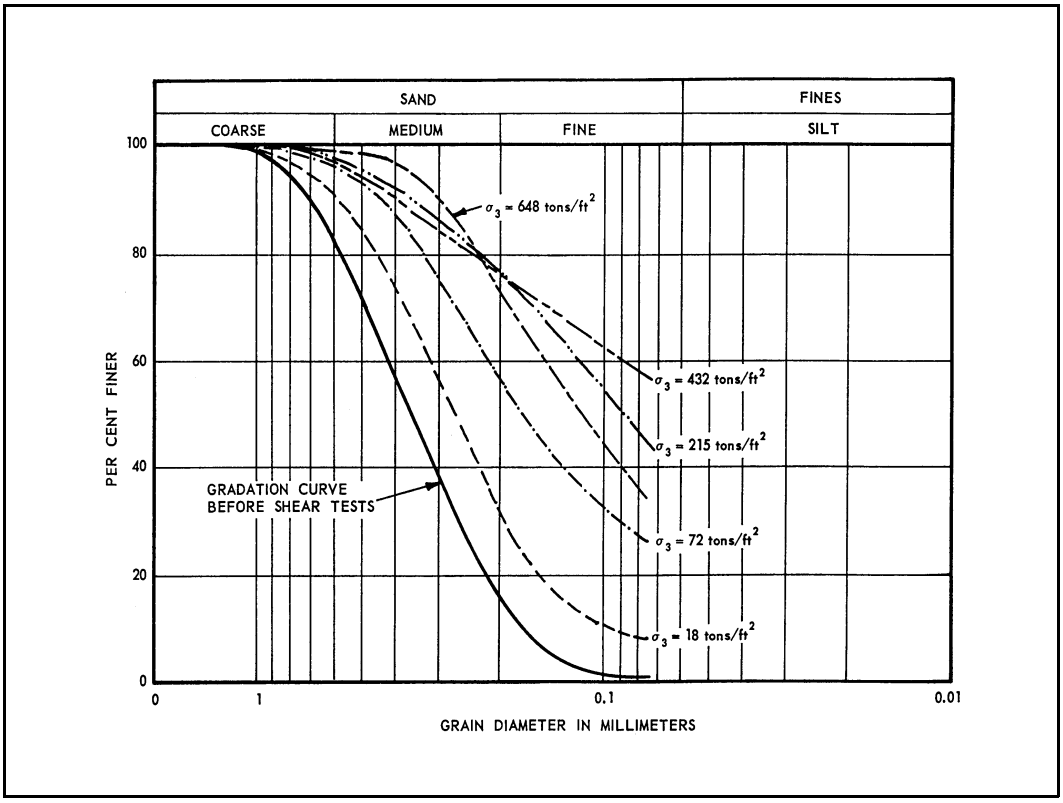

Figure 2.8. Changes in material grading due to triaxial compression testing (from Vesic and Barksdale 1963)

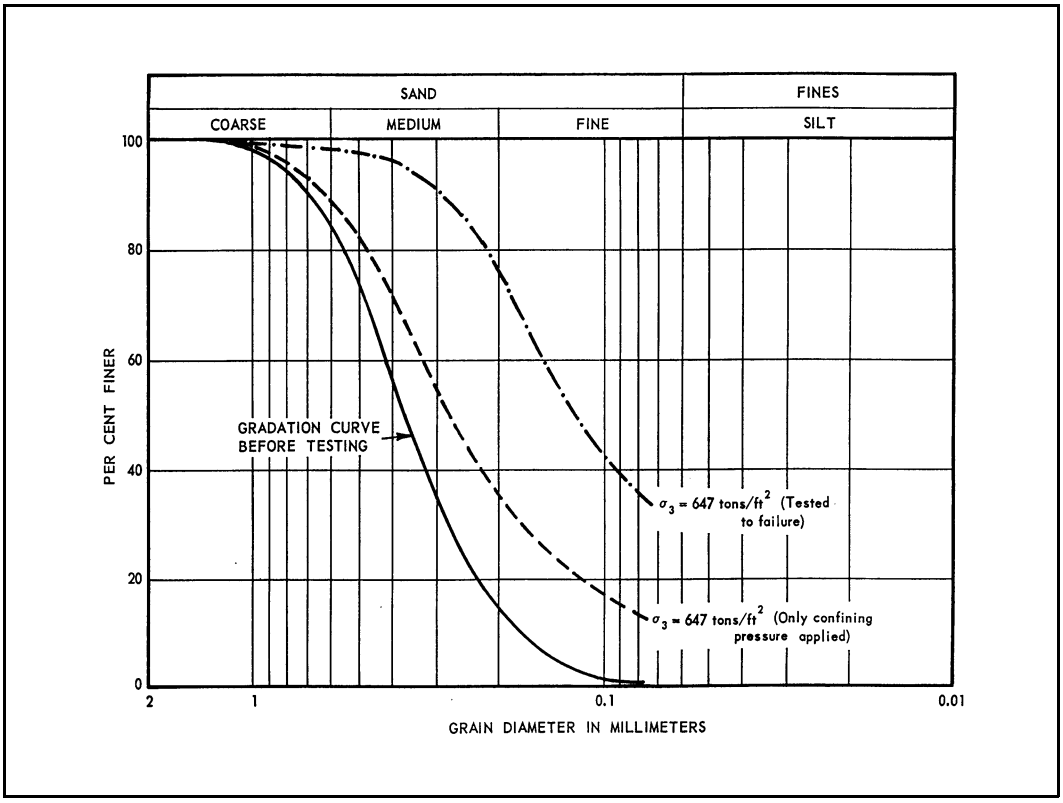

Figure 2.9. Comparison of posttest gradings from hydrostatic and triaxial compression tests (from Vesic and Barksdale 1963)

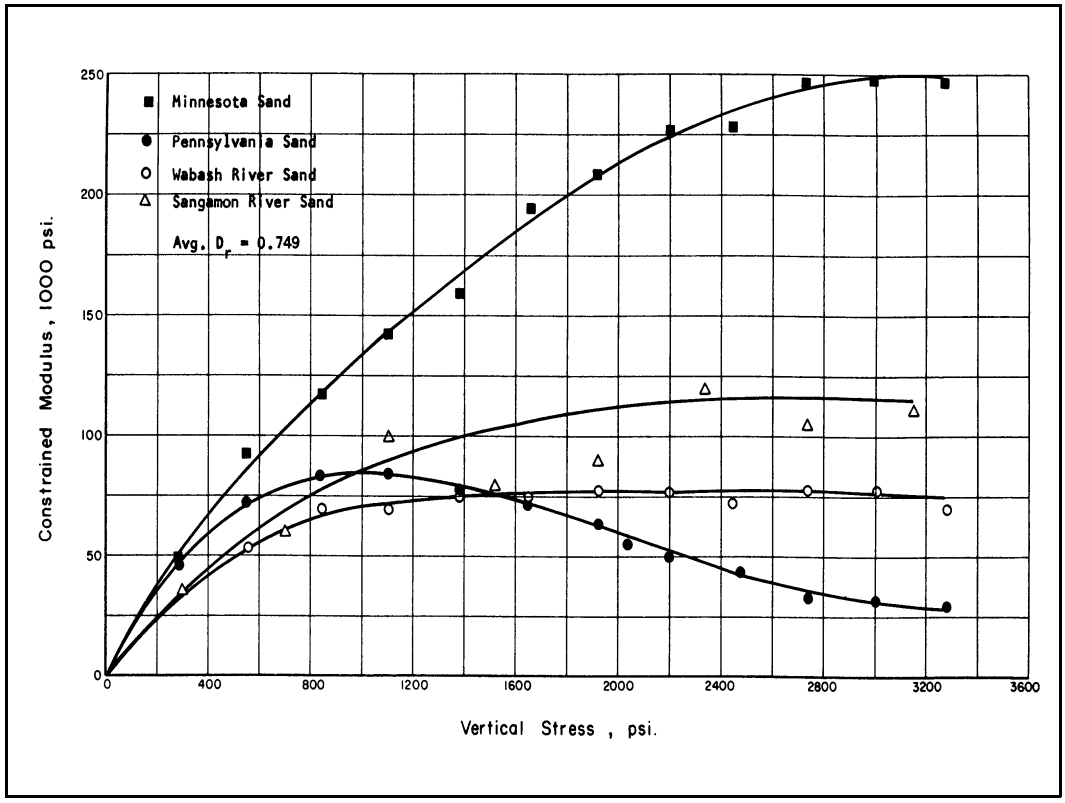

Figure 2.10 Constrained modulus versus vertical stress for four sands (from Hendron 1963)

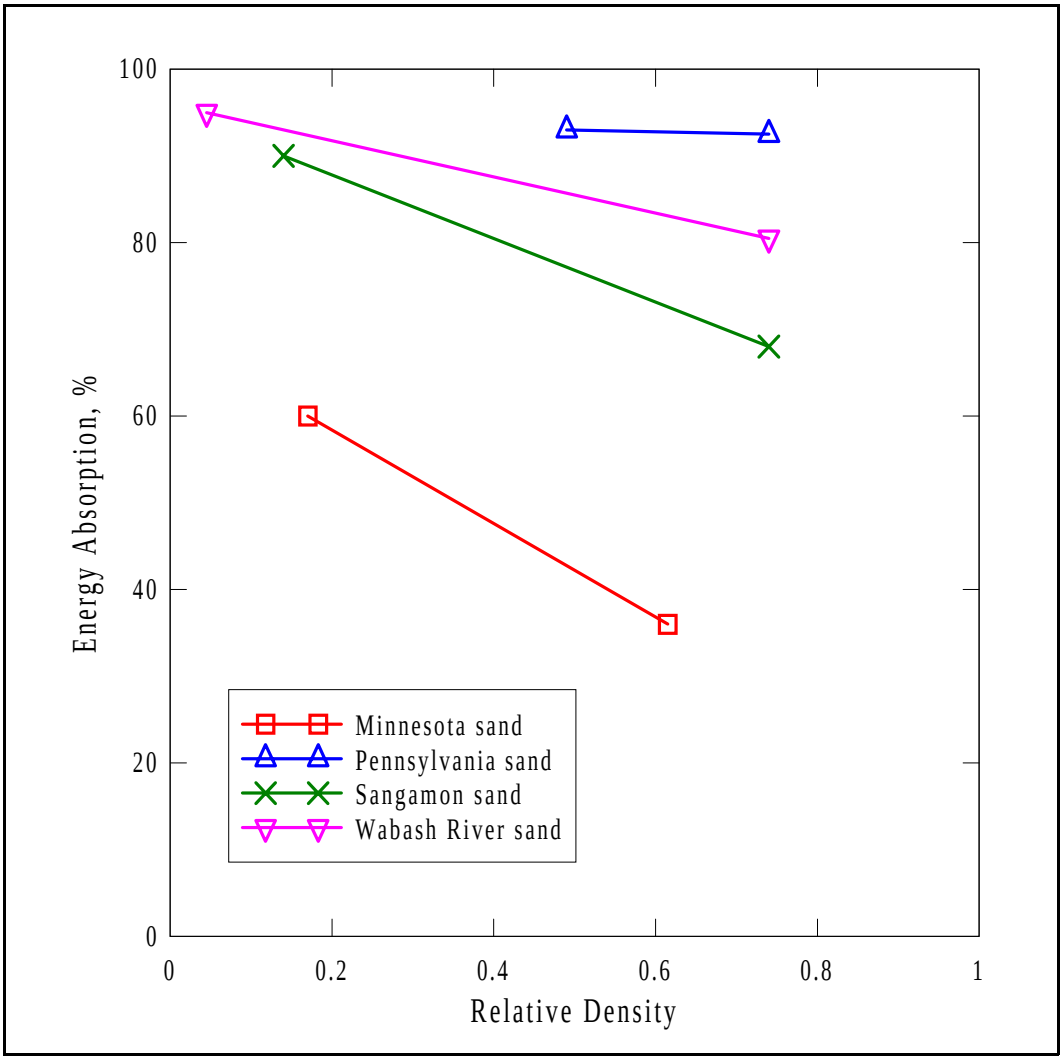

Figure 2.11. Energy absorption during the first cycle of loading as a function of relative density (after Hendron 1963)

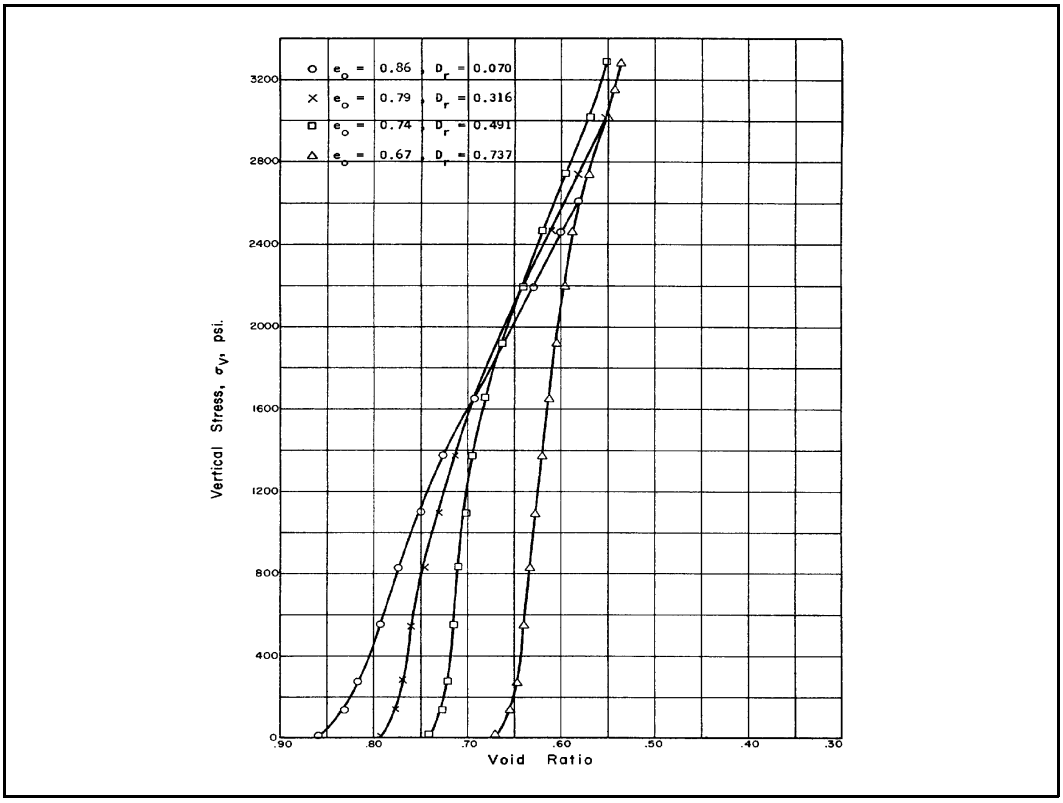

Figure 2.12. Variation in vertical stress versus void ratio during uniaxial strain loading (from Hendron 1963)

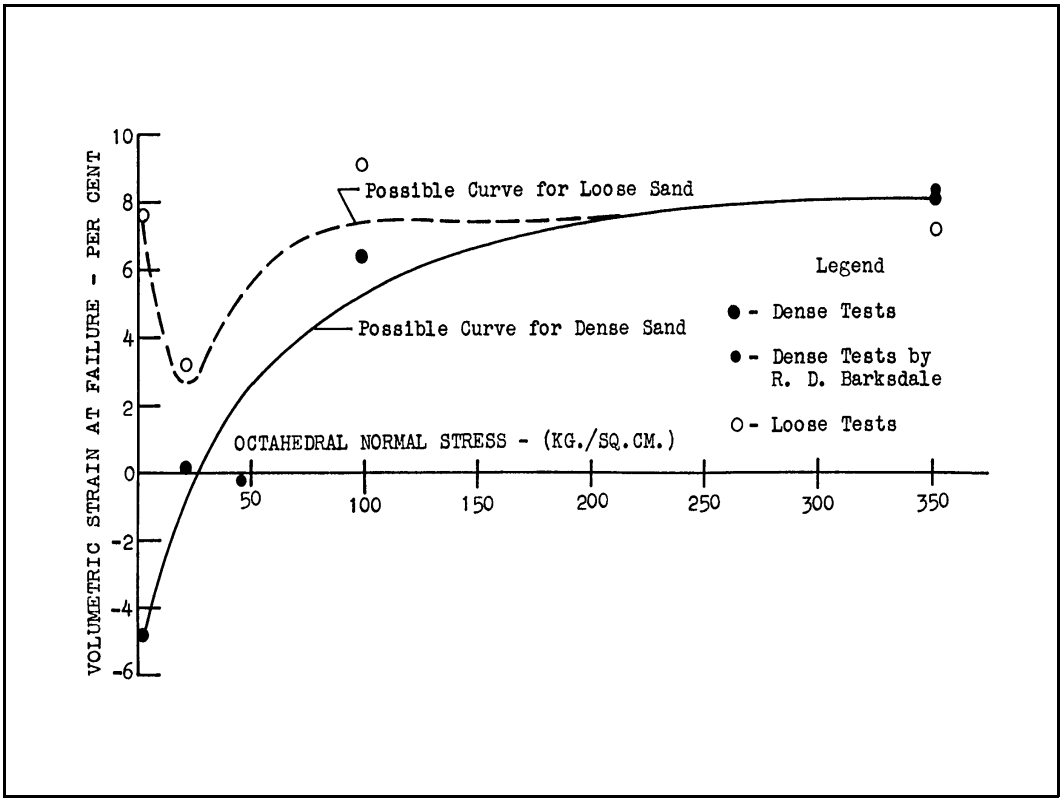

Figure 2.13. Volumetric strain at failure versus octahedral normal stress (from Clough 1964)

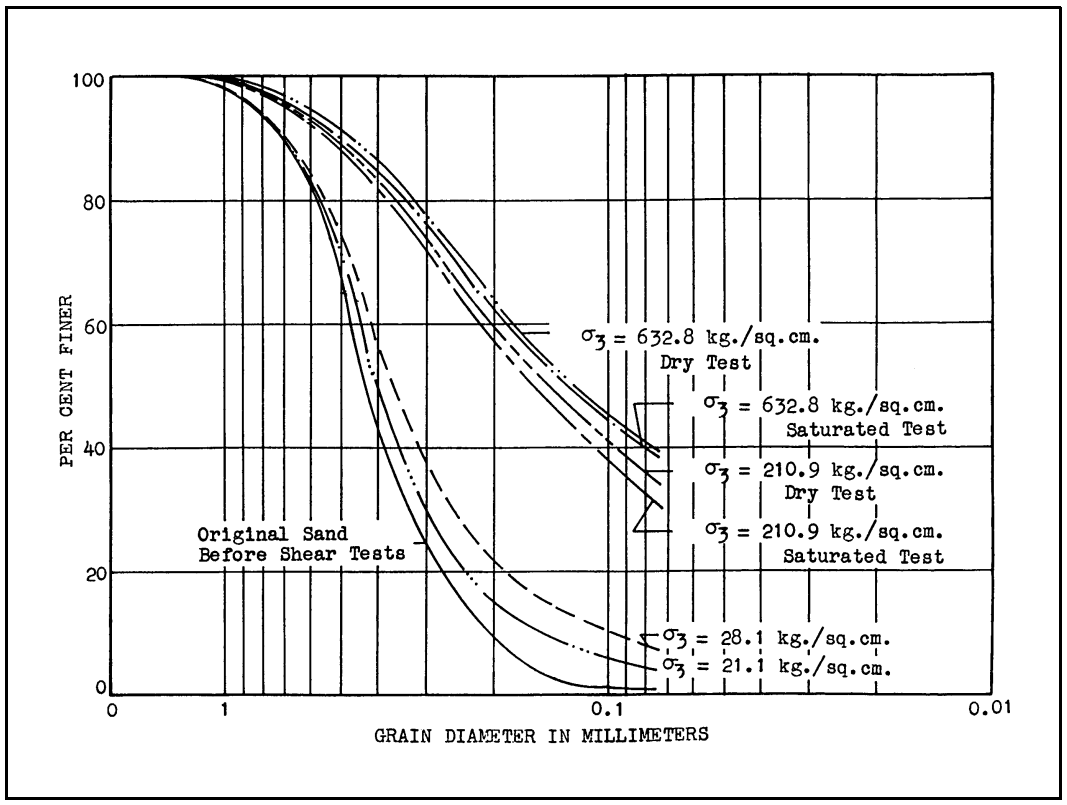

Figure 2.14. Changes in grading at various confining pressures (from Clough 1964)

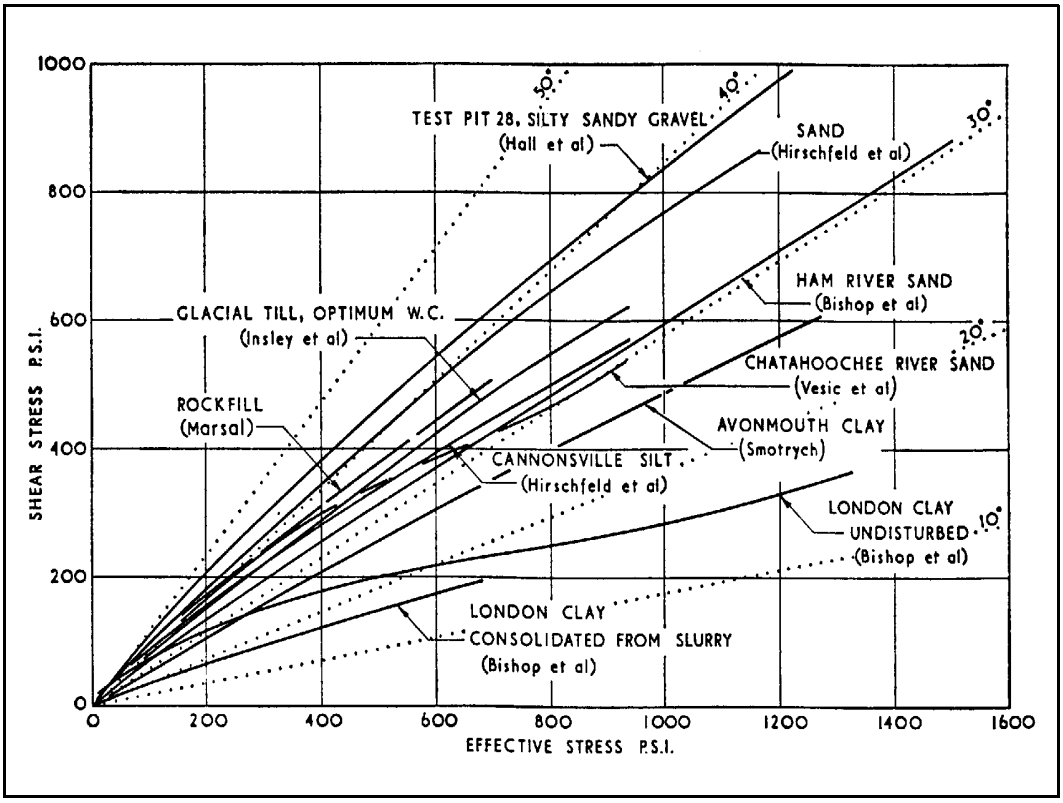

Figure 2.15. Failure envelopes for various soils (from Bishop 1965a)

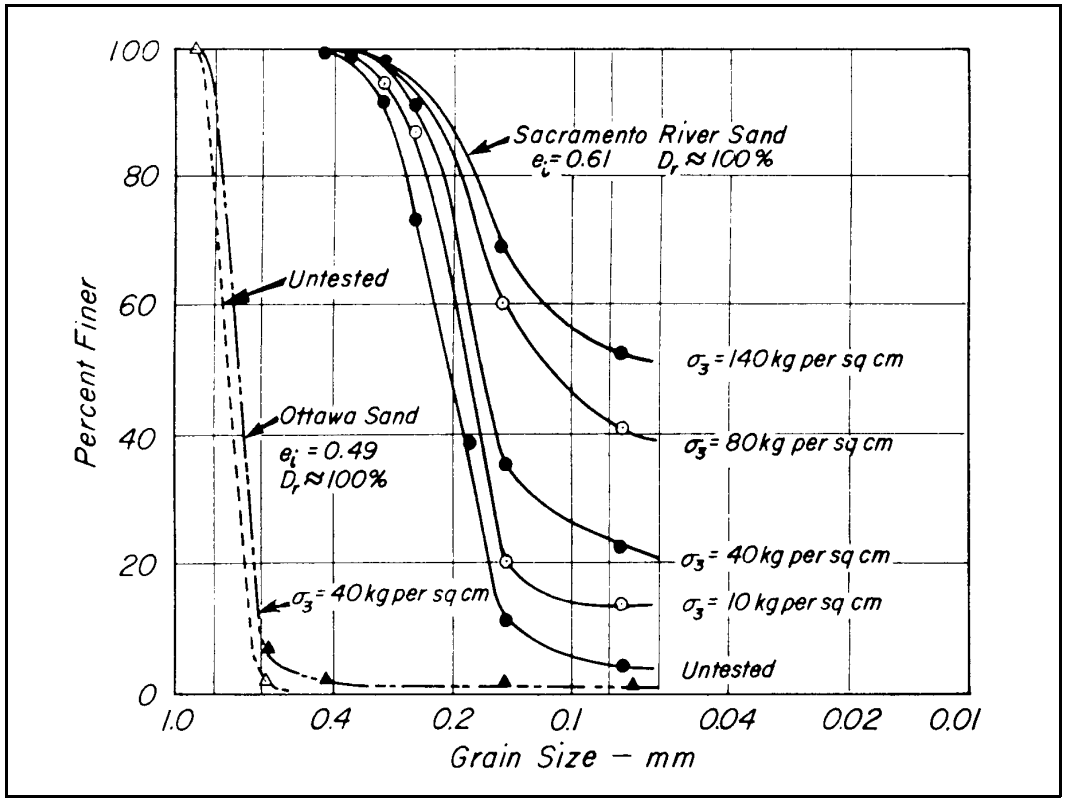

Figure 2.16. Changes in grading during drained triaxial compression tests (from Lee and Seed 1966)

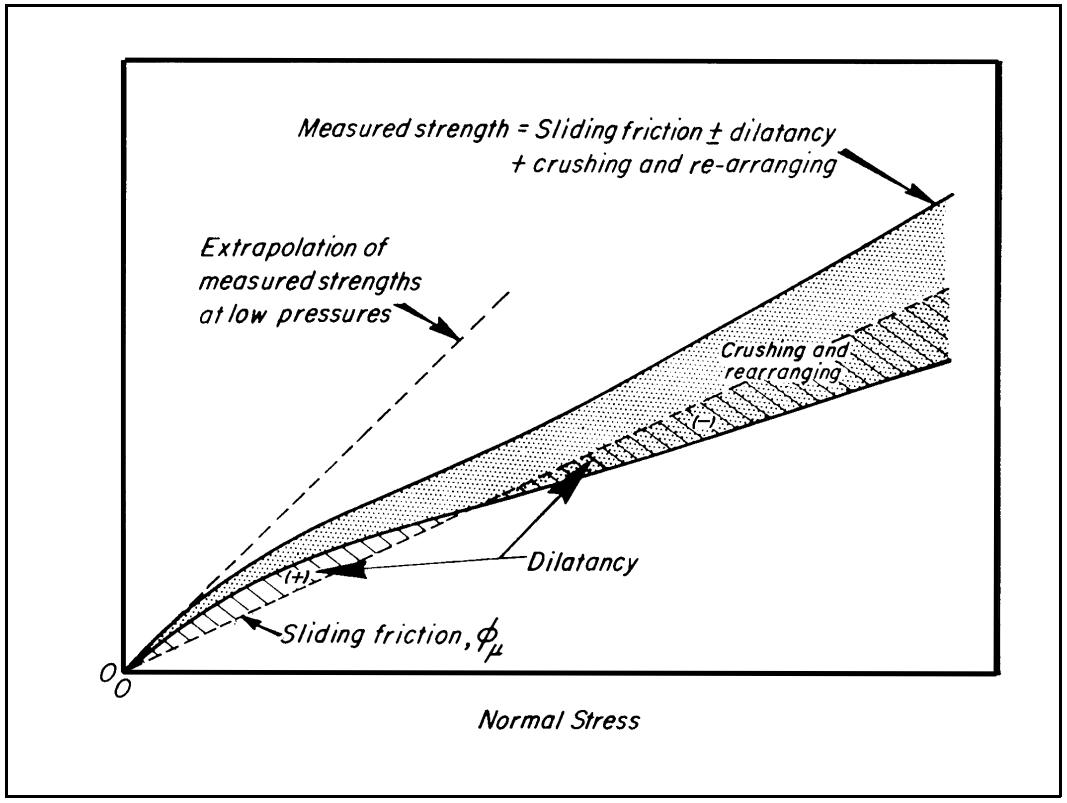

Figure 2.17. Strength components for drained triaxial compression tests on sand (from Lee and Seed 1966)

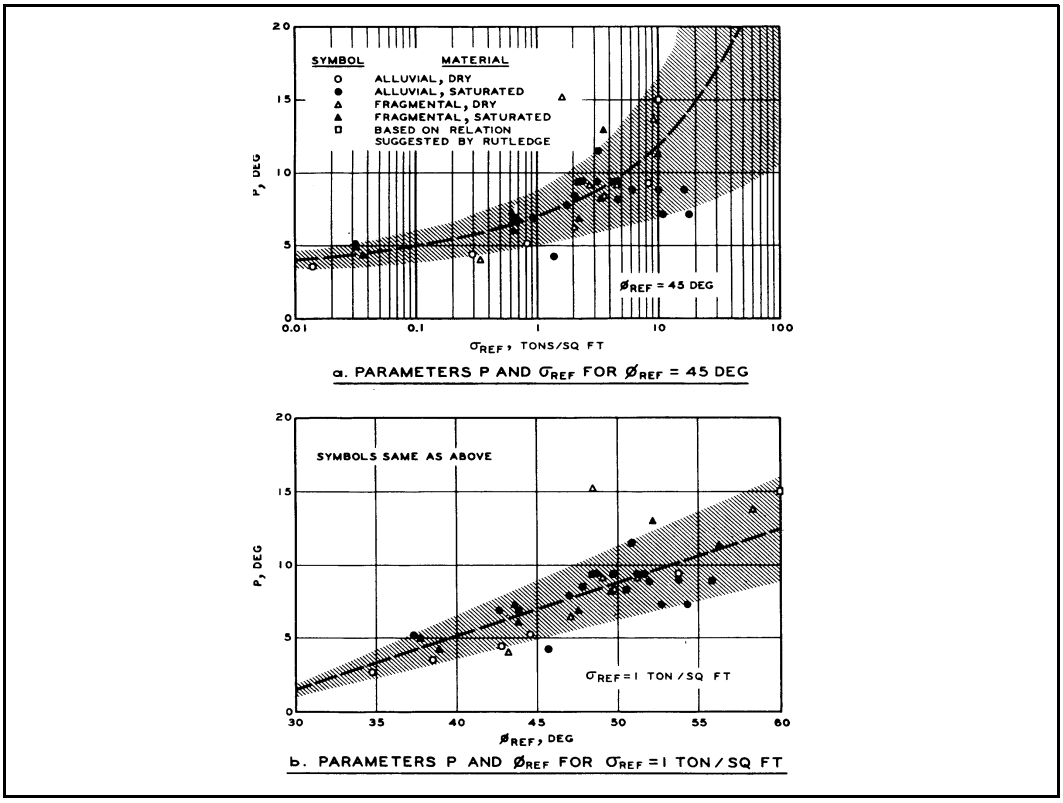

Figure 2.18. Summary of strength parameters (from Banks and MacIver 1969)

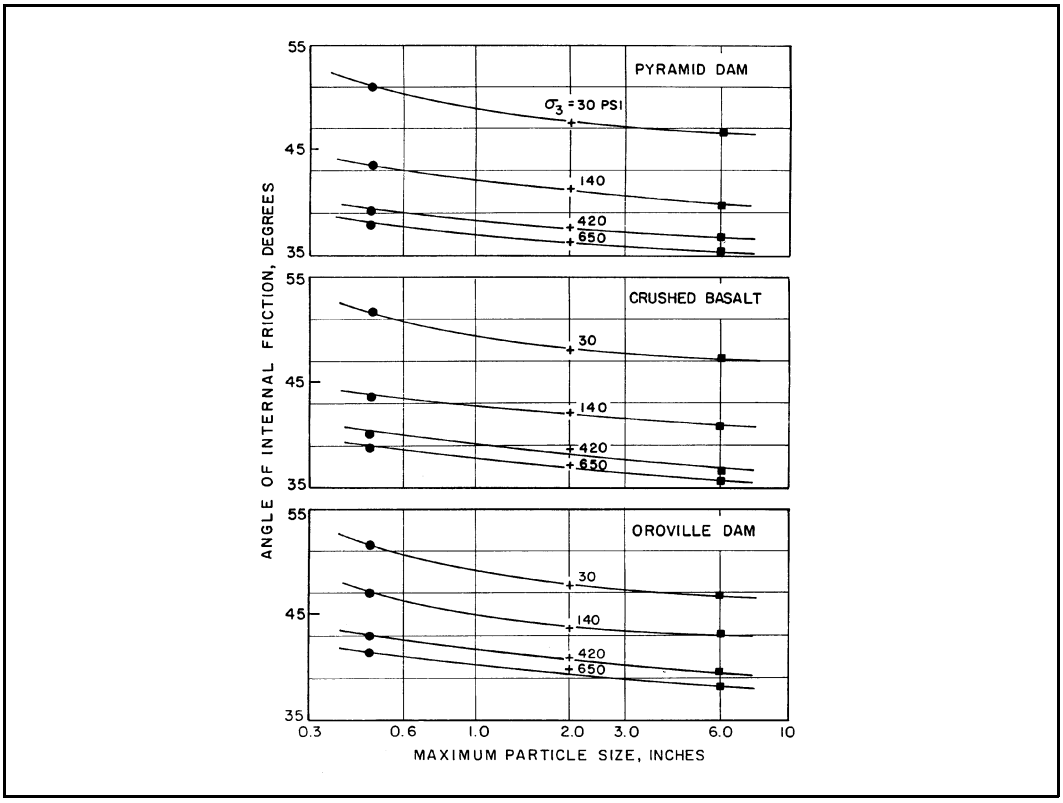

Figure 2.19. Effect of maximum particle size on angle of internal friction (from Marachi, et al. 1969)

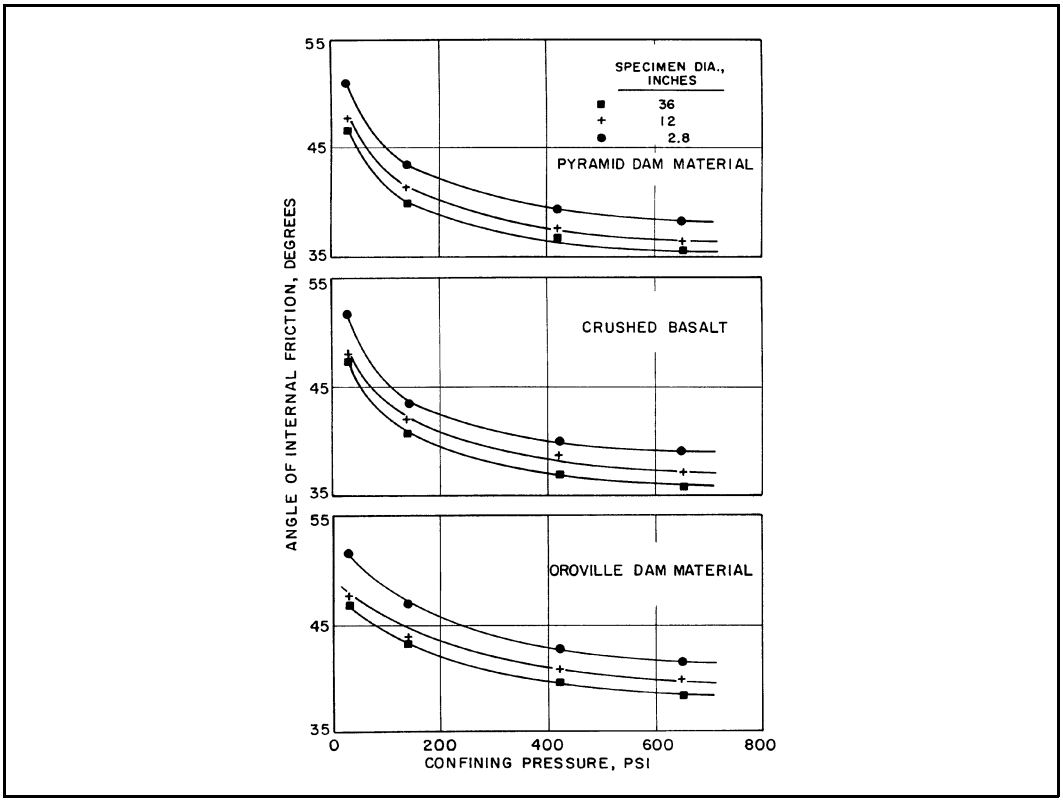

Figure 2.20. Effect of confining pressure on angle of internal friction (from Marachi, et al. 1969)

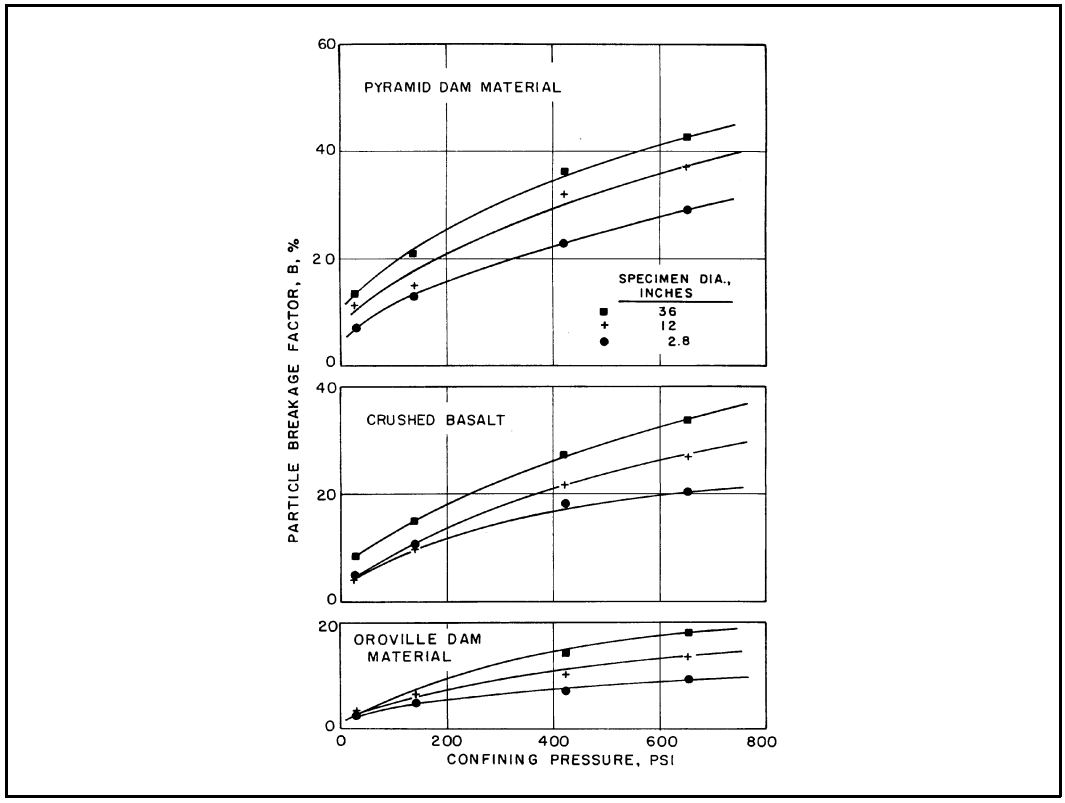

Figure 2.21 Particle breakage factor versus confining pressure (from Marachi, et al. 1969)

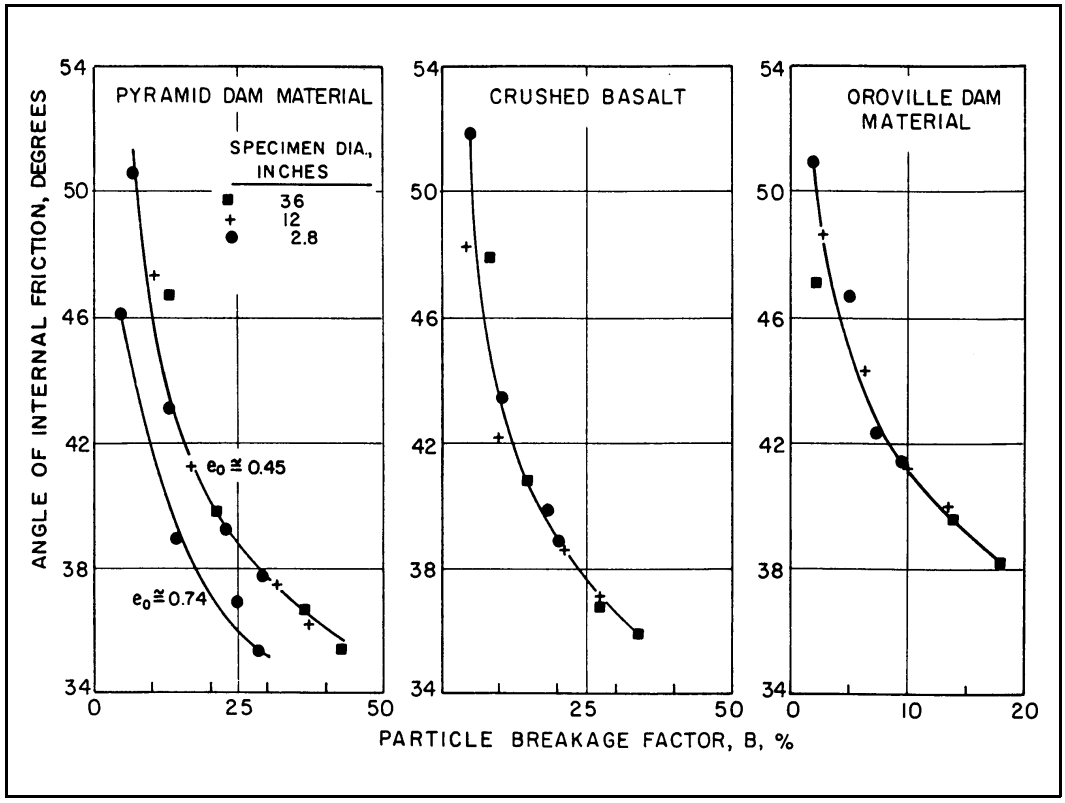

Figure 2.22 Angle of internal friction versus particle breakage factor (from Marachi, et al. 1969)

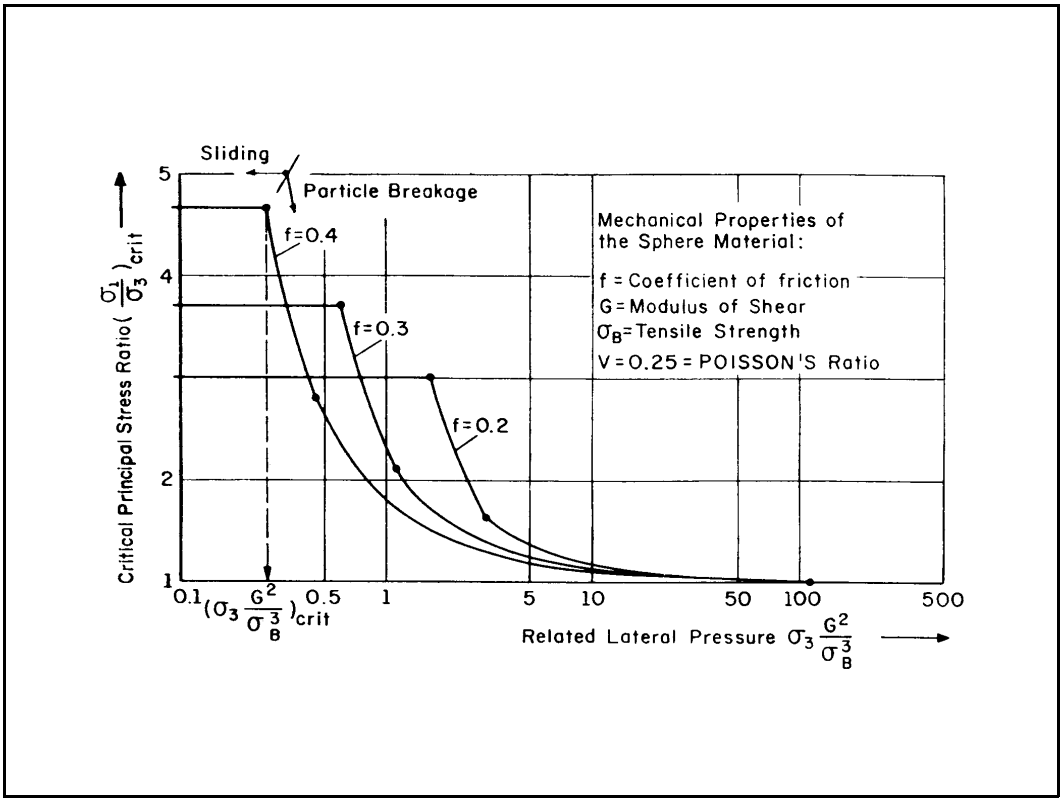

Figure 2.23. Critical stress states for densest packing of elastic-brittle spheres (from Leussink and Brauns 1969)

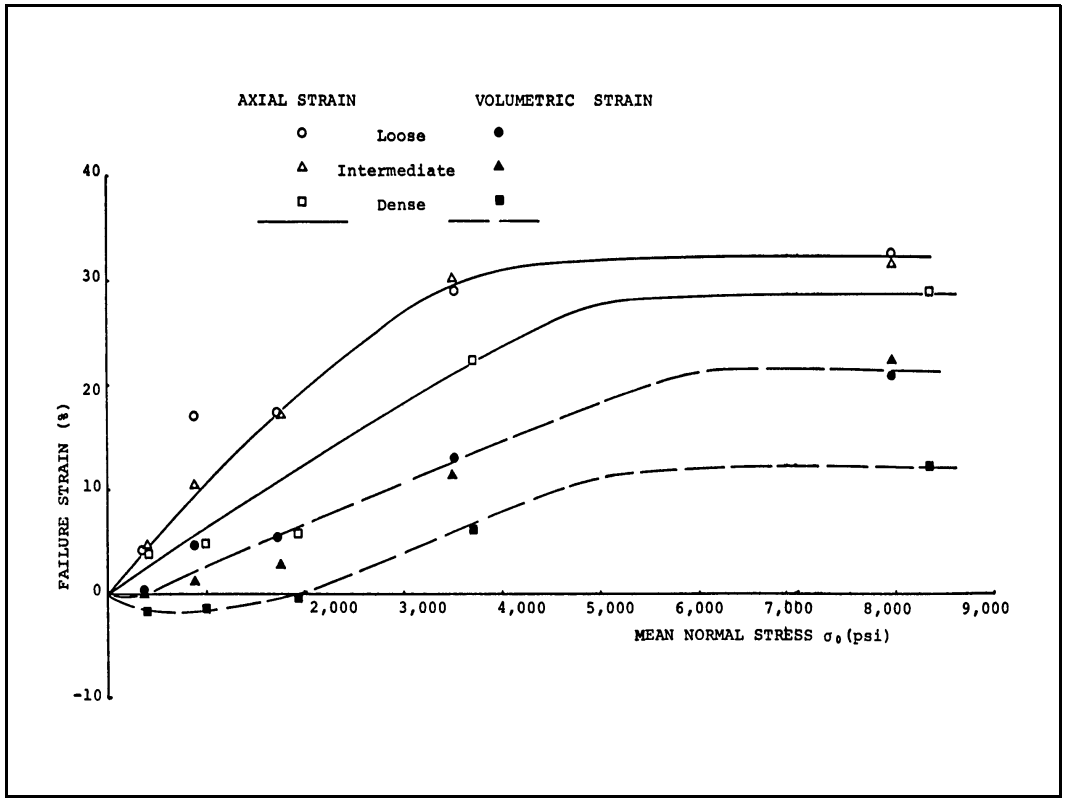

Figure 2.24 Failure strains versus mean normal stress for Ottawa sand (from Tai 1970)

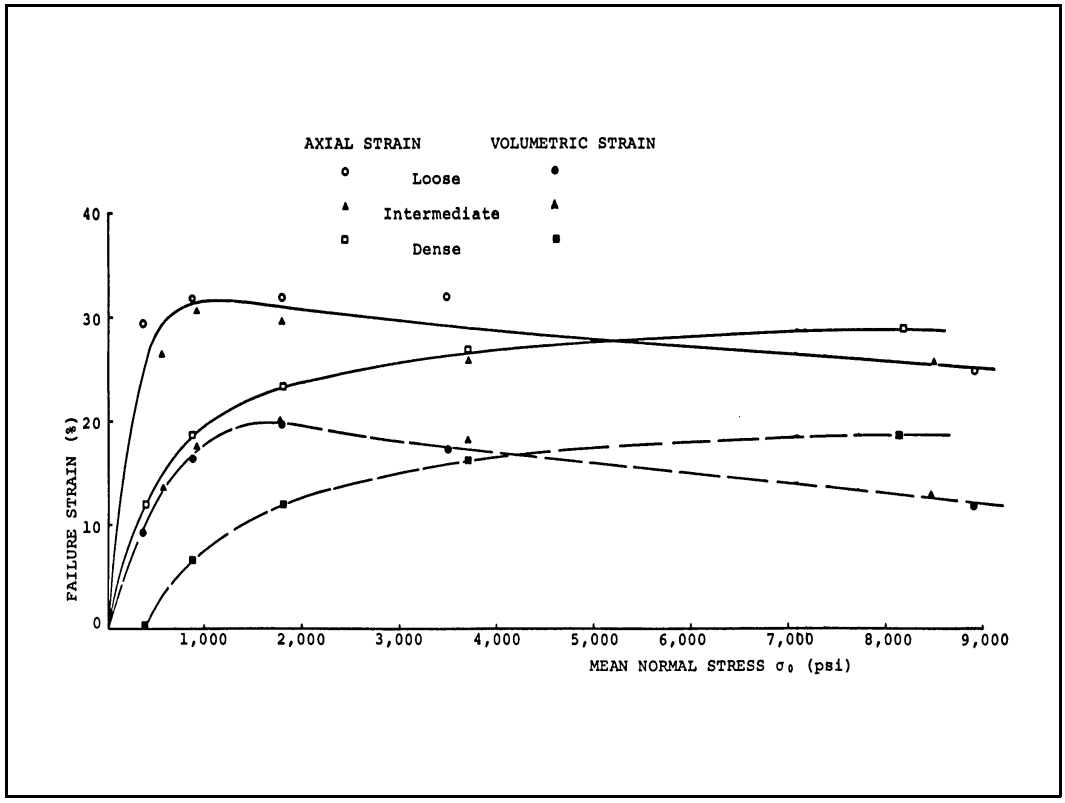

Figure 2.25 Failure strains versus mean normal stress for Chattahoochee River sand (from Tai 1970)

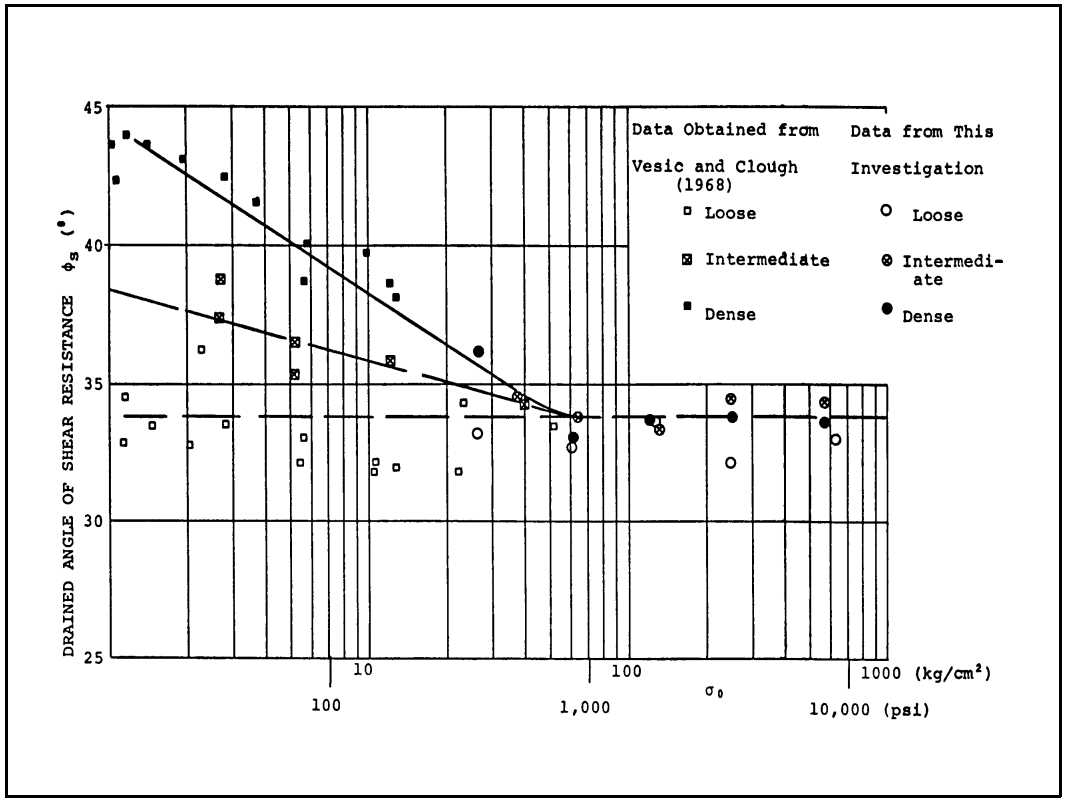

Figure 2.26. Secant friction angle versus mean normal stress for Chattahoochee River sand (from Tai 1970)

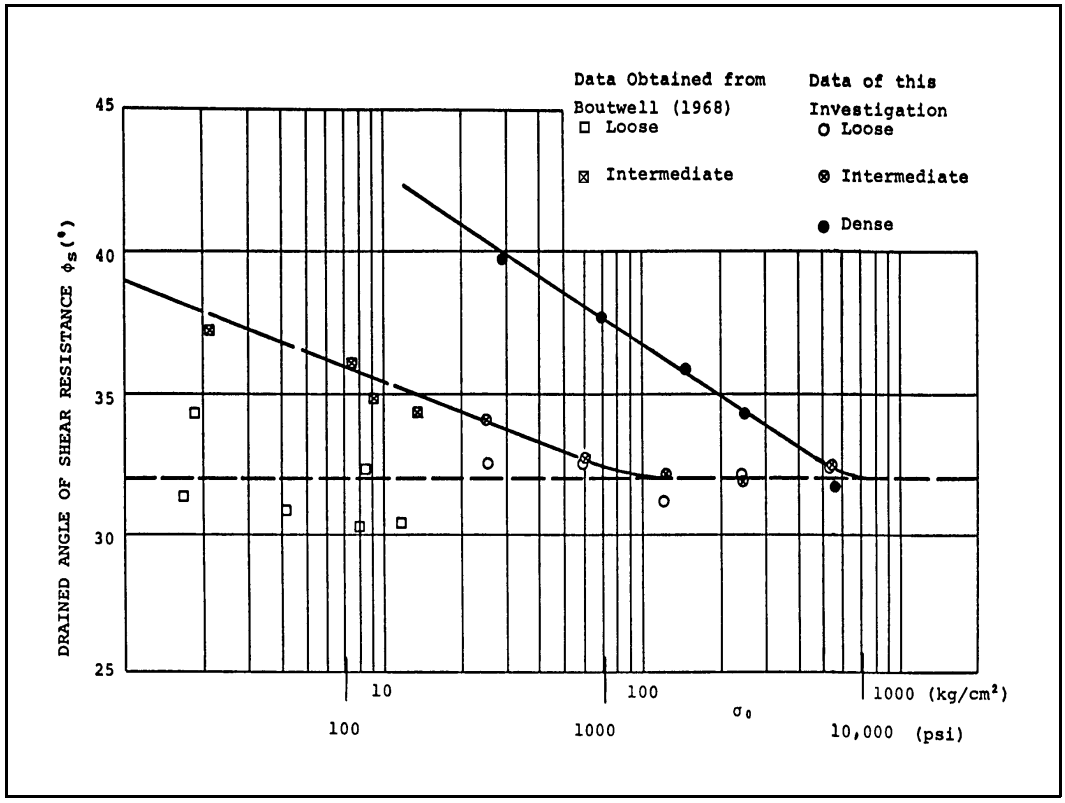

Figure 2.27. Secant friction angle versus mean normal stress for Ottawa sand (from Tai 1970)

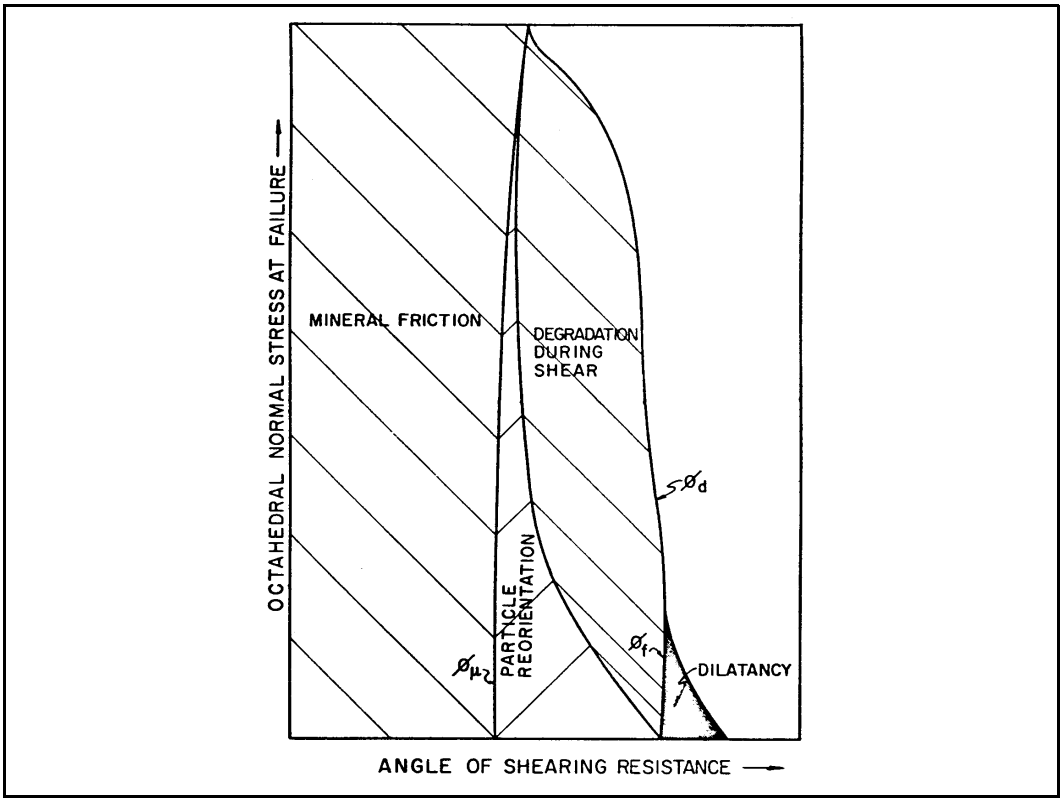

Figure 2.28. Components of shearing resistance for hard minerals (from Murphy 1970)

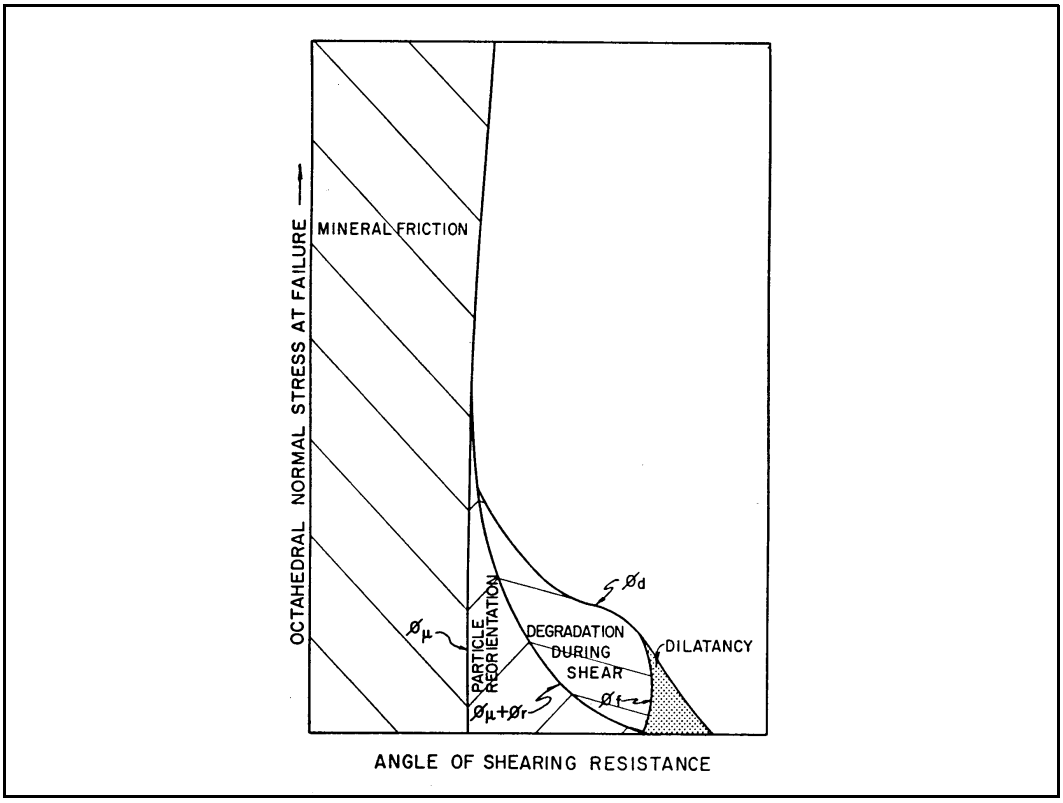

Figure 2.29. Components of shearing resistance for soft minerals (from Murphy 1970)

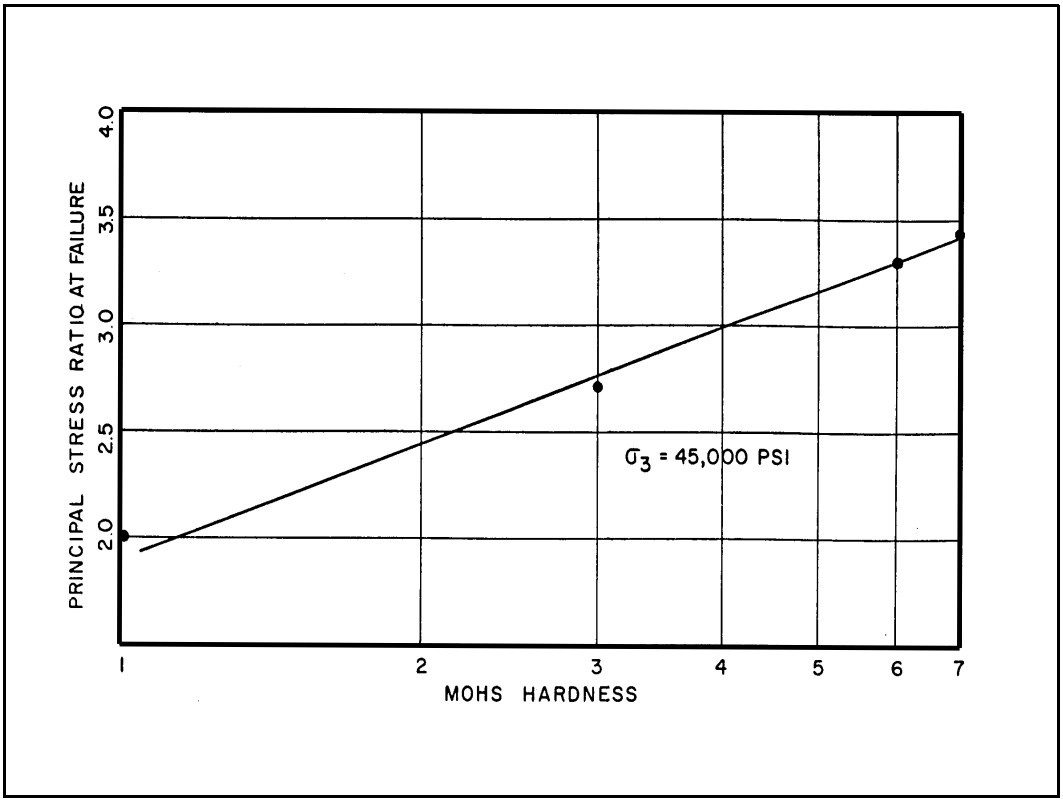

Figure 2.30. Strength versus hardness relationship (from Murphy 1970)

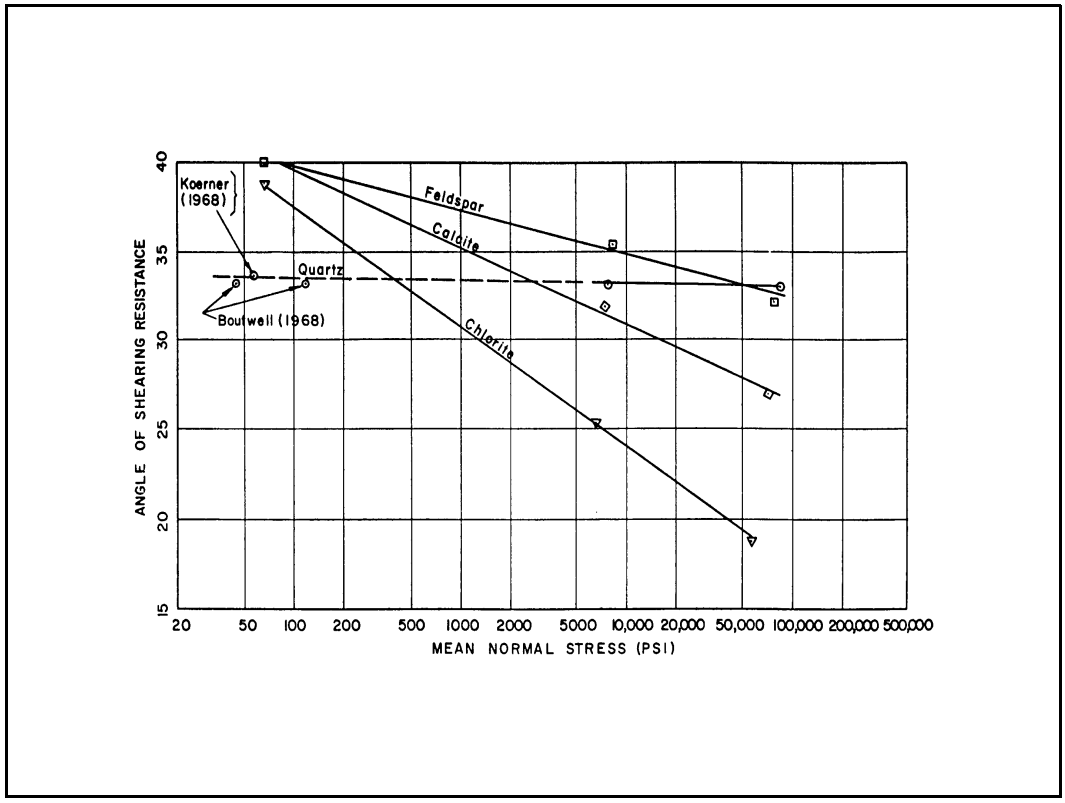

Figure 2.31. Secant friction angle versus mean normal stress (from Murphy 1970)

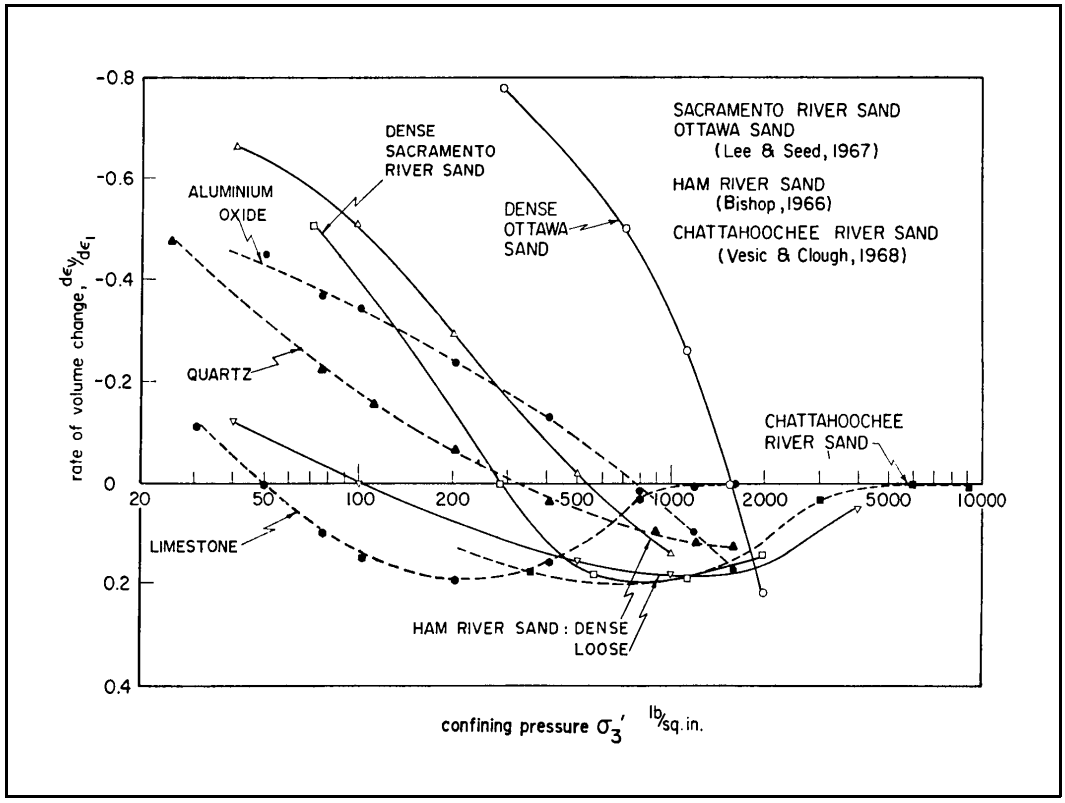

Figure 2.32. Relationship between dilantancy rate and confining pressure (from Lo and Roy 1973)

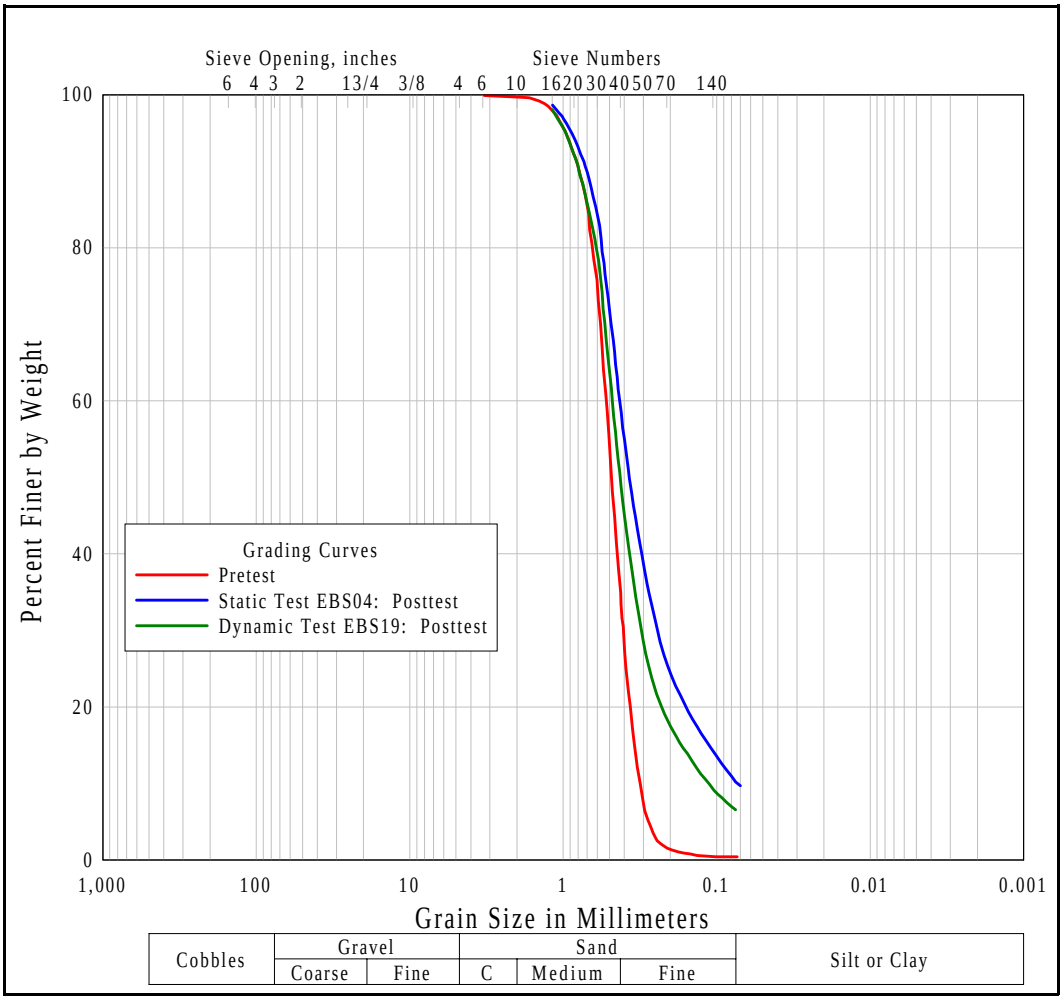

Figure 2.33. Beach sand grading curves

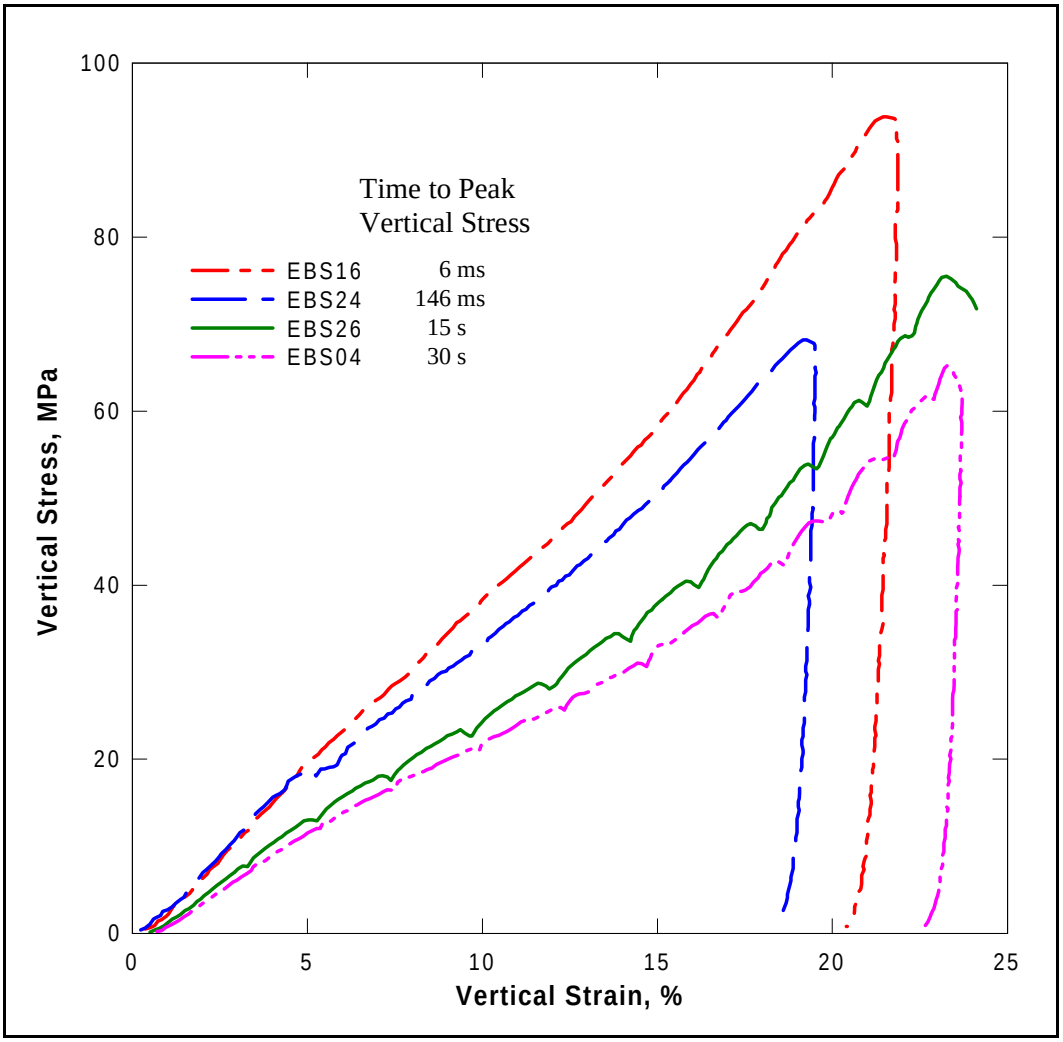

Figure 2.34. Beach sand UX stress-strain curves at four loading rates

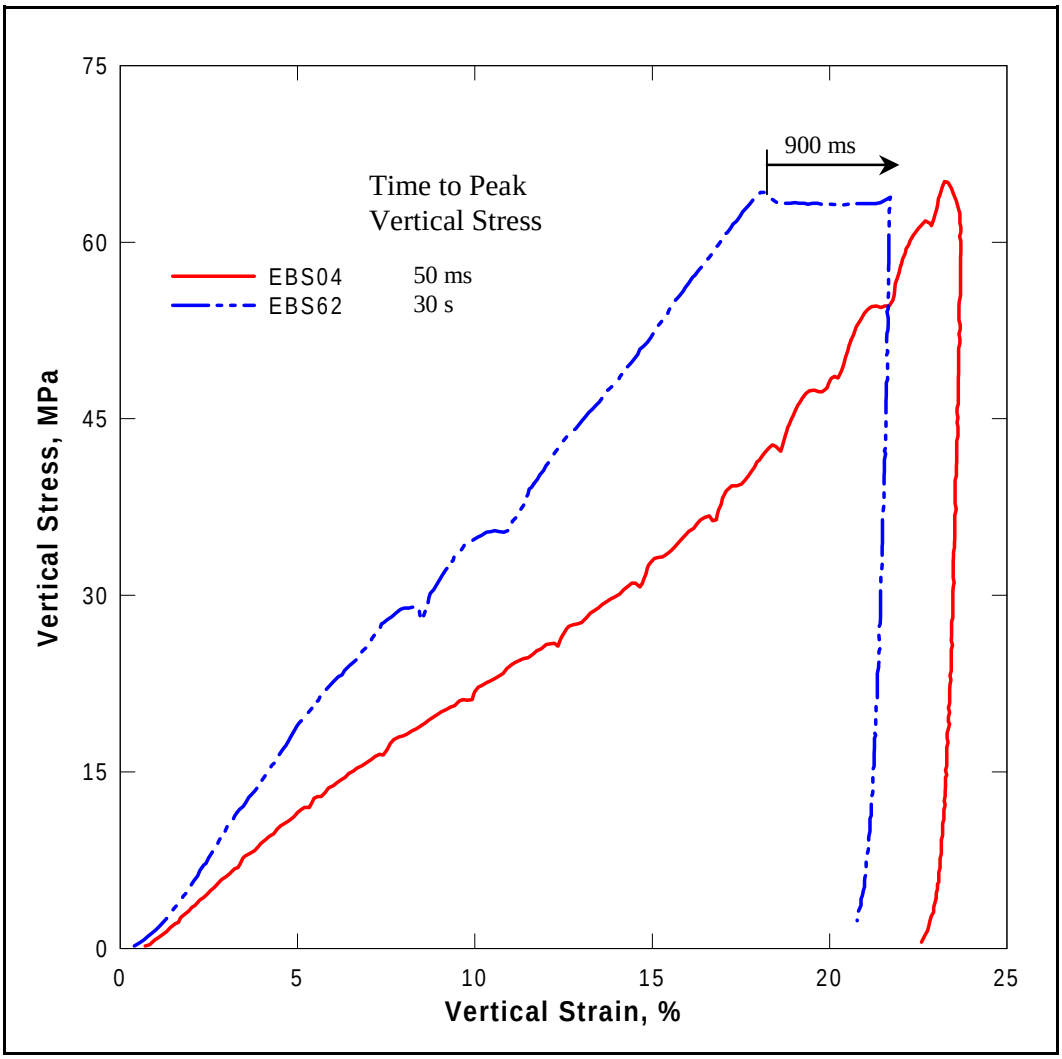

Figure 2.35. Beach sand static and dynamic UX stress-strain curves

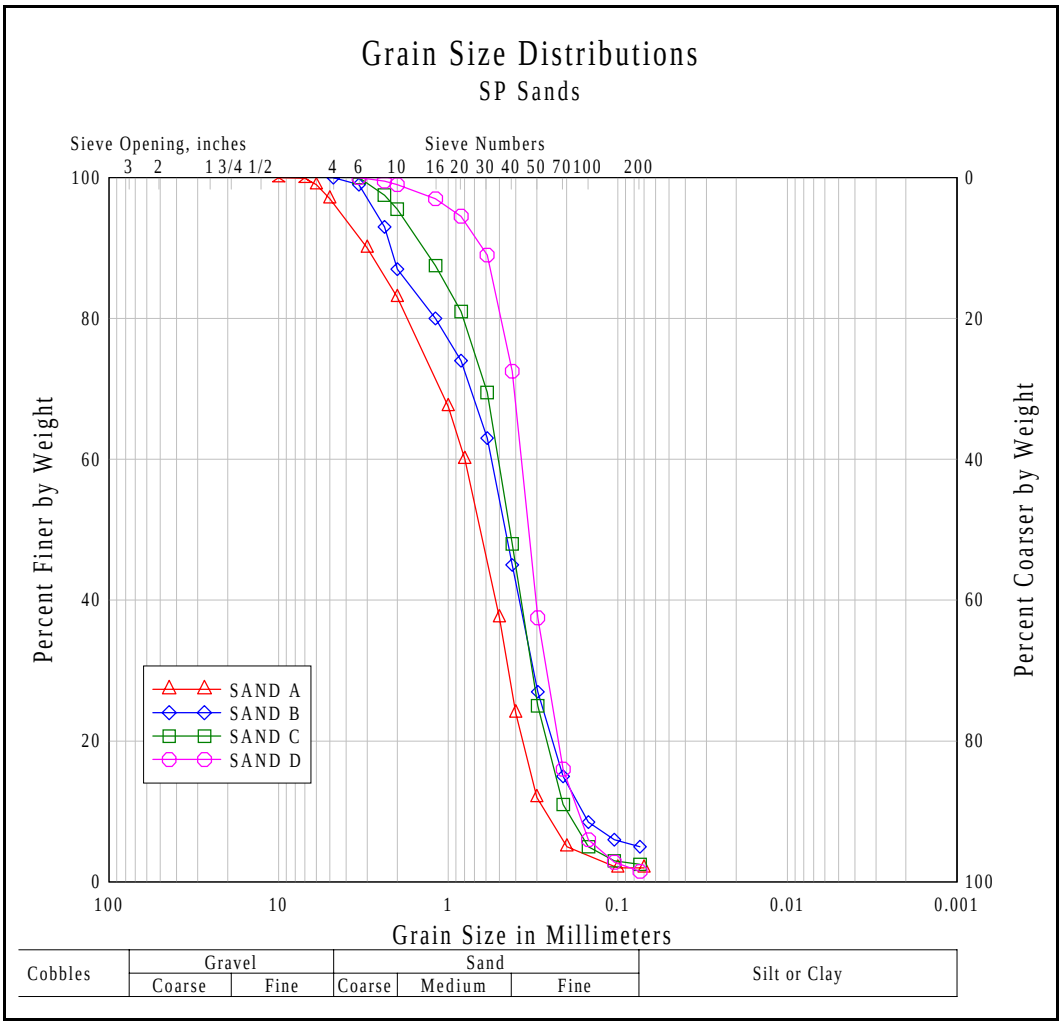

Figure 2.36. Grading curves for Sands A-D

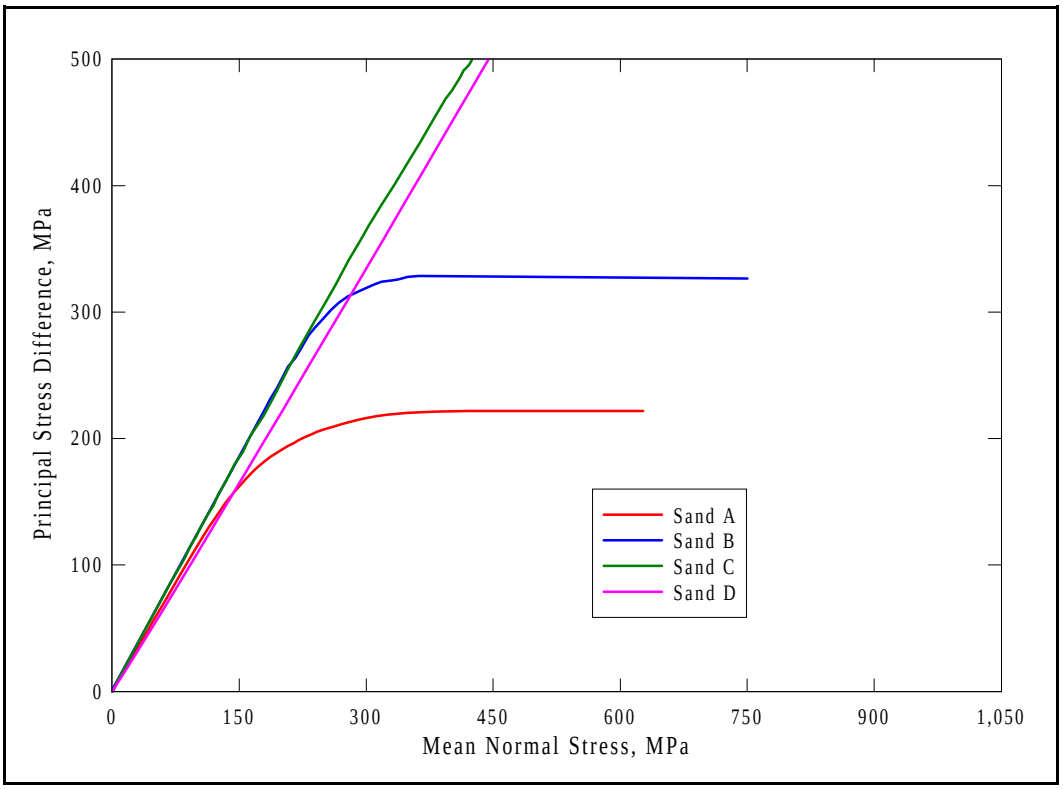

Figure 2.37. Failure envelopes for Sands A-D

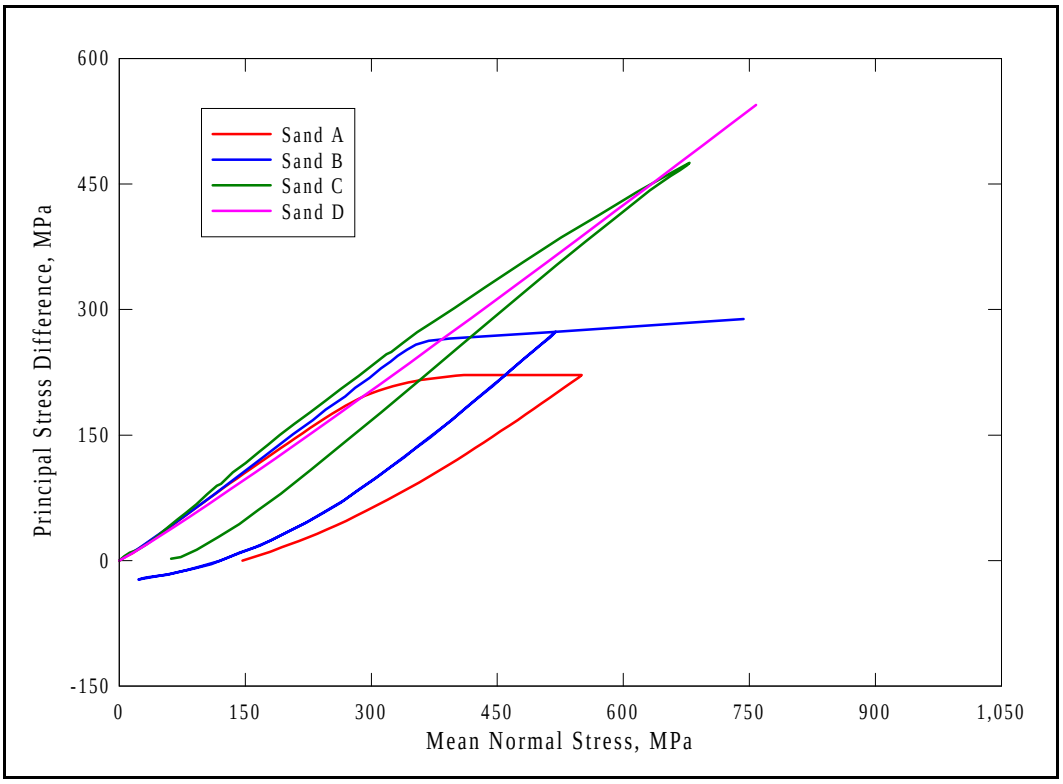

Figure 2.38. K_o stress paths for Sands A-D

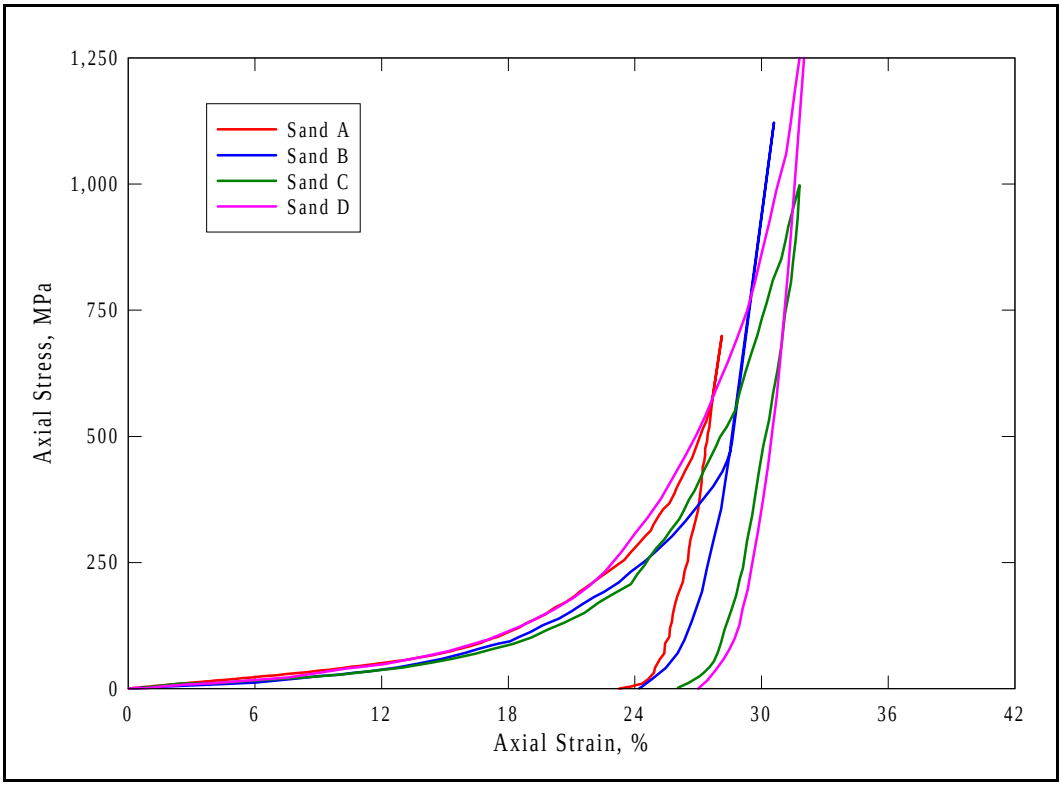

Figure 2.39. K_o stress-strain curves for Sands A-D

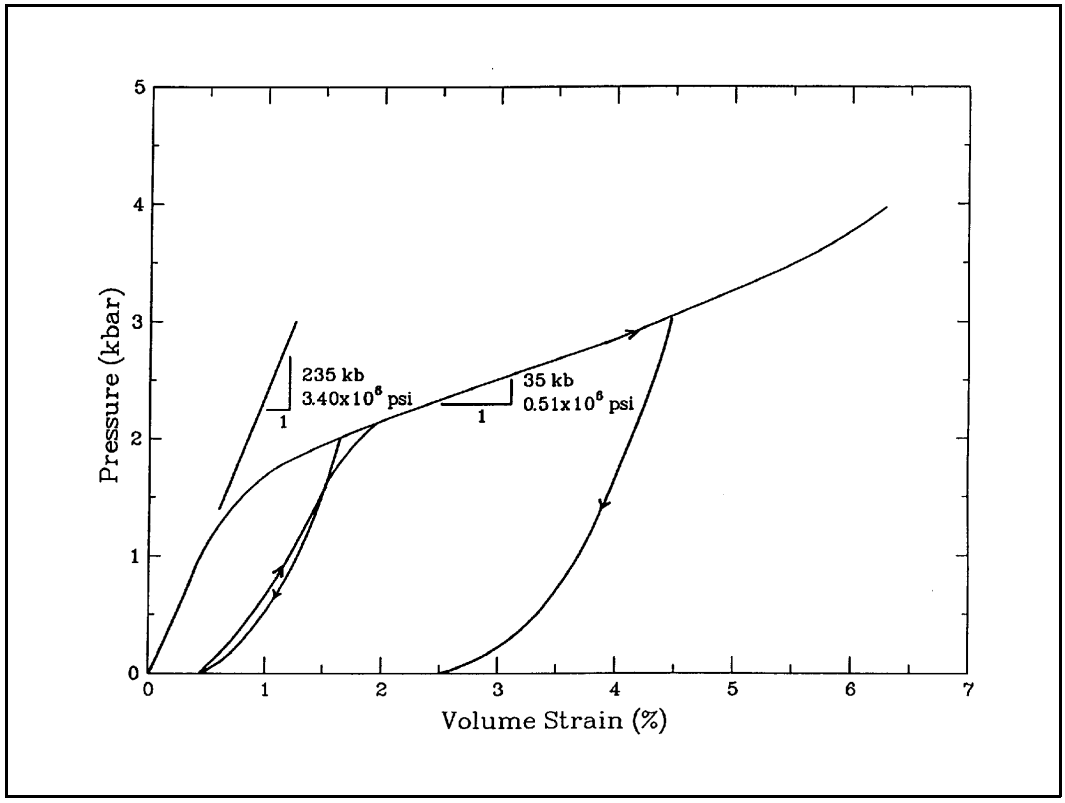

Figure 2.40. Drained pressure-volume response for Salem limestone (from Chitty and Blouin 1993)

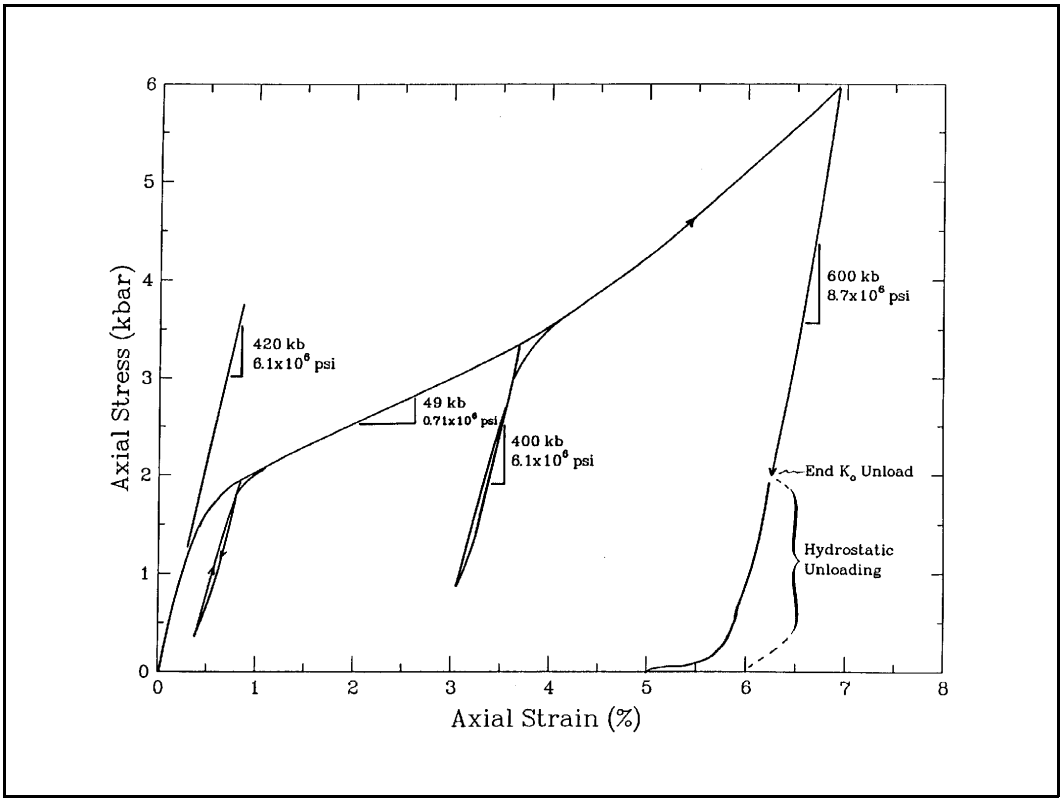

Figure 2.41. Drained K_o stress-strain response for Salem limestone (from Chitty and Blouin 1993)

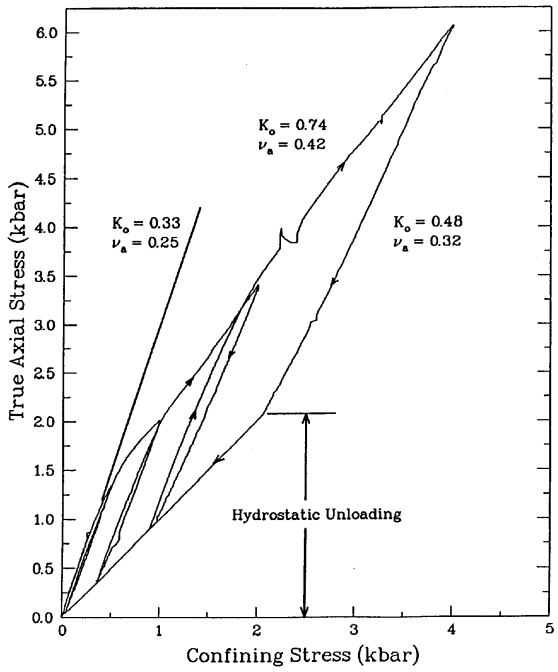

Figure 2.42. Drained K_o stress-path response for Salem limestone (from Chitty and Blouin 1993)

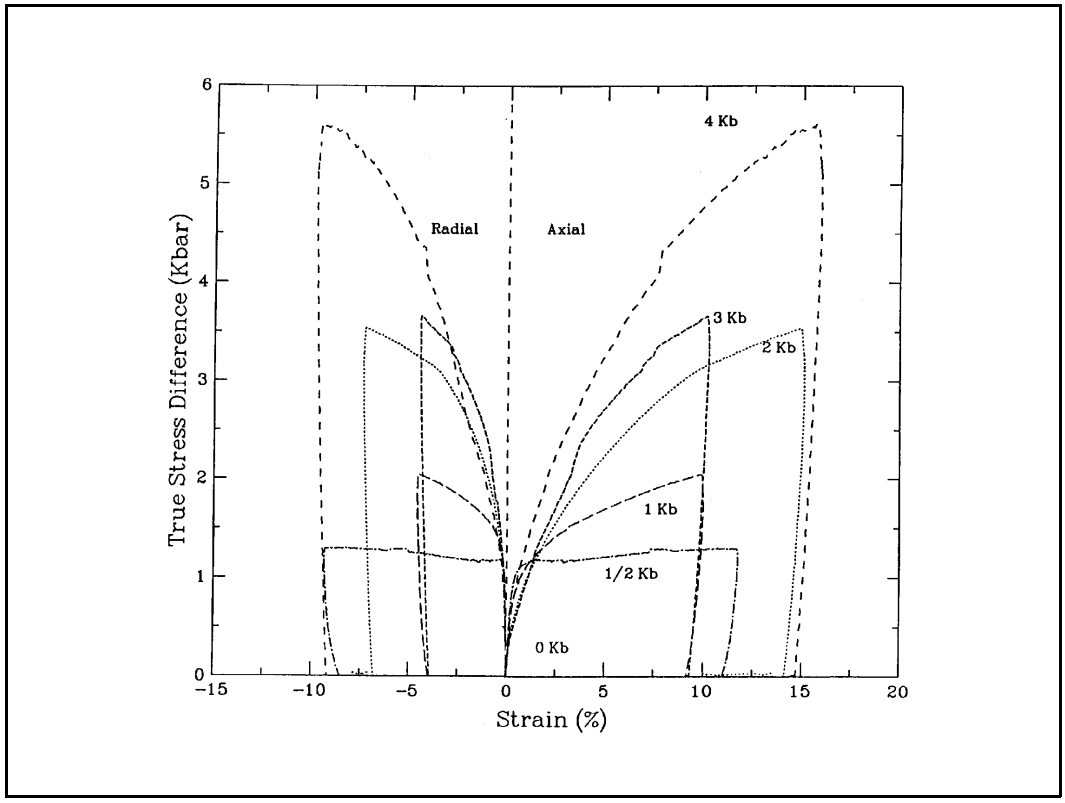

Figure 2.43. Stress-strain responses from drained Salem limestone TX tests (from Chitty and Blouin 1993)

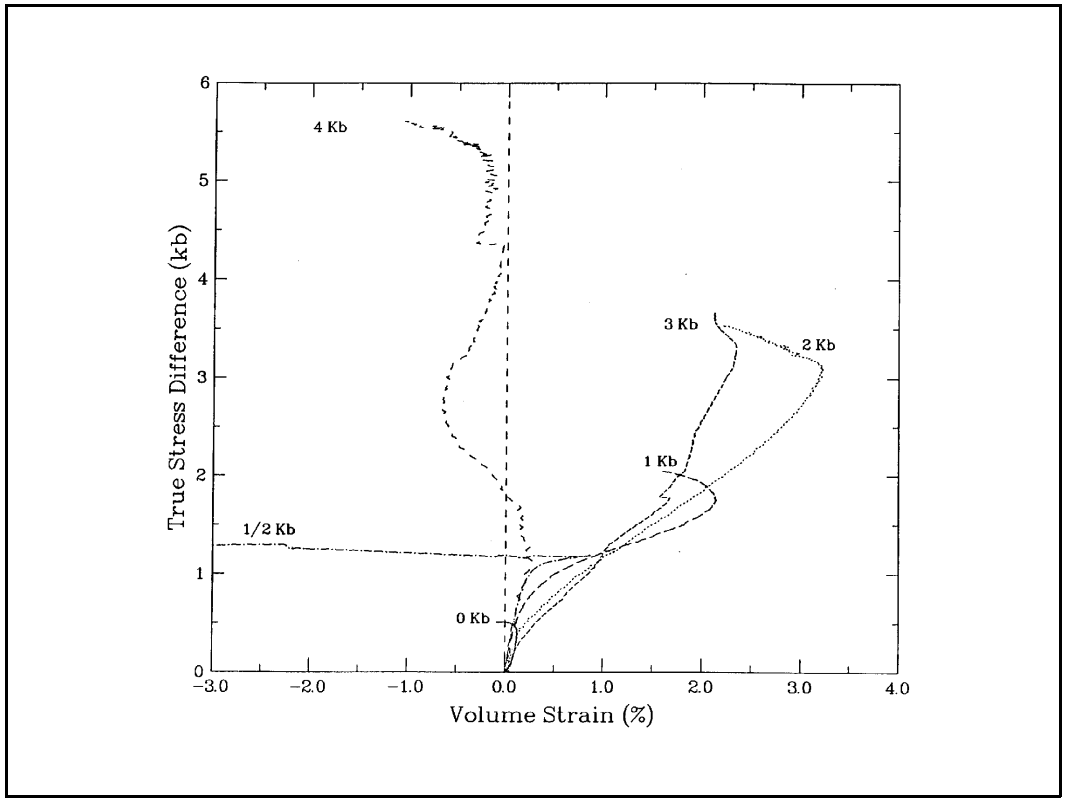

Figure 2.44. Volume strains during shear from drained Salem limestone TX tests (from Chitty and Blouin 1993)

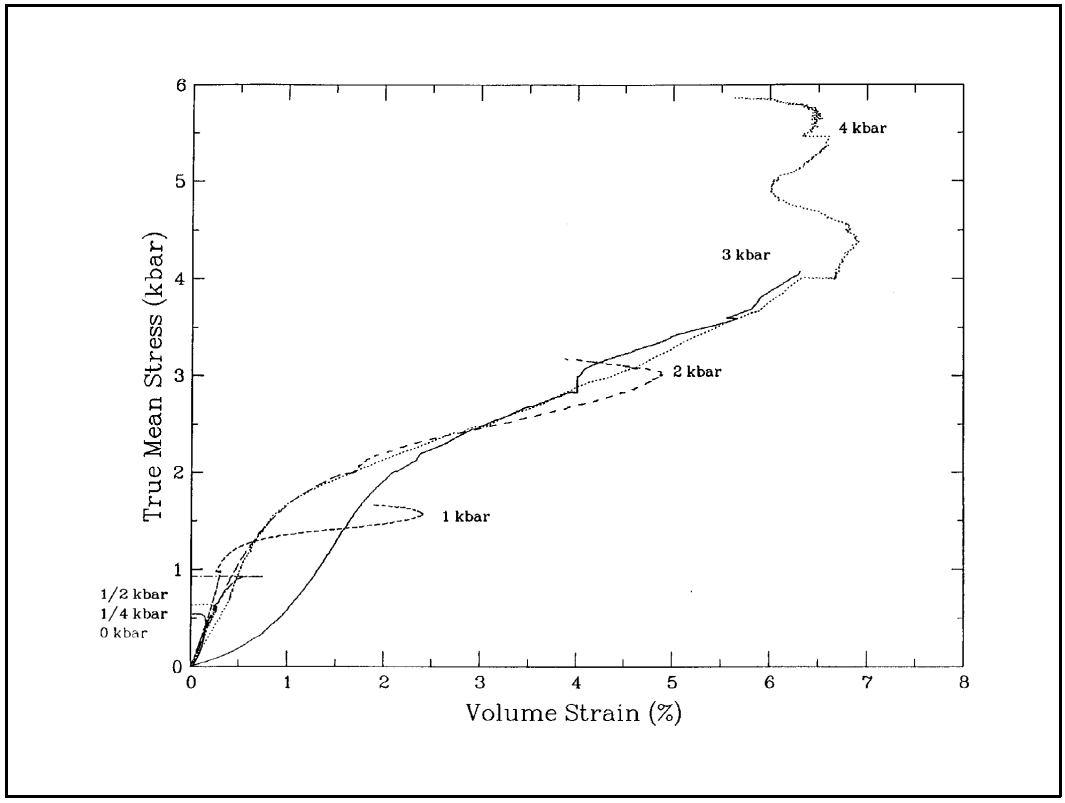

Figure 2.45. Pressure-volume responses from drained Salem limestone TX tests (from Chitty and Blouin 1993)

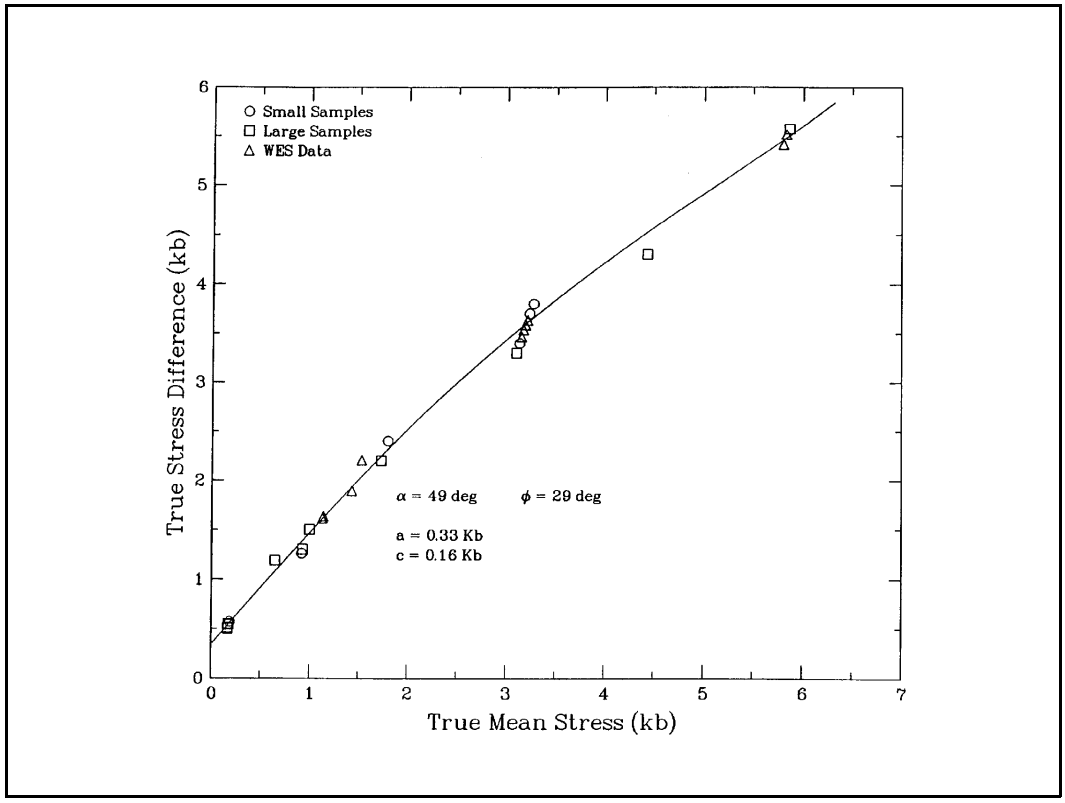

Figure 2.46. Failure envelope generated from drained Salem limestone TX data (from Chitty and Blouin 1993)

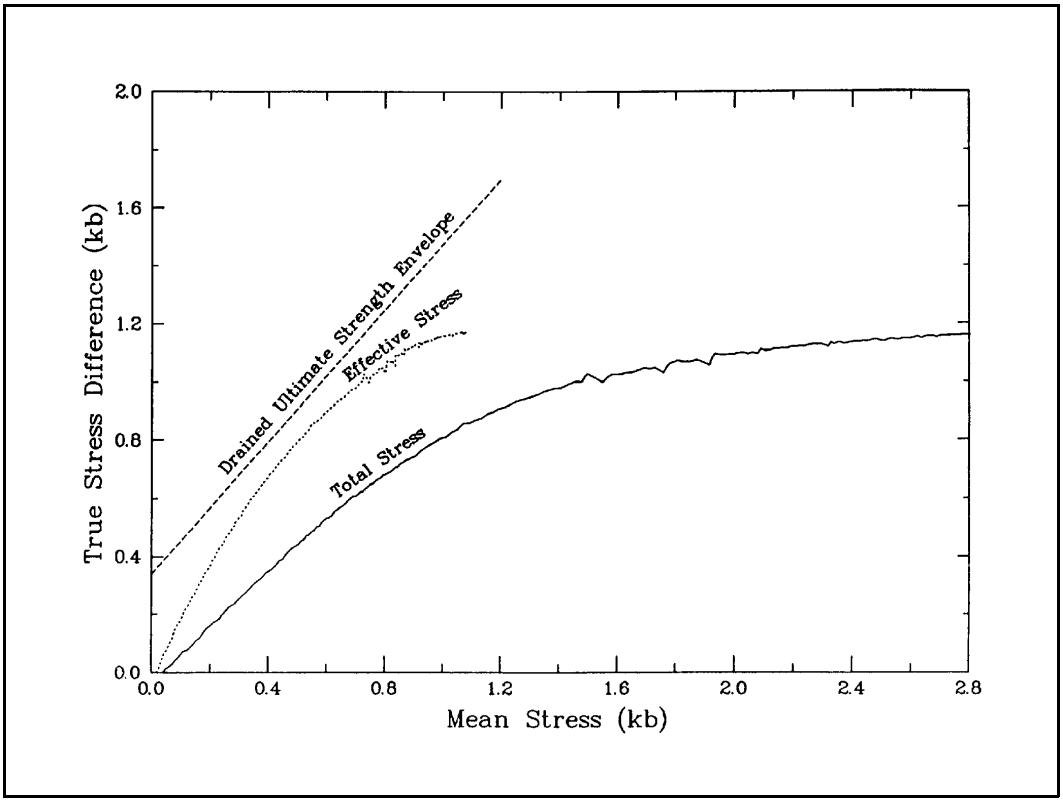

Figure 2.47. Stress paths from an undrained Salem limestone K_o test (from Chitty and Blouin 1993)

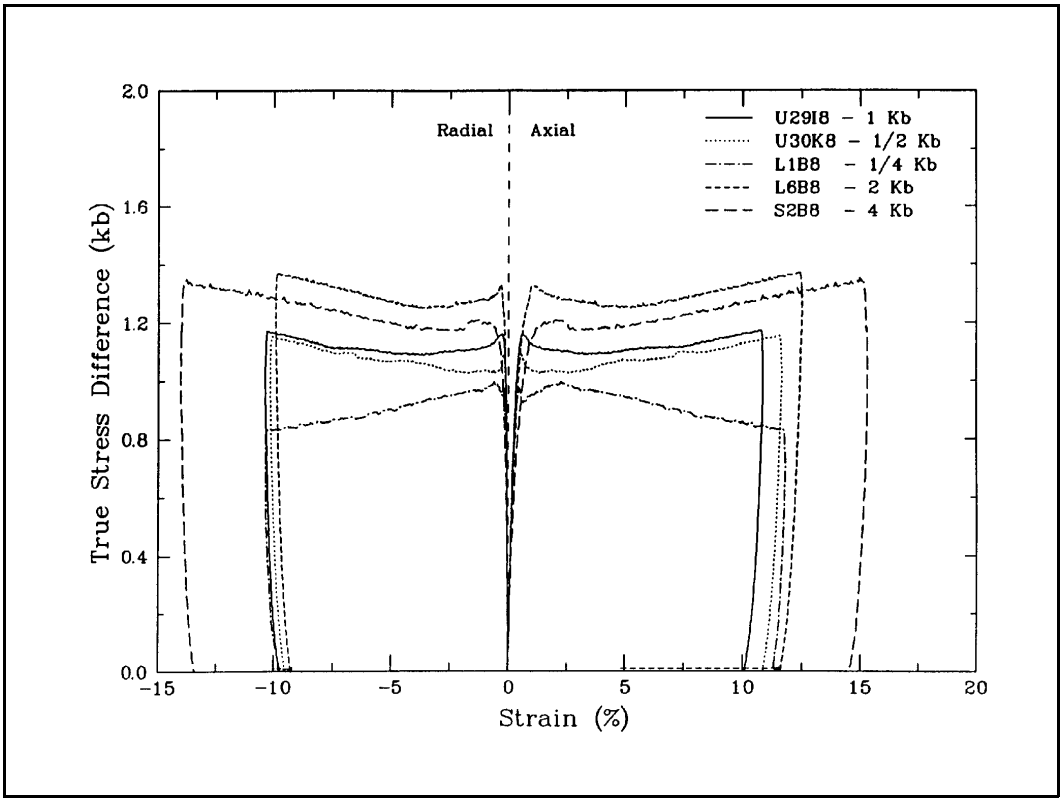

Figure 2.48. Stress-strain curves from undrained Salem limestone TX tests (from Chitty and Blouin 1993)

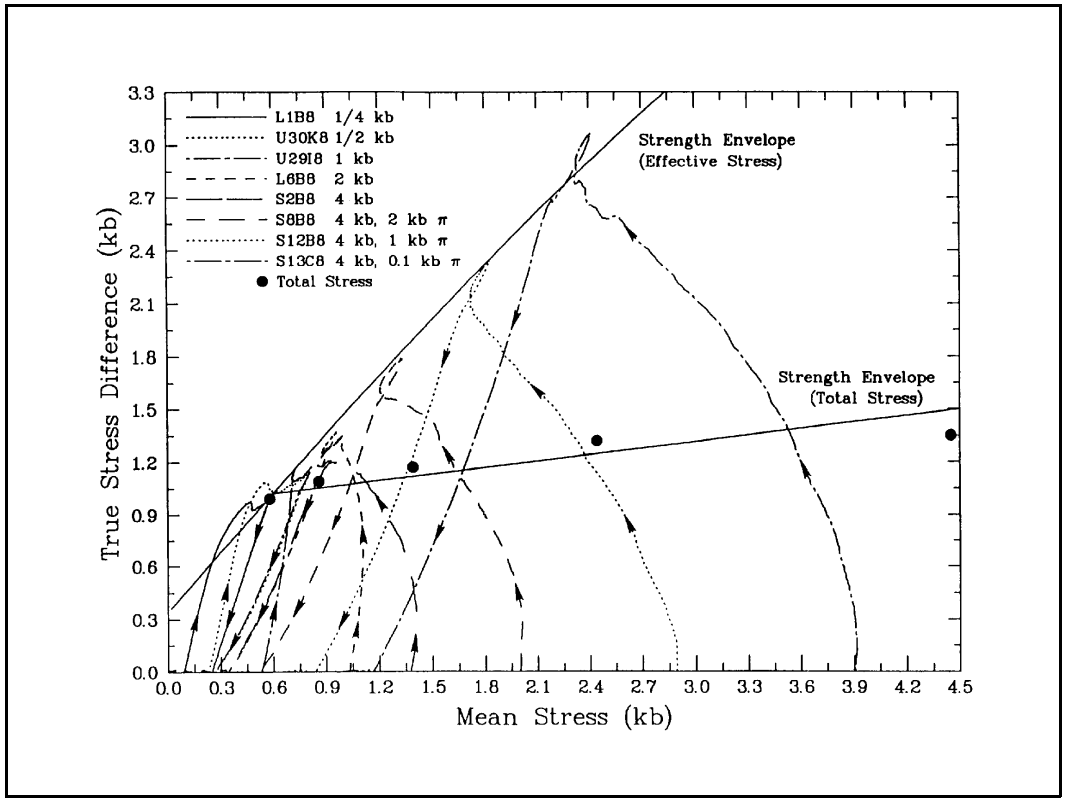

Figure 2.49. Effective stress paths from undrained Salem limestone TX tests (from Chitty and Blouin 1993)